

# A Divide-and-Conquer Bayesian Approach to Large-Scale Kriging

Rajarshi Guhaniyogi <sup>\*1</sup>, Cheng Li <sup>†2</sup>, Terrance D. Savitsky <sup>‡3</sup>, and Sanvesh Srivastava <sup>§4</sup>

<sup>1</sup>*Department of Applied Mathematics and Statistics, UC Santa Cruz*

<sup>2</sup>*Department of Statistics and Applied Probability, National University of Singapore*

<sup>3</sup>*U. S. Bureau of Labor Statistics*

<sup>4</sup>*Department of Statistics and Actuarial Science, The University of Iowa*

May 26, 2022

## Abstract

Flexible hierarchical Bayesian modeling of massive data is challenging due to poorly scaling computations in large sample size settings. This article is motivated by spatial process models for analyzing geostatistical data, which typically entail computations that become prohibitive as the number of spatial locations becomes large. We propose a three-step divide-and-conquer strategy within the Bayesian paradigm to achieve massive scalability for *any* spatial process model. We partition the data into a large number of subsets, apply a readily available Bayesian spatial process model on every subset in parallel, and optimally combine the posterior distributions estimated across all the subsets into a pseudo posterior distribution that conditions on the entire data. The combined pseudo posterior distribution is used for predicting the responses at arbitrary locations and for performing posterior inference on the model parameters and the residual spatial surface. We call this approach “Distributed Kriging” (DISK). It offers significant advantages in applications where the entire data are or can be stored across multiple machines. Under the standard theoretical setup, we show that if the number of subsets is not too large, then the Bayes  $L_2$ -risk of estimating the true residual spatial surface using the DISK posterior distribution decays to zero at a nearly optimal rate. While DISK is a general approach to distributed nonparametric regression, we focus on its applications in spatial statistics and demonstrate its empirical performance using a stationary full-rank and a nonstationary low-rank model based on Gaussian process (GP) prior. A variety of simulations and a geostatistical analysis of the Pacific Ocean sea surface temperature data validate our theoretical results.

**Keywords:** Distributed Bayesian inference; Gaussian process; modified predictive process; large and complex spatial data; Wasserstein distance; Wasserstein barycenter.

---

<sup>\*</sup>guhaniyogi@ucsc.edu

<sup>†</sup>stalic@nus.edu.sg

<sup>‡</sup>savitsky.terrance@bls.gov

<sup>§</sup>sanvesh-srivastava@uiowa.edu

# 1 Introduction

A fundamental challenge in geostatistics is the analysis of massive spatially-referenced data. Due to the recent influx of data with complex spatial associations, sophisticated spatial modeling has become an enormously active area of research; see, for example, [28, 13, 4]. Massive spatial data provide scientists with an unprecedented opportunity to hypothesize and test complex theories. This leads to the implementation of rather complex hierarchical GP-based models that are computationally intractable for large  $n$ , where  $n$  is the number of spatial locations, due to the  $O(n^3)$  computational cost and the  $O(n^2)$  storage cost. This article develops a general distributed Bayesian approach, called Distributed Kriging (DISK), for boosting the scalability of any state-of-the-art spatial process model based on GP prior to multiple folds using the divide-and-conquer technique.

The literature on process-based modeling of massive spatial data is large, so we only provide a selective review. Briefly, these methods seek “dimension-reduction” by endowing the spatial covariance matrix either with a low-rank or a sparse structure. Low-rank structures represent spatial surface using  $r$  *a priori* chosen basis functions. They include fixed-rank kriging [12], or predictive process and its variants [6, 24, 34, 5, 60]; see [78] and [4] for comprehensive reviews. The time complexity for fitting spatial models with a low-rank structure decreases from  $O(n^3)$  to  $O(nr^2)$  floating point operations (flops); however, practical considerations show that when  $n$  is large,  $r$  must grow roughly as  $O(\sqrt{n})$  for accurate estimation, implying that  $O(nr^2)$  flops are also expensive in low-rank structures. On the other hand, sparse structures intuit that spatial correlation between two distantly located observations is nearly zero, so little information is lost by assuming conditional independence given the intermediate locations. For example, covariance tapering [41, 19, 25, 63] uses compactly supported covariance functions to create sparse spatial covariance matrices that approximate the full covariance matrix. Alternately, one could introduce sparsity in the inverse covariance (precision) matrix using conditional independence assumptions or composite likelihoods [75, 59, 70, 20, 15, 71, 36]. In related literature on computer experiments, localized approximations of GP models are proposed, see, for example, [30, 82, 54]. GP-based modeling using low-rank or sparse structures has also received significant attention in machine learning; see [55, 10] for recent reviews.

Some variants of dimension-reduction methods partition the spatial domain into sub-regions containing fewer spatial locations. Each of these sub-regions is modeled using a GP which are then hierarchically combined by borrowing information from across the sub-regions. Examples include non-stationary models [4], multi-level and multi-resolution models [27, 52, 40, 35], and the Bayesian Treed GP models [31]. These models usually achieve scalability by assuming block-independence at some level of the hierarchy, usually across sub-regions, but may lose scalability when they borrow across sub-regions. In an unrelated thread, [45] propose parameter estimation in the GP-based geostatistical model using resampling based on stochastic approximation. Besides being fully frequentist in nature, it is less clear as to how such an idea would be extended to enable analysis of more general nonstationary models with massive data.

The proposed DISK framework is a three-step approach for distributed Bayesian inference in any model based on spatial process. First, we divide the  $n$  spatial locations into  $k$  subsets such that each subset has representative samples from all regions of the spatial domain. Second, we choose any spatial model and estimate the posterior distributions for inference and prediction in parallel across  $k$  subsets after raising the likelihood to a power of  $k$  in each subset. The pseudo posterior distribution obtained after modifying the likelihood for each subset of data is referred to as the “subset posterior.” Since each subset posterior distribution conditions on  $(1/k)$ -fraction of the full data, the modification by raising the likelihood to the power  $k$  ensures that variance of each subset posterior distribution is of the same order (as a function of  $n$ ) as that of the full data posterior distribution. Third, the  $k$  subset posterior distributions are combined into a single pseudo probability distribution, called the DISK pseudo posterior (henceforth, DISK posterior), that conditions on the full data and replaces the computationally expensive full data posterior distribution for the purpose of prediction and inference. Computationally, the main innovations are in the first and third steps, where general partitioning and combining schemes are unavailable in process-based modeling of spatial data. Theoretically, we provide guarantees on the rate of decay of the Bayes  $L_2$ -risk in estimating the true residual spatial surface using the DISK posterior as a function of  $n$ ,  $k$ , and analytic properties of the true spatial surface. This involves two new upper bounds. First, an upper bound for the Bayes risk of the DISK posterior is developed assuming each subset size approaches to infinity. Second, we provide an in depth analysis of the bias-variance tradeoff in estimating the true spatial surface using the DISK posterior and develop upper bounds on  $k$  (as a function on  $n$ ) that lead to near optimal performance as  $n$  tends to infinity.

Motivated by large and complex data, there has been significant interest in adopting the divide-and-conquer technique for distributed Bayesian inference [50, 76, 77, 32, 62, 33, 48, 80]. DISK is significantly different from these as it is based on combining the collection of  $k$  subset posterior distributions through their barycenter, a notion of geometric center that generalizes the Euclidean mean to a space of probability measures. There are recent approaches based on combining subset inferences, either through the posterior means and covariance matrices of parameters across the  $k$  subsets [62] or by employing a “product of experts” [51, 17]. These approaches are intuitively appealing for GP regression, but lead to theoretically sub-optimal uncertainty quantification [72] and are less suited when a GP or its derivative is embedded in a more general hierarchical model; for example, GP-based classification [37]. Recent developments on distributed variational GP [26] are impractical for  $n > 10^7$  and no theoretical results are available on the quality of approximation of the full posterior distribution. There are recent works on combining subset posterior distributions through their geometric centers, such as the mean or the median, but they are restricted to parametric models [46, 67, 44, 61, 47, 68]. Extensions to general nonparametric models, including those based on stochastic processes, are missing, except for some empirical results on nonparametric regression using GP [46, 67] and theoretical guarantees for both these methods in the Gaussian white noise model [72]. Combining subset posterior distributions of a stochastic process is challenging for two major reasons. First, it requires estimation of a function, an infinite dimensional parameter.

Second, and most importantly, stochastic process models induce complex dependencies among observations that is challenging to capture with a combination of subset posterior distributions that are estimated independently without accounting for the inter-subset dependence.

Divide-and-conquer nonparametric regression, which includes kriging as a special case, has received significant attention lately in the optimization literature, though the Bayesian literature is relatively lightly populated. The bias-variance decomposition of the  $L_2$ -risk in the estimation of true regression function in divide-and-conquer kernel ridge regression is known [84, 81]. Bayesian divide-and-conquer nonparametric regression has been mostly studied from the theoretical perspective [11, 64, 65, 72]. Filling the methodological gap, the DISK framework provides a general approach to enhance the scalability of *any* process-based model for Bayesian nonparametric regression, including models based on spatial processes. For example, if the application of spatial process models is feasible for a subset of size  $m$ , then one can run them on  $k$  subsets in parallel and DISK allows prediction and inference using  $n = mk$  spatial locations. The values of  $m$  and  $k$  depend mainly upon the available computational resources and the model, but our theoretical results provide guidance on choosing  $k$  depending on the analytic properties of the true spatial process. For clarity of exposition, we illustrate the empirical performance of the DISK framework with the stationary GP and the modified predictive process (MPP) [24] priors. The MPP is a low-rank nonstationary GP prior that allows accurate modeling of spatial surfaces whose variability or smoothness changes with the location. MPP, like any low-rank model, faces computational bottlenecks when  $n$  is large, and either computational efficiency or accuracy worsens when MPP is applied to even  $10^4$  observations. Our numerical results establish that DISK with MPP scales to  $10^6$  observations without compromising on either computational efficiency or accuracy in inference and prediction. We expect this conclusion to hold for other popular structured GP priors.

The remainder of the manuscript evolves as follows. In Section 2 we outline a Bayesian hierarchical mixed model framework that incorporates models based on both the full-rank and the low-rank GP priors. Our DISK approach will work with posterior samples from such models. Section 3 develops the framework for DISK, discusses how to compute the DISK posterior distribution, and offers theoretical insights into the DISK for general GPs and their approximations. A detailed simulation study followed by an analysis of the Pacific ocean sea surface temperature data are illustrated in Section 4 to justify the use of DISK for real data. Finally, Section 5 discusses what DISK achieves, and proposes a number of future directions to explore.

## 2 Hierarchical Bayesian inference for GP-based spatial models

Consider the standard univariate spatial regression model for the data observed at location  $\mathbf{s}$  in a compact spatial domain  $\mathcal{D}$ ,

$$y(\mathbf{s}) = \mathbf{x}(\mathbf{s})^T \boldsymbol{\beta} + w(\mathbf{s}) + \epsilon(\mathbf{s}), \quad (1)$$

where  $y(\mathbf{s})$  is a univariate response at  $\mathbf{s}$ ,  $\mathbf{x}(\mathbf{s})$  is a  $p \times 1$  predictor vector at  $\mathbf{s}$ ,  $\boldsymbol{\beta}$  is a  $p \times 1$  predictor coefficient,  $w(\mathbf{s})$  is the realization of an unknown spatial function  $w(\cdot)$  at  $\mathbf{s}$ , and  $\epsilon(\mathbf{s})$  is the realization of white-noise process  $\epsilon(\cdot)$  at  $\mathbf{s}$  and is independent of  $w(\cdot)$ . The Bayesian implementation of the model in (1) customarily assumes (a) that  $\boldsymbol{\beta}$  *a priori* follows a Gaussian distribution with mean  $\boldsymbol{\mu}_\beta$  and covariance matrix  $\boldsymbol{\Sigma}_\beta$  and (b) that  $w(\cdot)$  and  $\epsilon(\cdot)$  *a priori* follow mean 0 GPs with covariance functions  $C_\alpha(\mathbf{s}_1, \mathbf{s}_2)$  and  $D_\alpha(\mathbf{s}_1, \mathbf{s}_2)$  that model  $\text{cov}\{w(\mathbf{s}_1), w(\mathbf{s}_2)\}$  and  $\text{cov}\{\epsilon(\mathbf{s}_1), \epsilon(\mathbf{s}_2)\}$ , respectively, where  $\alpha$  are the process parameters indexing the two families of covariance functions and  $\mathbf{s}_1, \mathbf{s}_2 \in \mathcal{D}$ ; therefore, the model parameters are  $\boldsymbol{\Omega} = \{\alpha, \beta\}$ . If  $\beta = 0$  in (1), then we obtain the setup for Bayesian nonparametric regression using GP prior, with  $\mathbf{s}$  as covariates and  $y(\mathbf{s})$  as the response. The training data consists of  $n$  predictors and responses, denoted as  $\{\mathbf{x}(\mathbf{s}_1), y(\mathbf{s}_1)\}, \dots, \{\mathbf{x}(\mathbf{s}_n), y(\mathbf{s}_n)\}$ , observed at  $n$  spatial locations, denoted as  $\mathcal{S} = \{\mathbf{s}_1, \dots, \mathbf{s}_n\}$ .

Standard Markov chain Monte Carlo (MCMC) algorithms exist for performing posterior inference on  $\boldsymbol{\Omega}$  and the values of  $w(\cdot)$  at a given set of locations  $\mathcal{S}^* = \{\mathbf{s}_1^*, \dots, \mathbf{s}_l^*\}$ , where  $\mathcal{S}^* \cap \mathcal{S} = \emptyset$ , and for predicting  $y(\mathbf{s}^*)$  for any  $\mathbf{s}^* \in \mathcal{S}^*$  [4]. Given  $\mathcal{S}$ , the prior assumptions on  $w(\cdot)$  and  $\epsilon(\cdot)$  imply that  $\mathbf{w}^T = \{w(\mathbf{s}_1), \dots, w(\mathbf{s}_n)\}$  and  $\boldsymbol{\epsilon}^T = \{\epsilon(\mathbf{s}_1), \dots, \epsilon(\mathbf{s}_n)\}$  are independent and follow  $N\{\mathbf{0}, \mathbf{C}(\alpha)\}$  and  $N\{\mathbf{0}, \mathbf{D}(\alpha)\}$ , respectively, where  $N(\mathbf{m}, \mathbf{V})$  denotes the density of a multivariate Gaussian distribution of appropriate dimension with mean  $\mathbf{m}$  and covariance matrix  $\mathbf{V}$  and the  $(i, j)$ th entries of  $\mathbf{C}(\alpha)$  and  $\mathbf{D}(\alpha)$  are  $C_\alpha(\mathbf{s}_i, \mathbf{s}_j)$  and  $D_\alpha(\mathbf{s}_i, \mathbf{s}_j)$ , respectively. The hierarchy in (1) is completed by assuming that  $\alpha$  *a priori* follows a distribution with density  $\pi(\alpha)$ . If  $\mathbf{y} = \{y(\mathbf{s}_1), \dots, y(\mathbf{s}_n)\}^T$  is the  $n \times 1$  response vector and  $\mathbf{X} = [\mathbf{x}(\mathbf{s}_1) : \dots : \mathbf{x}(\mathbf{s}_n)]^T$  is the  $n \times p$  matrix of predictors, where  $p < n$ , then the MCMC algorithm for sampling  $\boldsymbol{\Omega}$ ,  $\mathbf{w}^{*T} = \{w(\mathbf{s}_1^*), \dots, w(\mathbf{s}_l^*)\}$ , and  $\mathbf{y}^{*T} = \{y(\mathbf{s}_1^*), \dots, y(\mathbf{s}_l^*)\}$  cycle through the following three steps until sufficient samples are drawn post convergence:

1. Integrate over  $\mathbf{w}$  in (1) and

- (a) sample  $\beta$  given  $\mathbf{y}$ ,  $\mathbf{X}$ , and  $\alpha$  from  $N(\mathbf{m}_\beta, \mathbf{V}_\beta)$ , where

$$\mathbf{V}_\beta = \left\{ \mathbf{X}^T \mathbf{V}(\alpha)^{-1} \mathbf{X} + \boldsymbol{\Sigma}_\beta^{-1} \right\}^{-1}, \quad \mathbf{m}_\beta = \mathbf{V}_\beta \left\{ \mathbf{X}^T \mathbf{V}(\alpha)^{-1} \mathbf{y} + \boldsymbol{\Sigma}_\beta^{-1} \boldsymbol{\mu}_\beta \right\}, \quad (2)$$

and  $\mathbf{V}(\alpha) = \mathbf{C}(\alpha) + \mathbf{D}(\alpha)$ ; and

- (b) sample  $\alpha$  given  $\mathbf{y}$ ,  $\mathbf{X}$ , and  $\beta$  using the Metropolis-Hastings algorithm with a normal random walk proposal.

2. Sample  $\mathbf{w}^*$  given  $\mathbf{y}$ ,  $\mathbf{X}$ ,  $\alpha$ , and  $\beta$  from  $N(\mathbf{m}_*, \mathbf{V}_*)$ , where

$$\mathbf{V}_* = \mathbf{C}_{*,*}(\alpha) - \mathbf{C}_*(\alpha) \mathbf{V}(\alpha)^{-1} \mathbf{C}_*(\alpha)^T, \quad \mathbf{m}_* = \mathbf{C}_*(\alpha) \mathbf{V}(\alpha)^{-1} (\mathbf{y} - \mathbf{X}\beta), \quad (3)$$

$\mathbf{C}_*(\alpha)$  and  $\mathbf{C}_{*,*}(\alpha)$  are  $l \times n$  and  $l \times l$  matrices, respectively, and the  $(i, j)$ th entries of  $\mathbf{C}_{*,*}(\alpha)$  and  $\mathbf{C}_*(\alpha)$  are  $C_\alpha(\mathbf{s}_i^*, \mathbf{s}_j^*)$  and  $C_\alpha(\mathbf{s}_i^*, \mathbf{s}_j)$ , respectively.

3. Sample  $\mathbf{y}^*$  given  $\alpha$ ,  $\beta$ , and  $\mathbf{w}^*$  from  $N\{\mathbf{X}^* \beta + \mathbf{w}^*, \mathbf{D}(\alpha)\}$ , where  $\mathbf{X}^{*T} = [\mathbf{x}(\mathbf{s}_1^*) : \dots : \mathbf{x}(\mathbf{s}_l^*)]$ .

Many Bayesian spatial models can be formulated in terms of (1) by assuming different forms of  $C_{\alpha}(\mathbf{s}_1, \mathbf{s}_2)$  and  $D_{\alpha}(\mathbf{s}_1, \mathbf{s}_2)$ ; see [4] and supplementary material for details on the MCMC algorithm.

MCMC computations face a major computational bottleneck due to matrix inversions involving  $\mathbf{C}(\alpha)$ . The steps 1(a), 1(b), and 2 for sampling  $\Omega$  and  $\mathbf{w}^*$  involve inversion of  $\mathbf{C}(\alpha) + \mathbf{D}(\alpha)$ . Irrespective of the form of  $\mathbf{D}(\alpha)$ , if no additional assumptions are made on the structure of  $\mathbf{C}(\alpha)$ , then the three steps require  $O(n^3)$  flops in computation and  $O(n^2)$  memory units in storage in every MCMC iteration. Spatial models with this form of posterior computations are based on a *full-rank* GP prior. In practice, if  $n \geq 10^4$ , then posterior computations in a model based on a full-rank GP prior are infeasible due to numerical issues in matrix inversions involving an unstructured  $\mathbf{C}(\alpha)$ .

This problem is solved by imposing additional structure on  $\mathbf{C}(\alpha)$ . Our focus is on those methods that impose a sparse or low-rank structure on the covariance function of a GP prior [55, 4]. Every method in this class expresses the covariance function in terms of  $r \ll n$  basis functions, in turn inducing a *low-rank* GP prior. We use the MPP as a representative example of this class of methods. Let  $\mathcal{S}^{(0)} = \{\mathbf{s}_1^{(0)}, \dots, \mathbf{s}_r^{(0)}\}$  be a set of  $r$  locations, known as the “knots,” which may or may not intersect with  $\mathcal{S}$ . Let  $\mathbf{c}(\mathbf{s}, \mathcal{S}^{(0)}) = \{C_{\alpha}(\mathbf{s}, \mathbf{s}_1^{(0)}), \dots, C_{\alpha}(\mathbf{s}, \mathbf{s}_r^{(0)})\}^T$  be an  $r \times 1$  vector and  $\mathbf{C}(\mathcal{S}^{(0)})$  be an  $r \times r$  matrix whose  $(i, j)$ th entry is  $C_{\alpha}(\mathbf{s}_i^{(0)}, \mathbf{s}_j^{(0)})$ . Using  $\mathbf{c}(\mathbf{s}_1, \mathcal{S}^{(0)}), \dots, \mathbf{c}(\mathbf{s}_n, \mathcal{S}^{(0)})$  and  $\mathbf{C}(\mathcal{S}^{(0)})$ , define the diagonal matrix  $\delta = \text{diag}\{\delta(\mathbf{s}_1), \dots, \delta(\mathbf{s}_n)\}$  with

$$\delta(\mathbf{s}_i) = C_{\alpha}(\mathbf{s}_i, \mathbf{s}_i) - \mathbf{c}^T(\mathbf{s}_i, \mathcal{S}^{(0)}) \mathbf{C}(\mathcal{S}^{(0)})^{-1} \mathbf{c}(\mathbf{s}_i, \mathcal{S}^{(0)}), \quad i = 1, \dots, n. \quad (4)$$

Let  $\mathbf{1}(\mathbf{a} = \mathbf{b}) = 1$  if  $\mathbf{a} = \mathbf{b}$  and 0 otherwise. Then, the MPP is a GP with the covariance function

$$\tilde{C}_{\alpha}(\mathbf{s}_1, \mathbf{s}_2) = \mathbf{c}^T(\mathbf{s}_1, \mathcal{S}^{(0)}) \mathbf{C}(\mathcal{S}^{(0)})^{-1} \mathbf{c}(\mathbf{s}_2, \mathcal{S}^{(0)}) + \delta(\mathbf{s}_1) \mathbf{1}(\mathbf{s}_1 = \mathbf{s}_2), \quad \mathbf{s}_1, \mathbf{s}_2 \in \mathcal{D}, \quad (5)$$

where  $\tilde{C}_{\alpha}(\mathbf{s}_1, \mathbf{s}_2)$  depends on the covariance function of the parent GP and the selected  $r$  knots, which define  $\mathbf{C}(\mathcal{S}^{(0)})$ ,  $\mathbf{c}^T(\mathbf{s}_1, \mathcal{S}^{(0)})$ , and  $\mathbf{c}^T(\mathbf{s}_2, \mathcal{S}^{(0)})$ . We have used a  $\tilde{\cdot}$  in (5) to distinguish the covariance function of a low-rank GP prior from that of its parent full-rank GP. If  $\tilde{\mathbf{C}}(\alpha)$  is a matrix with  $(i, j)$ th entry  $\tilde{C}_{\alpha}(\mathbf{s}_i, \mathbf{s}_j)$ , then the posterior computations using MPP, a low-rank GP prior, replace  $\mathbf{C}(\alpha)$  by  $\tilde{\mathbf{C}}(\alpha)$  in the steps 1(a), 1(b), and 2. The (low) rank  $r$  structure imposed by  $\mathbf{C}(\mathcal{S}^{(0)})$  implies that  $\tilde{\mathbf{C}}(\alpha)^{-1}$  computation requires  $O(nr^2)$  flops using the Woodbury formula [38].

Spatial models based on a low-rank GP prior, including MPP, suffer from computational bottlenecks in massive data settings. The computational complexity of posterior computations for a rank- $r$  GP prior is  $O(nr^2)$ , which is linear in  $n$ ; however, practical considerations often necessitate that  $r = O(\sqrt{n})$  for accurate inference and prediction. This severely limits the computational advantages of low-rank GP priors, including MPP, especially in applications with large  $n$  [15]. The next few sections develop our DISK framework, which is key in extending any GP-based spatial model to massive data using the divide-and-conquer technique without compromising either on the quality of inference and prediction or on the computational cost.

### 3 Distributed Kriging

#### 3.1 First step: partitioning of spatial locations

We partition the  $n$  spatial locations into  $k$  subsets. The value of  $k$  depends on the chosen spatial model, and it is large enough to ensure efficient posterior computations on any subset. The default partitioning scheme is to randomly allocate the locations into  $k$  subsets, but we specify a technical condition later which ensures that every subset has locations from all regions of the spatial domain. For theoretical and notational simplicity, we also assume that the  $k$  subsets are non-overlapping and that every subset has  $m$  spatial locations so that  $n = mk$ . Let  $\mathcal{S}_j$  be the set of spatial locations in subset  $j$  ( $j = 1, \dots, k$ ). Our simplifying assumptions imply that  $\cup_{j=1}^k \mathcal{S}_j = \mathcal{S}$ ,  $\mathcal{S}_j \cap \mathcal{S}_{j'} = \emptyset$  for  $j \neq j'$ , and  $\mathcal{S}_j = \{\mathbf{s}_{j1}, \dots, \mathbf{s}_{jm}\}$ , where  $\mathbf{s}_{ji} = \mathbf{s}_{i'}$  for some  $\mathbf{s}_{i'} \in \mathcal{S}$  and for every  $j = 1, \dots, k$  and  $i = 1, \dots, m$ . Denote the data in the  $j$ th partition as  $\{\mathbf{y}_j, \mathbf{X}_j\}$  ( $j = 1, \dots, k$ ), where  $\mathbf{y}_j = \{y(\mathbf{s}_{j1}), \dots, y(\mathbf{s}_{jm})\}^T$  is a  $m \times 1$  vector and  $\mathbf{X}_j = [\mathbf{x}(\mathbf{s}_{j1}) : \dots : \mathbf{x}(\mathbf{s}_{jm})]^T$  is a  $m \times p$  matrix of predictors corresponding to the spatial locations in  $\mathcal{S}_j$  with  $p < m$ .

The univariate spatial regression models using either a full-rank or a low-rank GP prior for the data observed at any location  $\mathbf{s}_{ji} \in \mathcal{S}_j \subset \mathcal{D}$  is given by

$$y(\mathbf{s}_{ji}) = \mathbf{x}(\mathbf{s}_{ji})^T \boldsymbol{\beta} + w(\mathbf{s}_{ji}) + \epsilon(\mathbf{s}_{ji}), \quad i = 1, \dots, m. \quad (6)$$

Let  $\mathbf{w}_j^T = \{w(\mathbf{s}_{j1}), \dots, w(\mathbf{s}_{jm})\}$  and  $\boldsymbol{\epsilon}_j^T = \{\epsilon(\mathbf{s}_{j1}), \dots, \epsilon(\mathbf{s}_{jm})\}$  be the realizations of GP  $w(\cdot)$  and white-noise process  $\epsilon(\cdot)$ , respectively, in the  $j$ th subset. After marginalizing over  $\mathbf{w}_j$  in the GP-based model for the  $j$ th subset, the likelihood of  $\boldsymbol{\Omega} = \{\boldsymbol{\alpha}, \boldsymbol{\beta}\}$  is given by

$$\ell_j(\boldsymbol{\Omega}) = N\{\mathbf{y}_j \mid \mathbf{X}_j \boldsymbol{\beta}, \mathbf{V}_j(\boldsymbol{\alpha})\}, \quad (7)$$

where  $N(\mathbf{y}_j \mid \mathbf{m}, \mathbf{V})$  represents the multivariate normal density of  $\mathbf{y}_j$  with mean  $\mathbf{m}$  and covariance matrix  $\mathbf{V}$ ,  $\mathbf{V}_j(\boldsymbol{\alpha}) = \mathbf{C}_j(\boldsymbol{\alpha}) + \mathbf{D}_j(\boldsymbol{\alpha})$  and  $\mathbf{V}_j(\boldsymbol{\alpha}) = \tilde{\mathbf{C}}_j(\boldsymbol{\alpha}) + \mathbf{D}_j(\boldsymbol{\alpha})$  for full-rank and low-rank GP priors, respectively, and  $\mathbf{C}_j(\boldsymbol{\alpha}), \tilde{\mathbf{C}}_j(\boldsymbol{\alpha}), \mathbf{D}_j(\boldsymbol{\alpha})$  are obtained by extending the definitions of  $\mathbf{C}(\boldsymbol{\alpha}), \tilde{\mathbf{C}}(\boldsymbol{\alpha}), \mathbf{D}(\boldsymbol{\alpha})$  to the  $j$ th subset. In a model based on full-rank or low-rank GP prior, the likelihood of  $\mathbf{w}_j$  given  $\mathbf{y}_j, \mathbf{X}_j$ , and  $\boldsymbol{\Omega}$  is

$$\ell_j(\mathbf{w}_j) = N\{\mathbf{y}_j - \mathbf{X}_j \boldsymbol{\beta} \mid \mathbf{w}_j, \mathbf{D}_j(\boldsymbol{\alpha})\}. \quad (8)$$

The likelihoods in (7) and (8) are used for defining the posterior distributions for  $\boldsymbol{\beta}, \boldsymbol{\alpha}, \mathbf{w}^*, \mathbf{y}^*$ , called  $j$ th subset posterior distributions, using a full-rank or a low-rank GP prior in subset  $j$ .

### 3.2 Second step: sampling from subset posterior distributions

We define subset posterior distributions by modifying the likelihoods in (7) and (8). More precisely, the density of the  $j$ th subset posterior distribution of  $\boldsymbol{\Omega}$  is given by

$$\pi_m(\boldsymbol{\Omega} \mid \mathbf{y}_j) = \frac{\{\ell_j(\boldsymbol{\Omega})\}^k \pi(\boldsymbol{\Omega})}{\int \{\ell_j(\boldsymbol{\Omega})\}^k \pi(\boldsymbol{\Omega}) d\boldsymbol{\Omega}}, \quad (9)$$

where we assume that  $\int \{\ell_j(\boldsymbol{\Omega})\}^k \pi(\boldsymbol{\Omega}) d\boldsymbol{\Omega} < \infty$ , and the subscript ‘ $m$ ’ denotes that the density conditions on  $m$  samples in the  $j$ th subset. The modification of likelihood to yield the subset posterior density in (9) is called *stochastic approximation* [46]. Raising the likelihood to the power of  $k$  is equivalent to replicating every  $y(\mathbf{s}_{ji})$   $k$  times ( $i = 1, \dots, m$ ). Thus, stochastic approximation accounts for the fact that the  $j$ th subset posterior distribution conditions on a  $(1/k)$ -fraction ( $k = n/m$ ) of the full data and ensures that its variance is of the same order (as a function of  $n$ ) as that of the full data posterior distribution. This is a common strategy adopted in divide-and-conquer based Bayesian inference in parametric models; see, for example, [44, 80] for recent applications.

With the proposed stochastic approximation in (9), the full conditional densities of  $j$ th subset posterior distributions for prediction and inference follow from their full data counterparts. The  $j$ th full conditional densities of  $\boldsymbol{\beta}$  and  $\boldsymbol{\alpha}$  in the GP-based models are given by

$$\pi_m(\boldsymbol{\beta} \mid \mathbf{y}_j, \boldsymbol{\alpha}) = \frac{\{\ell_j(\boldsymbol{\Omega})\}^k \pi(\boldsymbol{\beta})}{\int \{\ell_j(\boldsymbol{\Omega})\}^k \pi(\boldsymbol{\beta}) d\boldsymbol{\beta}}, \quad \pi_m(\boldsymbol{\alpha} \mid \mathbf{y}_j, \boldsymbol{\beta}) = \frac{\{\ell_j(\boldsymbol{\Omega})\}^k \pi(\boldsymbol{\alpha})}{\int \{\ell_j(\boldsymbol{\Omega})\}^k \pi(\boldsymbol{\alpha}) d\boldsymbol{\alpha}}, \quad (10)$$

where  $\pi(\boldsymbol{\beta}) = N(\boldsymbol{\mu}_\beta, \boldsymbol{\Sigma}_\beta)$ ,  $\pi(\boldsymbol{\alpha})$  is the prior density of  $\boldsymbol{\alpha}$ , and we assume that  $\int \{\ell_j(\boldsymbol{\Omega})\}^k \pi(\boldsymbol{\beta}) d\boldsymbol{\beta}$  and  $\int \{\ell_j(\boldsymbol{\Omega})\}^k \pi(\boldsymbol{\alpha}) d\boldsymbol{\alpha}$  respectively are finite. The  $j$ th full conditional densities of  $\mathbf{y}^*$  and  $\mathbf{w}^*$  are calculated after modifying the likelihood of  $\mathbf{w}_j$  in (7) using stochastic approximation. Given  $\mathbf{y}_j$ ,  $\mathbf{X}_j$ , and  $\boldsymbol{\Omega}$ , straightforward calculation yields that the  $j$ th subset posterior predictive density of  $\mathbf{w}^*$  is  $\pi_m(\mathbf{w}^* \mid \mathbf{y}_j, \boldsymbol{\Omega}) = N(\mathbf{w}^* \mid \mathbf{m}_{j*}, \mathbf{V}_{j*})$ , where

$$\mathbf{V}_{j*} = \mathbf{C}_{*,*}(\boldsymbol{\alpha}) - \mathbf{C}_{*j}(\boldsymbol{\alpha}) \mathbf{V}_j(\boldsymbol{\alpha})^{-1} \mathbf{C}_{*j}(\boldsymbol{\alpha})^T, \quad \mathbf{m}_{j*} = \mathbf{C}_{*j}(\boldsymbol{\alpha}) \mathbf{V}_j(\boldsymbol{\alpha})^{-1} (\mathbf{y}_j - \mathbf{X}_j \boldsymbol{\beta}), \quad (11)$$

where  $\mathbf{V}_j(\boldsymbol{\alpha}) = \mathbf{C}_j(\boldsymbol{\alpha}) + k^{-1} \mathbf{D}_j(\boldsymbol{\alpha})$  and  $\tilde{\mathbf{V}}_j(\boldsymbol{\alpha}) = \tilde{\mathbf{C}}_j(\boldsymbol{\alpha}) + k^{-1} \mathbf{D}_j(\boldsymbol{\alpha})$  for full-rank and low-rank GP priors, respectively, and  $\mathbf{C}_{*,*}(\boldsymbol{\alpha})$ ,  $\mathbf{C}_{*j}(\boldsymbol{\alpha})$  are  $l \times l$ ,  $l \times m$  matrices obtained by extending the definition in (3) to subset  $j$  for full-rank and low-rank GP priors with covariance functions  $C_\alpha(\cdot, \cdot)$  and  $\tilde{C}_\alpha(\cdot, \cdot)$ , respectively. We note that the stochastic approximation exponent,  $k$ , scales  $\mathbf{D}_j(\boldsymbol{\alpha})$  in  $\mathbf{V}_j(\boldsymbol{\alpha})$  so that the uncertainty in subset posterior distributions are scaled to that of the full data posterior. The  $j$ th subset posterior predictive density of  $\mathbf{y}^*$  given the samples of  $\mathbf{w}^*$  and  $\boldsymbol{\Omega}$  in the  $j$ th subset is  $N\{\mathbf{y}^* \mid \mathbf{X}^* \boldsymbol{\beta} + \mathbf{w}^*, \mathbf{D}_j(\boldsymbol{\alpha})\}$ . We employ the same three-step sampling algorithm, as earlier introduced, specialized to subset  $j$  ( $j = 1, \dots, k$ ), sampling  $\{\boldsymbol{\beta}, \boldsymbol{\alpha}, \mathbf{y}^*, \mathbf{w}^*\}$  in each subset across multiple MCMC iterations; see supplementary material for detailed derivations of subset posterior sampling algorithms in the full-rank and low-rank GP priors.

The computational complexity of  $j$ th subset posterior computations follows from their full data



counterparts if we replace  $n$  by  $m$ . Specifically, the computational complexities for sampling a subset posterior distribution are  $O(m^3)$  and  $O(mr^2)$  flops if the model in (6) uses a full-rank or a low-rank GP prior, respectively. Since the subset posterior computations are performed in parallel across  $k$  subsets, the computational complexities for obtaining  $B$  post burn-in subset posterior samples from  $k$  subsets are  $O(km^3) = O(nm^2)$  and  $O(kmr^2) = O(nr^2)$  flops in models based on full-rank and low-rank GP priors, respectively.

The combination step of subset posteriors using the DISK framework outlined below is more widely applicable compared to other divide-and-conquer type approaches because it does not rely on any model- or data-specific assumptions, such as independence, except that every subset posterior distribution has a density with respect to the Lebesgue measure and has finite second moments.

### 3.3 Third step: combination of subset posterior distributions

#### 3.3.1 Wasserstein distance and Wasserstein barycenter

The combination step relies on the Wasserstein barycenter, so we provide some background on this topic. Let  $(\Theta, \rho)$  be a complete separable metric space and  $\mathcal{P}(\Theta)$  be the space of all probability measures on  $\Theta$ . The Wasserstein space of order 2 is a set of probability distributions defined as

$$\mathcal{P}_2(\Theta) = \left\{ \mu \in \mathcal{P}(\Theta) : \int_{\Theta} \rho^2(\theta, \theta_0) \mu(d\theta) < \infty \right\}, \quad (12)$$

where  $\theta_0 \in \Theta$  is arbitrary and  $\mathcal{P}_2(\Theta)$  does not depend on the choice of  $\theta_0$ . The Wasserstein distance of order 2, denoted as  $W_2$ , metrizes  $\mathcal{P}_2(\Theta)$ . Let  $\mu, \nu$  be two probability measures in  $\mathcal{P}_2(\Theta)$  and  $\Pi(\mu, \nu)$  be the set of all probability measures on  $\Theta \times \Theta$  with marginals  $\mu$  and  $\nu$ , then  $W_2$  distance between  $\mu$  and  $\nu$  is defined as

$$W_2(\mu, \nu) = \left( \inf_{\pi \in \Pi(\mu, \nu)} \int_{\Theta \times \Theta} \rho^2(x, y) d\pi(x, y) \right)^{\frac{1}{2}}. \quad (13)$$

Let  $\nu_1, \dots, \nu_k \in \mathcal{P}_2(\Theta)$ , then the Wasserstein barycenter of  $\nu_1, \dots, \nu_k$  is defined as

$$\bar{\nu} = \operatorname{argmin}_{\nu \in \mathcal{P}_2(\Theta)} \sum_{j=1}^k \frac{1}{k} W_2^2(\nu, \nu_j). \quad (14)$$

It is known that  $\bar{\nu} \in \mathcal{P}_2(\Theta)$  is the unique solution of a linear program [1].

If  $\nu_1, \dots, \nu_k$  in (14) represent the  $k$  subset posterior distributions, then Wasserstein barycenter  $\bar{\nu}$  provides a general notion of obtaining the mean of  $k$  subset posterior distributions. If the  $k$  subset posteriors are combined using  $\bar{\nu}$ , then  $\bar{\nu}$  has finite second moments, conditions on the full data, and does not rely on model-specific or data-specific assumptions. If  $\nu_1, \dots, \nu_k$  are analytically intractable but MCMC samples are available from them, then an empirical approximation of the Wasserstein barycenter can be estimated by solving a sparse linear program or by averaging empirical subset posterior quantiles [14, 9, 67, 44, 69].

### 3.3.2 Combination scheme

In the DISK framework, we combine the collection of posterior samples from the  $k$  subset posterior distributions for  $\beta$ ,  $\alpha$ ,  $\mathbf{w}^*$ , and  $\mathbf{y}^*$  through their respective Wasserstein barycenters. Our combination scheme relies on the following key result. If  $\theta$  is a one-dimensional functional of the full data posterior distribution and the  $j$ th subset posterior distribution for  $\theta$  is denoted by  $\nu_j$ , then the  $q$ th quantile of the Wasserstein barycenter for  $\theta$ , denoted as  $\bar{\nu}$ , is estimated from the collection of  $k$  subset posterior samples as

$$\hat{\bar{\nu}}^q = \frac{1}{k} \sum_{j=1}^k \hat{\nu}_j^q, \quad q = \xi, 2\xi, \dots, 1 - \xi, \quad (15)$$

where  $\xi$  is the grid-size of the quantiles,  $\hat{\nu}_j^q$  is the estimate of  $q$ th quantile of  $\nu_j$  obtained using MCMC samples from  $\nu_j$ , and  $\hat{\bar{\nu}}^q$  is the estimate of the  $q$ th quantile of  $\bar{\nu}$  [44].

The post burn-in samples from the  $k$  subset posterior distributions are combined using (15). Let  $\{\beta_{j(b)}\}_{b=1}^B$ ,  $\{\alpha_{j(b)}\}_{b=1}^B$ ,  $\{\mathbf{w}_{j(b)}^*\}_{b=1}^B$ ,  $\{\mathbf{y}_{j(b)}^*\}_{b=1}^B$  ( $j = 1, \dots, k$ ) be the collection of  $B$  post burn-in MCMC samples from the  $k$  subsets;  $\beta_{ji(b)}$  and  $\alpha_{ji'(b)}$  be the  $b$ th post burn-in MCMC samples for the  $i$ th and  $i'$ th marginals of  $\beta$  and  $\alpha$  from their  $j$ th subset posteriors, where  $i = 1, \dots, p$ ,  $i' = 1, \dots, s$ ,  $p$  is the dimension of  $\beta$ , and  $s$  is the dimension of  $\alpha$ . If  $\bar{\beta}$ ,  $\bar{\alpha}$ ,  $\bar{\mathbf{w}}^*$ , and  $\bar{\mathbf{y}}^*$  represent the random variables that follow the DISK posterior distributions for  $\beta$ ,  $\alpha$ ,  $\mathbf{w}^*$ , and  $\mathbf{y}^*$ , then MCMC-based estimates of the DISK posterior are obtained through their quantile estimates as follows:

1. Use (15) to estimate the  $q$ th quantiles of the  $i$ th and  $i'$ th marginals of the DISK posteriors for  $\beta$  and  $\alpha$ , respectively, as

$$\hat{\bar{\beta}}_i^q = \frac{1}{k} \sum_{j=1}^k \hat{\beta}_{ji}^q, \quad i = 1, \dots, p, \quad \hat{\bar{\alpha}}_{i'}^q = \frac{1}{k} \sum_{j=1}^k \hat{\alpha}_{ji'}^q, \quad i' = 1, \dots, s, \quad (16)$$

where  $\hat{\beta}_{ji}^q$  and  $\hat{\alpha}_{ji'}^q$  are the estimates of  $q$ th quantiles of  $i$ th and  $i'$ th marginals of  $j$ th subset posterior distributions for  $\beta$  and  $\alpha$  obtained from  $\{\beta_{j(b)}\}_{b=1}^B$  and  $\{\alpha_{j(b)}\}_{b=1}^B$ .

2. Use (15) to estimate the pointwise  $q$ th quantiles of  $\bar{w}(\mathbf{s}_i^*)$  and  $\bar{y}(\mathbf{s}_i^*)$  as

$$\hat{\bar{w}}^q(\mathbf{s}_i^*) = \frac{1}{k} \sum_{j=1}^k \hat{w}_j^q(\mathbf{s}_i^*), \quad \hat{\bar{y}}^q(\mathbf{s}_i^*) = \frac{1}{k} \sum_{j=1}^k \hat{y}_j^q(\mathbf{s}_i^*), \quad i = 1, \dots, l, \quad (17)$$

where  $\hat{w}_j^q(\mathbf{s}_i^*)$  and  $\hat{y}_j^q(\mathbf{s}_i^*)$  are the estimates of  $q$ th quantiles of  $w(\mathbf{s}_i^*)$  and  $y(\mathbf{s}_i^*)$  of the  $j$ th subset posterior distributions for  $w(\mathbf{s}_i^*)$  and  $y(\mathbf{s}_i^*)$  obtained from  $\{\mathbf{w}_{j(b)}^*\}_{b=1}^B$  and  $\{\mathbf{y}_{j(b)}^*\}_{b=1}^B$ .

A key feature of the DISK combination scheme is that given the subset posterior samples, the combination step is agnostic to the choice of a model. Specifically, (15) remains the same for models based on a full-rank prior or a low-rank GP prior, such as MPP, given MCMC samples from the  $k$  subset posterior distributions. Since the averaging over  $k$  subsets takes  $O(k)$  flops and  $k < n$ ,

the total time for computing the empirical quantile estimates of the DISK posterior in inference or prediction requires  $O(k) + O(m^3)$  and  $O(k) + O(nm^2)$  flops in models based on full-rank and low-rank GP priors. Assuming that we have abundant computational resources,  $k$  is chosen large enough so that  $O(m^3)$  computations are feasible. This would enable applications of the DISK framework in models based on both full-rank and low-rank GP priors in massive  $n$  settings.

### 3.4 Illustrative example: linear regression

We develop intuitions behind the DISK posterior in this section by studying its theoretical properties in multivariate linear regression. The spatial linear model in (1) reduces to a linear regression model with error variance 1 if  $\epsilon(\mathbf{s})$  follows  $N(0, 1)$  and there is no spatial effect; that is,  $w(\mathbf{s}) = 0$  for every  $\mathbf{s} \in \mathcal{D}$ . A flat prior on  $\beta$  implies that the “full data” posterior distribution of  $\beta$  given  $\mathbf{y}$ , denoted as  $\Pi_n$ , has density  $N\{\hat{\beta}, (\mathbf{X}^T \mathbf{X})^{-1}\}$ , where  $\hat{\beta} = (\mathbf{X}^T \mathbf{X})^{-1} \mathbf{X}^T \mathbf{y}$ . Using notations similar to the earlier sections, the  $j$ th subset posterior distribution has density  $N\{\hat{\beta}_j, k^{-1}(\mathbf{X}_j^T \mathbf{X}_j)^{-1}\}$ , where  $\hat{\beta}_j = (\mathbf{X}_j^T \mathbf{X}_j)^{-1} \mathbf{X}_j^T \mathbf{y}_j$  ( $j = 1, \dots, k$ ) and the factor of  $k^{-1}$  in the posterior covariance matrix comes from stochastic approximation. The Wasserstein barycenter of the  $k$  subset posterior distributions, denoted as  $\bar{\Pi}_n$ , is Gaussian with density  $N(\bar{\mathbf{m}}, \bar{\mathbf{V}})$ , where

$$\bar{\mathbf{m}} = \frac{1}{k} \sum_{j=1}^k \hat{\beta}_j \text{ and } \bar{\mathbf{V}} \text{ is such that } \frac{1}{k} \sum_{j=1}^k \left\{ \bar{\mathbf{V}}^{1/2} k^{-1} (\mathbf{X}_j^T \mathbf{X}_j)^{-1} \bar{\mathbf{V}}^{1/2} \right\}^{1/2} = \bar{\mathbf{V}}; \quad (18)$$

see Section 6.3 in [1]. The DISK framework replaces  $N\{\hat{\beta}, (\mathbf{X}^T \mathbf{X})^{-1}\}$  with  $N(\bar{\mathbf{m}}, \bar{\mathbf{V}})$  for inference and predictions in massive data settings.

The covariance matrix  $\bar{\mathbf{V}}$  in (18) is estimated via fixed point iterations; however,  $\bar{\mathbf{V}}$  is analytically tractable when  $\mathbf{X}_1, \dots, \mathbf{X}_k$  have identical left and right singular vectors [2]. If  $\mathbf{U}$  and  $\mathbf{V}$  are  $m \times p$  and  $p \times p$  orthogonal matrices and  $\mathbf{D}_j = \text{diag}(d_{j1}, \dots, d_{jp})$  is a  $p \times p$  diagonal matrix containing singular values of  $\mathbf{X}_j$ , then  $\mathbf{X}_j = \mathbf{U} \mathbf{D}_j \mathbf{V}^T$ ,  $\mathbf{X}_j^T \mathbf{X}_j = \mathbf{V} \mathbf{D}_j^2 \mathbf{V}^T$ , and  $\mathbf{X}^T \mathbf{X} = \mathbf{V} (\sum_{j=1}^k \mathbf{D}_j^2) \mathbf{V}^T$ . The mean vector and covariance matrix of  $\bar{\Pi}_n$  reduce to  $\bar{\mathbf{m}} = \frac{1}{k} \sum_{j=1}^k \mathbf{V} \mathbf{D}_j^{-1} \mathbf{U}^T \mathbf{y}_j$  and  $\bar{\mathbf{V}} = \mathbf{V} \left( \frac{1}{k^{3/2}} \sum_{j=1}^k \mathbf{D}_j^{-1} \right)^2 \mathbf{V}^T$ . Let  $\beta_0$  be the true value of  $\beta$  and  $\bar{\beta}$ ,  $\beta$  be the random variables with distributions  $\bar{\Pi}$ ,  $\Pi_n$ . Assume that  $c_D \sqrt{m} \leq d_{jr}$  for some universal positive constant  $c_D$  and for  $j = 1, \dots, k$ , and  $r = 1, \dots, p$ , then the Bayes  $L_2$ -risk of the DISK posterior in estimating  $\beta_0$  is

$$\mathbb{E}_{\beta_0} \|\bar{\beta} - \beta_0\|_2^2 = \mathbb{E}_{\beta_0} \{ \mathbb{E} (\|\bar{\beta} - \beta_0\|_2^2 \mid \mathbf{y}) \} \leq 2pc_D^{-2} n^{-1} = O(\mathbb{E}_{\beta_0} \|\beta - \beta_0\|_2^2),$$

where  $p$  is fixed,  $\|\cdot\|_2$  is the Euclidean norm, and  $\mathbb{E}_{\beta_0}$  represents expectation with respect to the density of  $\mathbf{y}$  obtained by fixing  $\beta = \beta_0$  in (1). This shows that the Bayes  $L_2$ -risk of the DISK posterior in estimating  $\beta_0$  is upper bounded by the Bayes  $L_2$ -risk of full data posterior distribution.

A result like the one above is crucial in developing intuition on the DISK posterior as an alternative to the full data posterior and are generally difficult to come by in the literature for models presented in Section 2. In the next two sections, we develop theoretical guarantees for the

DISK posterior as an alternative to the full posterior in estimating the residual spatial surface.

### 3.5 Bayes $L_2$ -risk of DISK: General convergence rates

Consider a special case when  $w(\cdot) = 0$  in (1). The regression model reduces to a finite dimensional model with parameters  $\mathbf{\Omega} = \{\boldsymbol{\beta}, \boldsymbol{\alpha}\}$  and the DISK posterior reduces to the recently developed WASP method [68]. If  $\mathbf{\Omega}_0$  is the true value of  $\mathbf{\Omega}$ , then it is known that when the data are independent, WASP converges in probability to a Dirac measure centered at  $\mathbf{\Omega}_0$  or to the full data posterior distribution of  $\mathbf{\Omega}$  at a near optimal rate, under certain assumptions as  $n, m \rightarrow \infty$  [68, 44]; however, in models based on spatial process, inference on the infinite dimensional true residual spatial surface, denoted as  $w_0(\cdot)$ , is of primary importance and no formal results are available in the regard. A notable exception is [72], which shows that combination using Wasserstein barycenter has optimal Bayes risk and adapts to the smoothness of  $w_0(\cdot)$  in the Gaussian white noise model. This model is a special case of (1) with additional smoothness assumptions on  $w_0(\cdot)$ .

We focus on providing theoretical guarantees for the DISK posterior distribution for estimating  $w_0(\cdot)$  using the spatial regression model in (1) with a GP prior on  $w(\cdot)$ , including the low-rank GP prior such as MPP, as  $n, m \rightarrow \infty$ . Recall that  $\mathcal{S}^*$  is the set of  $l$  reference locations in  $\mathcal{D}$  and  $\mathcal{S}^* \cap \mathcal{S} = \emptyset$ . Let  $\mathbf{w}_0^* = \{w_0(\mathbf{s}_1^*), \dots, w_0(\mathbf{s}_l^*)\}^T$  be the true residual spatial surface generating the data at the locations in  $\mathcal{S}^*$  and  $\mathbf{w}^* = \{w(\mathbf{s}_1^*), \dots, w(\mathbf{s}_l^*)\}^T$  be the realization of GP  $w(\cdot)$  at the locations in  $\mathcal{S}^*$ . Following the standard theoretical setup in [73], we assume that  $\boldsymbol{\beta} = \mathbf{0}$ ,  $\boldsymbol{\alpha}$  is known, and  $\mathbf{D}(\boldsymbol{\alpha}) = \tau_0^2 \mathbf{I}$ , where  $\tau_0^2$  is the known non-spatial error variance, so that (1) reduces to

$$y(\mathbf{s}_i) = w(\mathbf{s}_i) + \epsilon(\mathbf{s}_i), \quad \epsilon(\mathbf{s}_i) \sim N(0, \tau_0^2), \quad i = 1, \dots, n, \quad w(\cdot) \sim \text{GP}\{0, C_{\boldsymbol{\alpha}}(\cdot, \cdot)\}. \quad (19)$$

This setup subsumes the low-rank GP priors, hence MPP, as MPP is a GP with covariance function  $\tilde{C}_{\boldsymbol{\alpha}}(\cdot, \cdot)$  in (5). We also assume that the data are generated using  $y(\mathbf{s}) = w_0(\mathbf{s}) + \epsilon(\mathbf{s})$ ,  $\mathbf{s} \in \mathcal{D}$ .

Adapting our discussing in Section 3.2 for the models in (6) to the one in (19), we have that  $\mathbf{y}_j$  given  $\mathbf{w}_j$  follows the Gaussian distribution with density  $N(\mathbf{w}_j, k^{-1} \tau_0^2 \mathbf{I})$  after stochastic approximation as in (11) and the GP prior on  $w(\cdot)$  implies that after integrating over  $\mathbf{w}_j$

$$\mathbf{y}_j \mid \mathbf{w}_j^* \sim N(\mathbf{A}_j \mathbf{w}_j^*, \boldsymbol{\Sigma}_j), \quad \mathbf{A}_j = \mathbf{C}_{*j}^T \mathbf{C}_{*,*}^{-1}, \quad \boldsymbol{\Sigma}_j = k^{-1} \tau_0^2 \mathbf{I} + \mathbf{C}_{j,j} - \mathbf{C}_{*j}^T \mathbf{C}_{*,*}^{-1} \mathbf{C}_{*j}, \quad (20)$$

where  $\mathbf{C}_{*,*}$ ,  $\mathbf{C}_{j,j}$ , and  $\mathbf{C}_{*j}$  are defined in (11). Let  $\mathbf{A}$  and  $\boldsymbol{\Sigma}$  represent the full data versions of  $\mathbf{A}_j$  and  $\boldsymbol{\Sigma}_j$  in (20). For any  $\mathbf{b} \in \mathbb{R}^l$ , we define two norms

$$\|\mathbf{b}\|_{\mathcal{S}_j} = \left( \frac{1}{m} \mathbf{b}^T \mathbf{A}_j^T \boldsymbol{\Sigma}_j^{-1} \mathbf{A}_j \mathbf{b} \right)^{1/2}, \quad \|\mathbf{b}\|_{\mathcal{S}} = \left( \frac{1}{n} \mathbf{b}^T \mathbf{A}^T \boldsymbol{\Sigma}^{-1} \mathbf{A} \mathbf{b} \right)^{1/2}. \quad (21)$$

Equivalently, for a generic function  $\tilde{\mathbf{b}}$  defined on the domain  $\mathcal{D}$ , if  $\mathbf{b}$  in (21) is the functional evaluation of  $\tilde{\mathbf{b}}$  at the testing locations  $\mathcal{S}^*$ , then  $\|\cdot\|_{\mathcal{S}_j}$  and  $\|\cdot\|_{\mathcal{S}}$  defined in (21) can be viewed as two Banach norms on the space of functions with the domain  $\mathcal{D}$ .

Based on the definitions and notation introduced previously, we make the following five assumptions for deriving the general convergence rates of the DISK posterior:

- A.1 (Compact domain) The spatial domain  $\mathcal{D}$  is a compact space in  $\|\cdot\|_2$  metric.
- A.2 (Norm equivalence) The partitions  $\mathcal{S}_1, \dots, \mathcal{S}_k$  of  $\mathcal{S}$  are such that there exist universal positive constants  $H_l < 1 < H_u$  independent of  $j$  such that  $H_l \|\cdot\|_{\mathcal{S}} \leq \|\cdot\|_{\mathcal{S}_j} \leq H_u \|\cdot\|_{\mathcal{S}}$  for  $j = 1, \dots, k$ .
- A.3 (Metric entropy) Suppose that  $\epsilon_m$  is a positive sequence that satisfies (i)  $\sqrt{m}\epsilon_m \geq 1$  for all  $m \geq 1$ ; (ii)  $\epsilon_m \rightarrow 0$  as  $m \rightarrow \infty$ ; (iii) with a slight abuse of notations, for every  $r > 1$ , there is a set  $\mathcal{F}_r$  such that for all  $m \geq 1$ ,  $D(\epsilon_m, \mathcal{F}_r, \|\cdot\|_{\mathcal{S}}) \leq e^{m\epsilon_m^2 H_l^2 r^2}$  and  $\Pi(\mathcal{F}_r) \geq 1 - e^{-2m\epsilon_m^2 r^2}$ , where  $D(\epsilon, \mathcal{F}_r, \|\cdot\|_{\mathcal{S}})$  is the minimum number of  $\|\cdot\|_{\mathcal{S}}$ -balls of radius  $\epsilon$  that cover  $\mathcal{F}_r$ .
- A.4 (Prior thickness) For the  $\epsilon_m$  sequence in Assumption A.3 and for all  $m \geq 1$ , the prior assigns positive mass to any small neighborhood around  $\mathbf{w}_0^*$ ,  $\Pi(w : \|\mathbf{w}^* - \mathbf{w}_0^*\|_{\mathcal{S}} \leq \epsilon_m) \geq e^{-mH_u^2 \epsilon_m^2}$ .
- A.5 The metrics  $\|\cdot\|_2^2$  and  $\|\cdot\|_{\mathcal{S}}^2$  are equivalent in that  $C_l \|\cdot\|_{\mathcal{S}}^2 \leq \|\cdot\|_2^2 \leq C_u \|\cdot\|_{\mathcal{S}}^2$  for some positive universal constants  $C_l$  and  $C_u$ .

Assumption A.1 is common to all models based on GP priors. Assumption A.2 specifies a technical condition on the partitioning scheme so that the realizations of the GP observed in the  $j$ th subset are similar to those in the full data, where such similarity is described in terms of the norms  $\|\cdot\|_{\mathcal{S}_j}$  and  $\|\cdot\|_{\mathcal{S}}$ . Assumption A.3 regulates the complexity of the sequence of sets  $\mathcal{F}_r$  in terms of  $\|\cdot\|_{\mathcal{S}}$ -metric entropy and specifies a condition on the probability assigned by GP prior to  $\mathcal{F}_r$ , ensuring that the prior probability of  $\mathcal{F}_r$  under the Gaussian measure induced by the GP prior increases with increasing  $\|\cdot\|_{\mathcal{S}}$ -metric entropy of  $\mathcal{F}_r$ . The subscript  $r$  here should not be confused with the number of knots in MPP. Assumption A.4 says that the GP prior assigns positive probability to arbitrarily small  $\|\cdot\|_{\mathcal{S}}$ -neighborhood around the true parameter  $\mathbf{w}_0^*$ . Assumption A.5 is a technical condition that is used in upper bounding the Bayes  $L_2$ -risk of Wasserstein barycenter in the estimation of  $\mathbf{w}_0^*$  if we have Bayes  $L_2$ -risk upper bounds for the subset posterior distributions.

We define the Bayes  $L_2$ -risk in the estimation of  $\mathbf{w}_0^*$  using the full data posterior as

$$\mathbb{E}_{0|\mathcal{S}, \mathcal{S}^*} \left\{ \mathbb{E} (\|\mathbf{w}^* - \mathbf{w}_0^*\|_2^2 \mid \mathbf{y}) \right\} = \mathbb{E}_{0|\mathcal{S}, \mathcal{S}^*} \left\{ \int \|\mathbf{w}^* - \mathbf{w}_0^*\|_2^2 d\Pi_n(w \mid \mathbf{y}) \right\}, \quad (22)$$

where  $\mathbb{E}_{0|\mathcal{S}, \mathcal{S}^*}$  is the expectation under the true space varying function  $w_0$  with respect to density of  $\mathbf{y}$  conditional on  $\mathcal{S}, \mathcal{S}^*$  in (19). The decay rate of the risk in (22) is known under assumptions that are similar to A.1, A.3, A.4 and are obtained by replacing  $m$  by  $n$  [73].

We present two theorems below that describe the asymptotic properties of the DISK posterior measured in this Bayes  $L_2$ -risk, for the spatial model specified in (19) with a prior  $\Pi$  on  $w(\cdot)$  and that satisfies assumptions A.1–A.5. The first theorem describes the Bayes  $L_2$ -risk of each subset posterior distributions in our case and is based on Proposition 11 in [73].

**Theorem 3.1** *If Assumptions A.1–A.5 hold for the  $j$ th subset posterior  $\Pi_m(\cdot \mid \mathbf{y}_j)$  with  $j = 1, \dots, k$ , then there exists a positive constant  $c(H_l)$  that only depends on  $H_l$ , such that as  $m \rightarrow \infty$ ,*

$$\mathbb{E}_{0|\mathcal{S}_j, \mathcal{S}^*} \{ \mathbb{E}(\|\mathbf{w}^* - \mathbf{w}_0^*\|_2^2 \mid \mathbf{y}_j) \} \leq C_u c(H_l) \epsilon_m^2,$$

where  $\mathbb{E}_{0|\mathcal{S}_j, \mathcal{S}^*}$  is the expectation under the true space varying function  $w_0$  with respect to the subset  $\mathbf{y}_j$  of size  $m$  conditional on  $\mathcal{S}_j, \mathcal{S}^*$ .

The proof of this theorem is in the supplementary material, along with other proofs in this section.

Theorem 3.1 holds for any  $\epsilon_m$  sequence that satisfies Assumptions A.3 and A.4. Explicit expressions for  $\epsilon_m$  are available if  $w_0(\cdot)$  and  $\mathcal{F}_r$  are restricted to class of functions with known regularity and  $\Pi$  is a GP prior with the Matérn or squared exponential covariance kernels. For any  $a, b > 0$ , let  $C^a[0, 1]^d$  and  $H^b[0, 1]^d$  be the Hölder and Sobolev spaces of functions on  $[0, 1]^d$  with regularity index  $a$  and  $b$ , respectively. Define  $\mathcal{D} = [0, 1]^d$  and  $C_\alpha$  to be the Matérn kernel with  $C_\alpha(\mathbf{s}, \mathbf{s}') = \frac{\sigma_0^2}{2^{\nu_0-1}\Gamma(\nu_0)} (\|\mathbf{s} - \mathbf{s}'\|_2 \phi_0)^{\nu_0} \mathcal{K}_{\nu_0}(\|\mathbf{s} - \mathbf{s}'\|_2 \phi_0)$  for  $\mathbf{s}, \mathbf{s}' \in \mathcal{D}$ , where  $\mathcal{K}_{\nu_0}$  is a modified Bessel function of the second kind with order,  $\nu_0$ , that controls the process smoothness,  $\phi_0$  is a length-scale parameter that controls the decay in spatial correlation and  $\Gamma$  is the Gamma function. If  $w_0 \in C^{b^*}[0, 1]^d \cap H^{b^*}[0, 1]^d$  and  $\mathcal{F}_r \subset C^{b^*}[0, 1]^d \cap H^{b^*}[0, 1]^d$  for  $r > 1$ , then  $\epsilon_m = m^{-\min(\nu_0, b^*)/(2\nu_0+d)}$  provided  $b^* > 0, \min(\nu_0, b^*) > d/2$ . Similarly, if  $\mathcal{D} = [0, 1]^d$ ,  $C_\alpha$  is the squared exponential kernel with  $C_\alpha(\mathbf{s}, \mathbf{s}') = \sigma_0^2 e^{-\phi_0 \|\mathbf{s} - \mathbf{s}'\|_2^2}$ , and  $w_0$  is an analytic function on  $\mathcal{D}$ , then  $\epsilon_m = (\log m)^{1/2}/\sqrt{m}$ ; see Theorems 5 and 10 in [73]. The squared exponential kernel is not relevant to spatial statistics, but we provide this additional result for a more general audience, especially in machine learning.

The second theorem below provides an upper bound on the Bayes  $L_2$ -risk of the DISK posterior,  $\bar{\Pi}(\cdot \mid \mathbf{y}_1, \dots, \mathbf{y}_k)$ , using the upper bounds on the  $k$  subset posterior distributions.

**Theorem 3.2** *If Assumptions A.1–A.5 hold for all subset posteriors  $\Pi_m(\cdot \mid \mathbf{y}_j)$  with  $j = 1, \dots, k$ , then as  $m \rightarrow \infty$ ,*

$$\mathbb{E}_{0|\mathcal{S}, \mathcal{S}^*} \{ \mathbb{E}(\|\mathbf{w}^* - \mathbf{w}_0^*\|_2^2 \mid \mathbf{y}_1, \dots, \mathbf{y}_k) \} = \mathbb{E}_{0|\mathcal{S}, \mathcal{S}^*} \left\{ \int \|\mathbf{w}^* - \mathbf{w}_0^*\|_2^2 d\bar{\Pi}(w \mid \mathbf{y}_1, \dots, \mathbf{y}_k) \right\} \leq C_u^2 c(H_l) \epsilon_m^2,$$

where  $\mathbb{E}_{0|\mathcal{S}, \mathcal{S}^*}$  is the expectation under the true space varying function  $w_0$  with respect to the full dataset of size  $n$  conditional on  $\mathcal{S}, \mathcal{S}^*$ .

The  $\epsilon_m$  sequence here is the same as in Theorem 3.1. If  $k \approx \log^a n$  for some  $a > 0$ , then  $m \approx n \log^{-a} n$ . With this choice of  $(m, k)$ , our previous discussion implies that  $\epsilon_m = n^{-c^*} \log^{ac^*} n$  for the Matérn, where  $c^* = \frac{\min(\nu_0, b^*)}{2a^*+d}$ , and  $\epsilon_m = (\log n)^{a/2+1/2}/\sqrt{n}$  for the squared exponential kernels. Both these rates are minimax optimal up to log factors in the estimation of  $w_0$ ; see [73] for proofs.

In applications, we are also interested in estimating functions of  $\mathbf{w}_0^*$ . An attractive property of the DISK posterior is that its theoretical guarantees extend to a large class of functions of  $\mathbf{w}^*$ . Let  $f$  be any function that maps  $\mathbf{w}^*$  to  $f(\mathbf{w}^*)$  and that  $f$  is bounded almost linearly by the  $\|\cdot\|_2$  metric. Then, we have the following corollary from a direct application of Lemma 8.5 in [8].

**Corollary 3.3** *Suppose that Assumptions A.1–A.5 hold for all subset posteriors  $\Pi_m(\cdot \mid \mathbf{y}_j)$  with  $j = 1, \dots, k$ . Let  $f$  be a continuous function that maps  $\mathbb{R}^l$  to  $\mathbb{R}^{l'}$  and satisfies  $\|f(\mathbf{w}^*)\|_2^2 \leq C_f(1 + \|\mathbf{w}^* - \mathbf{w}_0^*\|_2^2)$  for any  $\mathbf{w}^* \in \mathbb{R}^l$ , where  $C_f > 0$  is a fixed constant. Let  $\overline{f_{\#}\Pi}(\cdot \mid \mathbf{y}_1, \dots, \mathbf{y}_k)$  represent the DISK posterior of  $f(\mathbf{w}^*)$ , then as  $m \rightarrow \infty$ ,*

$$\int \|\mathbf{f} - \mathbf{f}(\mathbf{w}_0^*)\|_2^2 d\overline{f_{\#}\Pi}(\mathbf{f} \mid \mathbf{y}_1, \dots, \mathbf{y}_k) = O_p(\epsilon_m^2),$$

where  $O_p$  is in the probability measure under the true space varying function  $w_0$  with respect to the full dataset of size  $n$  conditional on  $\mathcal{S}, \mathcal{S}^*$ .

### 3.6 Bayes $L_2$ -risk of DISK: Bias-variance tradeoff and the choice of $k$

While Section 3.5 describes asymptotic optimality results for the DISK posterior when  $n, m \rightarrow \infty$ , a common problem in applications is the choice of  $k$  for a large  $n$ . The risk for the DISK posterior derived in Theorem 3.2 and Corollary 3.3 is applicable to any prior distribution that satisfies Assumptions A.3 and A.4. If  $k \approx \log^a n$  for some  $a > 0$ , then the DISK posterior gives near minimax optimal performance in the estimation of  $w_0$  for the two covariance kernels. In practice, however, we want to choose a  $k$  that is much larger than  $\log^a n$  due to the abundance of computational resources. If the number of subsets  $k$  is very small, then the biases in subset posterior distributions are small due to a large  $m$  but the variance of the DISK posterior is large due to the small  $k$ . In contrast, if  $k$  is very large, then the biases in subset posterior distributions are large due to a small subset size  $m$  but the variance of the DISK posterior can be small due to the large  $k$ . An optimal choice of  $k$  balances the bias-variance tradeoff and minimizes the risk of the DISK posterior.

We introduce some definitions used in stating the results in this section. Let  $\mathbb{P}_{\mathbf{s}}$  be a probability distribution over  $\mathcal{D}$ ,  $L_2(\mathbb{P}_{\mathbf{s}})$  be the  $L_2$  space under  $\mathbb{P}_{\mathbf{s}}$ , the inner product in  $L_2(\mathbb{P}_{\mathbf{s}})$  is defined as  $\langle f, g \rangle_{L_2(\mathbb{P}_{\mathbf{s}})} = \mathbb{E}_{\mathbb{P}_{\mathbf{s}}}(fg)$  for any  $f, g \in L_2(\mathbb{P}_{\mathbf{s}})$ , and  $\{\phi_i(\mathbf{s}) : i = 1, 2, \dots\}$  be an orthonormal basis with respect to  $\mathbb{P}_{\mathbf{s}}$ . Assume that the kernel has the series expansion  $C_{\alpha}(\mathbf{s}, \mathbf{s}') = \sum_{i=1}^{\infty} \mu_i \phi_i(\mathbf{s}) \phi_i(\mathbf{s}')$  with respect to  $\mathbb{P}_{\mathbf{s}}$  for any  $\mathbf{s}, \mathbf{s}' \in \mathcal{D}$ , where  $\mu_1 \geq \mu_2 \geq \dots \geq 0$  are the eigenvalues of  $C_{\alpha}$ . The trace of the kernel  $C_{\alpha}$  is defined as  $\text{tr}(C_{\alpha}) = \sum_{i=1}^{\infty} \mu_i$ . Any  $f \in L_2(\mathbb{P}_{\mathbf{s}})$  has the series expansion  $f(\mathbf{s}) = \sum_{i=1}^{\infty} \theta_i \phi_i(\mathbf{s})$ , where  $\theta_i = \langle f, \phi_i \rangle_{L_2(\mathbb{P}_{\mathbf{s}})}$ . The reproducing kernel Hilbert space (RKHS)  $\mathbb{H}$  attached to  $C_{\alpha}$  is the space of all functions  $f \in L_2(\mathbb{P}_{\mathbf{s}})$  such that the  $\mathbb{H}$ -norm  $\|f\|_{\mathbb{H}} = \sum_{i=1}^{\infty} \theta_i^2 / \mu_i < \infty$ . The RKHS  $\mathbb{H}$  is the completion of the linear space of functions defined as  $\sum_{i=1}^I a_i C_{\alpha}(\mathbf{s}_i, \cdot)$ , where  $I$  is a positive integer,  $\mathbf{s}_i \in \mathcal{D}$ , and  $a_i \in \mathbb{R}$  ( $i = 1, \dots, I$ ); see [74] for greater details.

Simplifying our setup in Section 3.5, we consider a random design scheme with the observed locations  $\mathcal{S} = \{\mathbf{s}_1, \dots, \mathbf{s}_n\}$  and  $\mathcal{S}^* = \{\mathbf{s}^*\}$ , where  $\mathbf{s}_1, \dots, \mathbf{s}_n, \mathbf{s}^*$  are mutually independent and follow  $\mathbb{P}_{\mathbf{s}}$ . The assumptions we impose below are used to derive analytic bounds for the bias and variance terms associated with the Bayes  $L_2$ -risk, and they are stronger than those in Section 3.5.

B.1 (RKHS) The true function  $w_0$  is an element of the RKHS  $\mathbb{H}$  attached to the kernel  $C_{\alpha}$ .

B.2 (Trace class kernel)  $\text{tr}(C_{\alpha}) < \infty$ .

B.3 (Moment condition) There are positive constants  $\rho$  and, with a slight abuse of notation,  $r \geq 2$  such that  $\mathbb{E}_{\mathbb{P}_{\mathbf{s}}} \{\phi_i^{2r}(\mathbf{s})\} \leq \rho^{2r}$  for every  $i = 1, 2, \dots, \infty$ , and  $\text{var} \{\epsilon(\mathbf{s})\} \leq \tau_0^2 < \infty$  for any  $\mathbf{s} \in \mathcal{D}$ .

Assumption B.1 is a stronger assumption than Assumption A.4 in Section 3.5. Assumption B.1 is not required in Section 3.5 because the DISK posterior can learn any continuous  $w_0$  for a large class of GP priors as  $n \rightarrow \infty$ , even if  $w_0 \notin \mathbb{H}$ . In general, the RKHS  $\mathbb{H}$  can be a much smaller space relative to the support of the GP prior, in the sense that the GP prior can assign zero probability to  $\mathbb{H}$  and positive probability to any neighborhood of arbitrary size around any continuous  $w_0$ . While we use Assumption B.1 mainly for technical simplicity in this section, it can be possibly relaxed by considering sieves with increasing Hilbert norms; see for example, Assumption B' and Theorem 2 in Zhang et al. [84]. In Assumption B.2,  $\text{tr}(C_{\alpha})$  measures the size of the covariance kernel and imposes conditions on the regularity of the functions that the DISK posterior can learn. Assumption B.3 controls the error in approximating  $C_{\alpha}(\mathbf{s}, \mathbf{s}')$  by a finite sum, and the superscript  $r$  here should not be confused with the number of knots in MPP or the  $r$  in Assumption A.3. Our results are valid for any error distribution that guarantees  $\text{var} \{\epsilon(\mathbf{s})\} \leq \tau_0^2$  for every  $\mathbf{s} \in \mathcal{D}$ , and it is trivially satisfied in (19).

We examine the Bayes  $L_2$ -risk of the DISK posterior for estimating  $w_0$  in (19). Under the setup of (19), let  $\mathbb{E}_{\mathbf{s}^*}$ ,  $\mathbb{E}_0$ ,  $\mathbb{E}_{\mathcal{S}}$ , and  $\mathbb{E}_{0|\mathcal{S}}$  respectively be the expectations with respect to the distributions of  $\mathbf{s}^*$ ,  $(\mathcal{S}, \mathbf{y})$ ,  $\mathcal{S}$ , and  $\mathbf{y}$  given  $\mathcal{S}$ . If  $\bar{w}(\mathbf{s}^*)$  is a random variable that follows the DISK posterior for estimating  $w_0(\mathbf{s}^*)$ , then  $\bar{w}(\mathbf{s}^*)$  has the density  $N(\bar{m}, \bar{v})$ , where

$$\bar{m} = \frac{1}{k} \sum_{j=1}^k \mathbf{c}_{j,*}^T (\mathbf{C}_{j,j} + \frac{\tau_0^2}{k} \mathbf{I})^{-1} \mathbf{y}_j, \quad \bar{v}^{1/2} = \frac{1}{k} \sum_{j=1}^k v_j^{1/2}, \quad v_j = c_{*,*} - \mathbf{c}_{j,*}^T (\mathbf{C}_{j,j} + \frac{\tau_0^2}{k} \mathbf{I})^{-1} \mathbf{c}_{j,*}, \quad (23)$$

$c_{*,*} = \text{cov}\{w(\mathbf{s}^*), w(\mathbf{s}^*)\}$ , and  $\mathbf{c}_{j,*}^T = [\text{cov}\{w(\mathbf{s}_{j1}), w(\mathbf{s}^*)\}, \dots, \text{cov}\{w(\mathbf{s}_{jm}), w(\mathbf{s}^*)\}]$ . The Bayes  $L_2$ -risk of the DISK posterior in estimating  $w_0$  is  $\mathbb{E}_0 [\mathbb{E}_{\mathbf{s}^*} \{\bar{w}(\mathbf{s}^*) - w_0(\mathbf{s}^*)\}^2]$ , and it is decomposed into squared bias, variance of mean of the DISK posterior, and variance of the DISK posterior terms as

$$\begin{aligned} \text{bias}^2 &= \mathbb{E}_{\mathbf{s}^*} \mathbb{E}_{\mathcal{S}} \{\mathbf{c}_*^T (k \mathbf{L} + \tau_0^2 \mathbf{I})^{-1} \mathbf{w}_0 - w_0(\mathbf{s}^*)\}^2, \\ \text{var}_{\text{mean}} &= \tau_0^2 \mathbb{E}_{\mathbf{s}^*} \mathbb{E}_{\mathcal{S}} \{\mathbf{c}_*^T (k \mathbf{L} + \tau_0^2 \mathbf{I})^{-2} \mathbf{c}_*\}, \quad \text{var}_{\text{DISK}} = \mathbb{E}_{\mathbf{s}^*} \mathbb{E}_{\mathcal{S}}(\bar{v}), \end{aligned} \quad (24)$$

where  $\mathbf{c}_*^T = (\mathbf{c}_{1,*}^T, \dots, \mathbf{c}_{k,*}^T)$ ,  $\mathbf{w}_{0j} = \{w_0(\mathbf{s}_{j1}), \dots, w_0(\mathbf{s}_{jk})\}$  ( $j = 1, \dots, k$ ),  $\mathbf{w}_0^T = \{\mathbf{w}_{01}, \dots, \mathbf{w}_{0k}\}$ , and  $\mathbf{L}$  is a block-diagonal matrix with  $\mathbf{C}_{1,1}, \dots, \mathbf{C}_{k,k}$  along the diagonal. The next theorem describes the asymptotic behavior of each of the three terms in (24).

**Theorem 3.4** *If Assumptions B.1–B.3 hold, then*

$$\text{Bayes } L_2 \text{ risk} = \mathbb{E}_{\mathcal{S}} \mathbb{E}_{0|\mathcal{S}} \mathbb{E}_{\mathbf{s}^*} \{\bar{w}(\mathbf{s}_*) - w_0(\mathbf{s}_*)\}^2 = \text{bias}^2 + \text{var}_{\text{mean}} + \text{var}_{\text{DISK}},$$

$$\text{bias}^2 \leq \frac{8\tau_0^2}{n} \|w_0\|_{\mathbb{H}}^2 + \|w_0\|_{\mathbb{H}}^2 \inf_{d \in \mathbb{N}} \left[ \frac{8n}{\tau_0^2} \rho^4 \text{tr}(C_{\alpha}) \text{tr}(C_{\alpha}^d) + \mu_1 \left\{ \frac{Ab(m, d, r) \rho^2 \gamma(\frac{\tau_0^2}{n})}{\sqrt{m}} \right\}^r \right],$$



$$\begin{aligned}
\text{var}_{\text{mean}} &\leq \frac{2n + 4\|w_0\|_{\mathbb{H}}^2}{k} \inf_{d \in \mathbb{N}} \left[ \mu_{d+1} + 12 \frac{n}{\tau_0^2} \rho^4 \text{tr}(C_{\alpha}) \text{tr}(C_{\alpha}^d) + \left\{ \frac{Ab(m, d, r) \rho^2 \gamma(\frac{\tau_0^2}{n})}{\sqrt{m}} \right\}^r \right] + \\
&\quad \frac{12}{k} \frac{\tau_0^2}{n} \|w_0\|_{\mathbb{H}}^2 + 12 \frac{\tau_0^2}{n} \gamma\left(\frac{\tau_0^2}{n}\right), \\
\text{var}_{\text{DISK}} &\leq 2 \frac{\tau_0^2}{n} \gamma\left(\frac{\tau_0^2}{n}\right) + \inf_{d \in \mathbb{N}} \left[ \text{tr}(C_{\alpha}^d) + \text{tr}(C_{\alpha}) \left\{ \frac{Ab(m, d, r) \rho^2 \gamma(\frac{\tau_0^2}{n})}{\sqrt{m}} \right\}^r \right], \tag{25}
\end{aligned}$$

where  $\mathbb{N}$  is the set of all positive integers,  $A$  is a positive constant,

$$\begin{aligned}
b(m, d, r) &= \max \left( \sqrt{\max(r, \log d)}, \frac{\max(r, \log d)}{m^{1/2-1/r}} \right), \\
\gamma(a) &= \sum_{i=1}^{\infty} \frac{\mu_i}{\mu_i + a} \text{ for any } a > 0, \quad \text{tr}(C_{\alpha}^d) = \sum_{i=d+1}^{\infty} \mu_i.
\end{aligned}$$

Theorem 3.4 is based on arguments similar to Theorem 1 in Zhang et al. [84], which has derived the risk bounds for the frequentist divide-and-conquer estimator in kernel ridge regression. We however are considering the divide-and-conquer scheme in the Bayesian context, so our risk bound in Theorem 3.4 involves two variance terms, including the DISK posterior variance term  $\text{var}_{\text{DISK}}$ , which has not been considered by Zhang et al. [84] and other divide-and-conquer literature before due to their interests in frequentist point estimation of  $w_0$ . The function  $\gamma(a)$  measures the effective dimensionality of  $C_{\alpha}$  with respect to  $L_2(\mathbb{P}_{\mathbf{s}})$  [83]. The function  $\text{tr}(C_{\alpha}^d)$  describes the tail behavior of the eigenvalues of  $C_{\alpha}$  [84]. The upper bound for  $\text{bias}^2$  and  $\text{var}_{\text{mean}}$  are the DISK analogues of the upper bounds in Lemma 6 and Lemma 7, respectively, of Zhang et al. [84].

From the risk bounds in Theorem 3.4, one can see that the first and second terms in the upper bound for  $\text{var}_{\text{DISK}}$  are dominated by the last and second terms in the upper bounds for  $\text{var}_{\text{mean}}$  and  $\text{bias}^2$ , respectively. Therefore, if we use the DISK posterior mean or a random draw from the DISK posterior to estimate  $w_0$ , we will observe the bias-variance tradeoff phenomenon similar to the one described in [84]: as  $k$  increases, the squared bias of the estimate increases, while the variation between the subset estimates decreases. Theoretically, this implies the existence of an optimal  $k^*$  such that the Bayes  $L_2$ -risk of the DISK posterior decreases for  $k \leq k^*$  and increases for  $k > k^*$ . Our empirical results in Section 4 demonstrate this bias-variance tradeoff.

For three types of commonly used kernels, the next theorem provides conditions on  $k$  such that the Bayes  $L_2$ -risk in (25) is nearly minimax optimal. The covariance kernel  $C_{\alpha}$  is a degenerate kernel of rank  $d^*$  if there is some constant positive integer  $d^*$  such that  $\mu_1 \geq \mu_2 \geq \dots \geq \mu_{d^*} > 0$  and  $\mu_{d^*+1} = \mu_{d^*+2} = \dots = \mu_{\infty} = 0$ . The covariance kernels in subset of regressors approximation [55] and predictive process [6] are degenerate with their ranks equaling the number of selected regressors and knots, respectively. The squared exponential kernel is very popular in machine learning. Its RKHS belongs to the class of RKHSs of kernels with exponentially decaying eigenvalues. Similarly, the class of RKHSs of kernels with polynomially decaying eigenvalues includes the Sobolev spaces with different orders of smoothness and the RKHS of the Matérn kernel. This kernel is most

relevant for spatial applications, but we provide the other two results for a more general audience.

**Theorem 3.5** *If Assumptions B.1–B.3 hold and  $r > 4$  in Assumption B.3, then, as  $n \rightarrow \infty$ ,*

- (i) *if  $C_\alpha$  is a degenerate kernel of rank  $d^*$  and  $k \leq cn^{\frac{r-4}{r-2}}/(\log n)^{\frac{2r}{r-2}}$  for some constant  $c > 0$ , then the  $L_2$ -risk of DISK posterior satisfies  $\mathbb{E}_{\mathbf{s}^*} \mathbb{E}_{\mathcal{S}} \mathbb{E}_{0|\mathcal{S}} \{\bar{w}(\mathbf{s}^*) - w_0(\mathbf{s}^*)\}^2 = O(n^{-1})$ ;*
- (ii) *if  $\mu_i \leq c_{1\mu} \exp(-c_{2\mu} i^2)$  for some constants  $c_{1\mu} > 0, c_{2\mu} > 0$  and all  $i \in \mathbb{N}$ , and for some constant  $c > 0$ ,  $k \leq cn^{\frac{r-4}{r-2}}/(\log n)^{\frac{3r-1}{r-2}}$ , then the  $L_2$ -risk of DISK posterior satisfies  $\mathbb{E}_{\mathbf{s}^*} \mathbb{E}_{\mathcal{S}} \mathbb{E}_{0|\mathcal{S}} \{\bar{w}(\mathbf{s}^*) - w_0(\mathbf{s}^*)\}^2 = O(\sqrt{\log n/n})$ ; and*
- (iii) *if  $\mu_i \leq c_\mu i^{-2\nu}$  for some constants  $c_\mu > 0, \nu > \frac{r-1}{r-4}$  and all  $i \in \mathbb{N}$ , and for some constant  $c > 0$ ,  $k \leq cn^{\frac{(r-4)\nu-(r-1)}{(r-2)\nu}}/(\log n)^{\frac{2r}{r-2}}$ , then the  $L_2$ -risk of DISK posterior satisfies  $\mathbb{E}_{\mathbf{s}^*} \mathbb{E}_{\mathcal{S}} \mathbb{E}_{0|\mathcal{S}} \{\bar{w}(\mathbf{s}^*) - w_0(\mathbf{s}^*)\}^2 = O\left(n^{-\frac{2\nu-1}{2\nu}}\right)$ .*

The rate of decay of the  $L_2$ -risks in (i) and (ii) are known to be minimax optimal [57, 84, 81], whereas the rate of decay of the  $L_2$ -risk in (iii) is slightly larger than the minimax optimal rate by a factor of  $n^{\frac{1}{2\nu(2\nu+1)}}$  [84]. The main advantage of the DISK posterior over its non-Bayesian counterparts is that it achieves optimal performance in the first two cases and a near optimal performance in the third case while being free of tuning parameter selection. In most applications  $\mathcal{D}$  is also compact, so that  $r$  in Assumption B.3 can be taken as infinity. This implies that the upper bounds on  $k$  in (i), (ii), and (iii) reduce to  $k = O(n/\log^2 n)$ ,  $k = O(n/\log^3 n)$ , and  $k = O(n^{\frac{\nu-1}{\nu}}/\log^2 n)$ , respectively.

Theoretical results similar to Theorems 3.4 and 3.5 are well studied in frequentist divide-and-conquer kernel ridge regression, but developing Bayesian analogues of these results remains an active area of research. Cheng and Shang have studied the theoretical properties of divide-and-conquer Bayesian nonparametric regression under various theoretical setups [11, 64, 65]. Recently, Szabo and van Zanten [72] have explored the convergence rate of the  $L_2$ -risk and coverage in the classical Gaussian white noise model. Focusing on the practical issue, we have developed a general method and related sampling algorithms for extending any method for Bayesian nonparametric regression based on GP prior to massive data settings using the divide-and-conquer technique. Theorem 3.4 describes the  $L_2$ -risk of our method, and Theorem 3.5 provides guidance on choosing the number of subsets. Under certain assumptions on  $w_0$ , our theoretical results reduce to those obtained in the previous works; however, none of the previous work focus on developing a computational method that is as widely applicable as DISK and is grounded in Bayesian asymptotic theory.

## 4 Experiments

### 4.1 Simulation setup

We compare DISK with its competitors on synthetic data based on its performance in learning the process parameters, interpolating the unobserved residual spatial surface, and predicting at new locations. This section presents two simulation studies. The first (*Simulation 1*) and second

simulations (*Simulation 2*) represent examples of a moderately large dataset with 12,025 locations and a large dataset with 1,002,025 locations, respectively. In Simulations 1 and 2, we randomly select the data at  $10^4$  and  $10^6$  locations, respectively, for model fitting and the remaining data at 2025 locations for assessing the performance of DISK and its competitors; therefore,  $n = 10^4$  and  $l = 2025$  in Simulation 1 and  $n = 10^6$  and  $l = 2025$  in Simulation 2.

We simulate the data following the scheme described in [30]. Specifically, we set  $\mathcal{D} = [-2, 2] \times [-2, 2] \subset \mathbb{R}^2$  and uniformly sample  $(n+l)$  spatial locations  $\mathbf{s}_i = (s_{i1}, s_{i2})$  in  $\mathcal{D}$  ( $i = 1, \dots, n+l$ ). For any  $s \in [-2, 2]$ , define the function  $f_0(s) = e^{-(s-1)^2} + e^{-0.8(s+1)^2} - 0.05 \sin\{8(s+0.1)\}$ . Assuming  $w_0(\mathbf{s}_i) = -f_0(s_{i1})f_0(s_{i2})$ , the response is simulated at  $(n+l)$  locations as

$$y(\mathbf{s}_i) = \beta_0 + w_0(\mathbf{s}_i) + \epsilon_i, \quad \epsilon_i \sim N(0, \tau_0^2), \quad i = 1, \dots, n+l. \quad (26)$$

The response surface simulated from (26) exhibits complex local behavior, which is challenging to capture using spatial process-based models. For both simulations, the intercept  $\beta_0$  and true error variance  $\tau_0^2$  are set to 1 and 0.01, respectively. The inferential and predictive results for both simulations are based on 10 replications. We compare DISK with a number of Bayesian and non-Bayesian spatial models in both simulations:

1. LatticeKrig [52] using the `LatticeKrig` package in R [56] with 3 number of resolutions [53];
2. nearest neighbor Gaussian process (NNGP) using the `spNNGP` package in R with the number of nearest neighbors (NN) as 5, 15, and 25 [16, 21];
3. full-rank Gaussian process (GP) using the `spBayes` package in R [22] with the full data;
4. modified predictive process (MPP) using the `spBayes` package in R with the full data; and
5. locally approximated Gaussian process (laGP) using the `laGP` package in R with method set to “nn” [30, 29].

All comparisons are performed in R. All five methods produce results in Simulation 1, but the first four methods fail due to numerical issues in Simulation 2. While laGP is not designed for full scale Bayesian inference, it is used as the benchmark for predictive point estimates and associated standard errors in (26) due to its popularity in fitting computer models. Similar to laGP, we obtain predictive point estimates with associated standard errors from the frequentist implementation of LatticeKrig. For the spatial process-based Bayesian models, we employ (1) with only an intercept  $\beta$ , putting a  $N(0, 100)$  prior on  $\beta$ , a GP prior on  $w(\cdot)$ , and  $\text{IG}(2, 0.1)$  prior on  $\tau^2$ , where  $\text{IG}(a, b)$  is the Inverse-Gamma distribution with mean  $a/(b+1)$  and variance  $b/\{(a-1)^2(a-2)\}$  for  $a > 2$ . Motivated by [73], we assume an exponential correlation in the random field given by  $\text{cov}\{w(\mathbf{s}), w(\mathbf{s}')\} = \sigma^2 e^{-\phi \|\mathbf{s} - \mathbf{s}'\|_2}$ ,  $\mathbf{s}, \mathbf{s}' \in \mathcal{D}$  and put  $\text{IG}(2, 2)$  prior on  $\sigma^2$  and a uniform prior on  $\phi$ . The MPP prior on  $w(\cdot)$  is a representative example of a low-rank and non-stationary GP prior. It is defined by setting the rank  $r$  as 200 and 400, respectively, where the  $r$  knots are selected randomly

from the domain  $\mathcal{D}$ . NNGP is chosen as a representative example of the current state-of-the-art Bayesian method for inference and predictions in massive spatial data.

The three-step DISK framework is fitted with the full-rank GP and the low-rank MPP priors using the algorithm outlined in (16) and (17), yielding DISK (GP) and DISK (MPP) procedures, respectively. We use consensus Monte Carlo (CMC; [62]) and semiparametric density product (SDP; [50]) as representative competitors for model-free subset posterior aggregation to highlight the advantages of DISK. Similar to DISK, these two approaches also operate in three steps. First, the data for  $n$  locations are randomly divided into  $k$  subsets. Second, the MPP-based model in (6) is fitted on every subset for CMC and SDP using the `spBayes` package. Unlike DISK, CMC and SDP do not employ stochastic approximation. Third, we use `parallelMCMCcombine` package with the default setting [49] for combining subset posterior samples in CMC and SDP, yielding CMC (MPP) and SDP (MPP) procedures, respectively. SDP (MPP) fails due to numerical issues when the posterior samples for predictions and the surface are combined. Identical priors, covariance functions, ranks, and knots are used for the non-distributed process models and their distributed counterparts for a fair comparison.

All experiments are run on an Oracle Grid Engine cluster with 2.6GHz 16 core compute nodes. The non-distributed methods (LatticeKrig, GP, MPP, NNGP, and laGP) and the distributed methods (CMC, DISK, and SDP) are allotted memory resources of 64GB and 16GB, respectively. Every MCMC sampling algorithm runs for 15,000 iterations, out of which the first 10,000 samples are discarded as burn-in samples and the rest of the chain is thinned by collecting every fifth sample. Convergence of the chains to their stationary distributions is confirmed using trace plots. All the interpolated spatial surfaces are obtained using the `MBA` package in R.

We compare the quality of prediction and estimation of residual spatial surface at  $l = 2025$  predictive locations  $\mathcal{S}^* = \{\mathbf{s}_1^*, \dots, \mathbf{s}_l^*\}$ . If  $w_0(\mathbf{s}_{i'}^*)$  represents the value of the spatial surface at  $\mathbf{s}_{i'}^* \in \mathcal{S}^*$ , then the estimates of bias, variance, and Bayes  $L_2$ -risk in estimating  $w_0(\cdot)$  are defined as

$$\text{bias}^2 = \frac{1}{l} \sum_{i'=1}^l \{\hat{w}(\mathbf{s}_{i'}^*) - w_0(\mathbf{s}_{i'}^*)\}^2, \text{ var} = \frac{1}{l} \sum_{i'=1}^l \text{var}\{w(\mathbf{s}_{i'}^*)\}, L_2\text{-risk} = \text{bias}^2 + \text{var}, \quad (27)$$

where  $\hat{w}(\mathbf{s}_{i'}^*)$  and  $\text{var}\{w(\mathbf{s}_{i'}^*)\}$  denote the estimate of  $w_0(\mathbf{s}_{i'}^*)$  obtained using any distributed or non-distributed methods and its variance, respectively. For sampling-based methods, we set  $\hat{w}(\mathbf{s}_{i'}^*)$  and  $\text{var}\{w(\mathbf{s}_{i'}^*)\}$  to be the median and the variance of the posterior samples for  $w(\mathbf{s}_{i'}^*)$ , respectively, for  $i' = 1, \dots, l$ . We also estimate the point-wise 95% credible or confidence intervals (CIs) of  $w(\mathbf{s}_{i'}^*)$  and predictive intervals (PIs) of  $y(\mathbf{s}_{i'}^*)$  for every  $\mathbf{s}_{i'} \in \mathcal{S}^*$  and compare the CI and PI coverages and lengths for every method. Also, the point predictive performance at the locations in  $\mathcal{S}^*$  are compared across competitors using the mean square prediction error (MSPE) defined as  $\text{MSPE} = \sum_{i'=1}^l \{\hat{y}(\mathbf{s}_{i'}^*) - y(\mathbf{s}_{i'}^*)\}^2 / l$ . Finally, we compare the performance of all the methods for parameter estimation using the posterior medians or point estimates and 95% CIs for  $\beta$ ,  $\sigma^2$ ,  $\tau^2$ , and  $\phi$ .

## 4.2 Simulated data analysis

### 4.2.1 Simulation 1: moderately large spatial data

We fit CMC (MPP), SDP (MPP), DISK (GP), and DISK (MPP) for  $k = 10, 20, 30, 40, 50$  along with other competitors. Focusing on the estimation of  $w_0(\mathbf{s}^*)$  for  $\mathbf{s}^* \in \mathcal{S}^*$ , CMC and DISK have smaller biases and larger variances than their non-distributed counterparts if  $k \leq 30$  (Table 1). The DISK estimator’s variance decreases and bias increases with increasing  $k$ , resulting in a decreasing MSE in the estimation of  $w_0$  initially and increasing after  $k = 20$  (Figure 2), which empirically verifies Theorem 3.4. The pointwise coverages of 95% CIs in DISK are similar to that of the non-distributed methods, except MPP and NNGP, for  $k \leq 30$  and are above the nominal value for all  $k$ . On the other hand, coverages of CMC and MPP are below the nominal value for every  $k$  and  $r$  and NNGP fails to cover  $w_0$  across all replications. The length of 95% CIs in DISK (GP) and DISK (MPP) are very close to that of their non-distributed version, whereas CMC’s and NNGP’s CIs greatly underestimate the posterior uncertainty. DISK (GP) and DISK (MPP) with  $k = 20$  are the best performers and closely match the empirical performance of LatticeKrig and laGP.

The results for DISK’s uncertainty quantification in parameter estimation and prediction results agree with those observed in the inference on the spatial surface (Table 2). All methods perform well in terms of MSPE and coverages and lengths of 95% PIs. DISK (GP) and DISK (MPP) (with  $k = 10, 20$ ) are more precise in the estimation of  $\beta$  compared to their non-distributed versions. All competitors exhibit a similar degree of accuracy in estimating  $\tau^2$ ,  $\sigma^2$ , and  $\phi$ . Providing an empirical confirmation of Theorem 3.4, increasing the number of subsets beyond 30 leads to poorer parameter estimation and uncertainty quantification due to a greater bias in the estimation of  $w_0$ .

An interesting feature of our comparisons is the dramatic difference between the performance of DISK (MPP) and MPP with the same choices of knots (Figure 1). The performance of MPP in spatial surface and parameter estimation using full data is sensitive to the choice of  $r$ , suffering greatly when  $r = 200$ . Contrary to this, DISK (MPP) has substantially smaller  $L_2$ -risk with the same number of knots used in each subset and its  $w_0$  estimate is almost indistinguishable from the true spatial surface. The performance of MPP is unstable when  $r/n$  is low due to poorly conditioned covariance matrix [3]. While the poor performance of full data MPP is attributed to this fact, this ratio is reasonably high in each subset for DISK (MPP), which contributes to its strikingly superior performance; in particular, using  $r$  knots in *each* subset of size  $m$  results in relatively high  $r/m$  ratio in DISK. While running NNGP with the `spNNGP` package, the inference from NNGP marginalized over  $w(\mathbf{s})$ ’s using the “response” option closely matches DISK in terms of inference on parameter estimates; however,  $\mathbf{w}^*$  cannot be estimated with “response” option, so we employ un-marginalized NNGP using the “sequential” option in the package. This results in severe auto-correlation among the latent variables and  $\beta$ , yielding NNGP’s poor performance across all three choices of the number of nearest neighbors. In an ongoing work, this issue is addressed by employing conjugate gradient algorithms to estimate latent variables in NNGP.

Table 1: Inference on the values of spatial surface at the locations in  $\mathcal{S}^*$  in Simulation 1. The numbers in parentheses are standard deviations over 10 simulation replications. The bias, variance, and Bayes  $L_2$ -risk in the estimation of  $w_0$  are defined in (27) and the coverage and credible intervals are calculated pointwise for the locations in  $\mathcal{S}^*$

	Bias <sup>2</sup>	Variance	$L_2$ -Risk	95% CI Coverage	95% CI Length
laGP	0.0004 (0.0000)	0.0100 (0.0002)	0.0103 (0.0002)	1.0000 (0.0000)	0.3890 (0.0036)
LatticeKrig	0.0002 (0.0000)	0.0003 (0.0000)	0.0005 (0.0000)	0.9867 (0.0033)	0.0703 (0.0006)
GP	0.0077 (0.0049)	0.0103 (0.0002)	0.0180 (0.0049)	1.0000 (0.0002)	0.3943 (0.0036)
MPP ( $r = 200$ )	0.3732 (0.3671)	0.0110 (0.0002)	0.3842 (0.3671)	0.0000 (0.0000)	0.4061 (0.0036)
MPP ( $r = 400$ )	0.0623 (0.0369)	0.0105 (0.0002)	0.0727 (0.0370)	0.2946 (0.4662)	0.3976 (0.0037)
NNGP					
NN= 5	0.4213 (0.1373)	0.0021 (0.0002)	0.4233 (0.1373)	0.0000 (0.0000)	0.1778 (0.0079)
NN= 15	0.4822 (0.0666)	0.0013 (0.0001)	0.4835 (0.0666)	0.0000 (0.0000)	0.1421 (0.0067)
NN= 25	0.4887 (0.0668)	0.0013 (0.0001)	0.4900 (0.0668)	0.0000 (0.0000)	0.1398 (0.0032)
CMC (MPP)					
$r = 200, k = 10$	0.0020 (0.0006)	0.0416 (0.0005)	0.0436 (0.0006)	0.8854 (0.0527)	0.1429 (0.0010)
$r = 200, k = 20$	0.0090 (0.0029)	0.0402 (0.0006)	0.0493 (0.0031)	0.1265 (0.1027)	0.1026 (0.0009)
$r = 200, k = 30$	0.0040 (0.0011)	0.0382 (0.0005)	0.0422 (0.0014)	0.3805 (0.1220)	0.0886 (0.0006)
$r = 200, k = 40$	0.0021 (0.0005)	0.0364 (0.0005)	0.0385 (0.0009)	0.5738 (0.0822)	0.0807 (0.0006)
$r = 200, k = 50$	0.0019 (0.0001)	0.0346 (0.0005)	0.0364 (0.0004)	0.6191 (0.0219)	0.0755 (0.0004)
CMC (MPP)					
$r = 400, k = 10$	0.0031 (0.0013)	0.0424 (0.0006)	0.0455 (0.0014)	0.7710 (0.1315)	0.1398 (0.0013)
$r = 400, k = 20$	0.0013 (0.0005)	0.0409 (0.0006)	0.0422 (0.0009)	0.8255 (0.0987)	0.1005 (0.0009)
$r = 400, k = 30$	0.0010 (0.0001)	0.0391 (0.0005)	0.0401 (0.0005)	0.8267 (0.0168)	0.0866 (0.0005)
$r = 400, k = 40$	0.0017 (0.0004)	0.0374 (0.0005)	0.0391 (0.0005)	0.6876 (0.0556)	0.0788 (0.0006)
$r = 400, k = 50$	0.0035 (0.0006)	0.0357 (0.0005)	0.0392 (0.0005)	0.4635 (0.0598)	0.0738 (0.0004)
DISK (GP)					
$k = 10$	0.0012 (0.0007)	0.0160 (0.0007)	0.0332 (0.0018)	1.0000 (0.0000)	0.4971 (0.0104)
$k = 20$	0.0008 (0.0005)	0.0106 (0.0004)	0.0221 (0.0005)	1.0000 (0.0000)	0.4041 (0.0070)
$k = 30$	0.0055 (0.0016)	0.0089 (0.0001)	0.0232 (0.0015)	1.0000 (0.0000)	0.3694 (0.0026)
$k = 40$	0.0136 (0.0019)	0.0085 (0.0001)	0.0306 (0.0018)	0.9946 (0.0048)	0.3612 (0.0026)
$k = 50$	0.0255 (0.0021)	0.0086 (0.0001)	0.0427 (0.0020)	0.7949 (0.0572)	0.3626 (0.0022)
DISK (MPP)					
$r = 200, k = 10$	0.0017 (0.0008)	0.0189 (0.0009)	0.0394 (0.0021)	1.0000 (0.0000)	0.5388 (0.0122)
$r = 200, k = 20$	0.0009 (0.0004)	0.0131 (0.0002)	0.0270 (0.0004)	1.0000 (0.0000)	0.4477 (0.0039)
$r = 200, k = 30$	0.0053 (0.0015)	0.0113 (0.0002)	0.0278 (0.0014)	1.0000 (0.0000)	0.4148 (0.0029)
$r = 200, k = 40$	0.0136 (0.0020)	0.0109 (0.0001)	0.0352 (0.0019)	0.9974 (0.0032)	0.4064 (0.0027)
$r = 200, k = 50$	0.0256 (0.0022)	0.0109 (0.0001)	0.0473 (0.0021)	0.8622 (0.0408)	0.4064 (0.0024)
DISK (MPP)					
$r = 400, k = 10$	0.0015 (0.0008)	0.0177 (0.0007)	0.0369 (0.0017)	1.0000 (0.0000)	0.5211 (0.0099)
$r = 400, k = 20$	0.0007 (0.0004)	0.0118 (0.0002)	0.0243 (0.0003)	1.0000 (0.0000)	0.4253 (0.0031)
$r = 400, k = 30$	0.0051 (0.0016)	0.0100 (0.0002)	0.0250 (0.0014)	1.0000 (0.0000)	0.3913 (0.0038)
$r = 400, k = 40$	0.0135 (0.0019)	0.0095 (0.0001)	0.0325 (0.0019)	0.9970 (0.0045)	0.3813 (0.0029)
$r = 400, k = 50$	0.0260 (0.0020)	0.0095 (0.0001)	0.0449 (0.0020)	0.8366 (0.0429)	0.3806 (0.0017)

#### 4.2.2 Simulation 2: large spatial data

Our ultimate goal is to apply DISK in massive data settings, so we evaluate its performance when  $n = 10^6$ . Simulation 1 compares DISK with its full data counterparts and other competitors across a variety of settings of  $k$  and  $r$ ; however, as mentioned earlier, massive size of the data in Simulation 2 prohibits the fitting of models based on full-rank and low-rank GPs, including MPP, LatticeKrig, and NNGP due to numerical issues, leaving only laGP as a feasible competitor. Since Simulation 1 demonstrates similar performance of DISK (MPP) and DISK (GP) with DISK (MPP) having a smaller run time, we use only DISK (MPP) for comparisons with laGP in Simulation 2. We use the identical three-step strategy for fitting DISK (MPP) as in Simulation 1 but with  $k = 500$  and with  $r = 400$  and  $r = 600$ . Notably,  $r$  is increased from 200 and 400 in Simulation 1 to 400 and 600 to account for the larger subset size in this simulation, maintaining a high  $r/m$  ratio.

The results for DISK's uncertainty quantification in parameter estimation and prediction agree with those observed in Simulation 1, but, unlike Simulation 1, DISK outperforms laGP in the estimation of  $w_0(\mathbf{s}^*)$  for  $\mathbf{s}^* \in \mathcal{S}^*$  for both choices of  $r$  (Tables 3 and 4). The point estimates of  $\beta$  and  $\tau^2$  are close to their true values with narrow 95% CIs. For  $\tau^2$ , the CI misses the truth, which is expected given that the full data GP in Simulation 1 underestimates  $\tau^2$ . In fact, every competitor,

including full data GP, identifies some portion of idiosyncratic variation as spatial variation due to the complex local variations in the simulated spatial surface. The bias, variance, and Bayes  $L_2$ -risk of DISK (MPP) for both  $rs$  are lower than those of laGP. The coverages of 95% CIs for laGP and DISK (MPP) are the same but the length of 95% CIs in DISK (MPP) are smaller than those of laGP for both  $rs$ . We conclude that DISK (MPP) matches the performance of laGP in prediction, where as it outperforms laGP in terms of estimation of parameters and  $w_0(\mathbf{s}^*)$  for  $\mathbf{s}^* \in \mathcal{S}^*$ .

### 4.3 Real data: Sea Surface Temperature data

One of most important ecological issues concerning our planet is climate change. It is generally accepted that the earth’s climate will change in response to radiative forces induced by the changes in atmospheric gases, cloud temperature, sea surface temperature (SST), water vapor, among others. A description of the evolution and dynamics of the SST is a key component of the study of the earth’s climate. SST data (in centigrade) from ocean samples have been collected by voluntary observing ships, buoys, and military and scientific cruises for decades. During the last 20 years or so, the SST database has been complemented by regular streams of remotely sensed observations from satellite orbiting the earth. A careful quantification of variability of SST data is important for climatological research, which includes determining the formation of sea breezes and sea fog and calibrating measurements from weather satellites [18]. A number of articles have appeared to address this issue in recent years; see [39, 7, 42, 43, 79].

We consider the problem of capturing the spatial trend and characterizing the uncertainties in the SST in the west coast of mainland U.S.A., Canada, and Alaska between  $40^\circ$ – $65^\circ$  north latitudes and  $100^\circ$ – $180^\circ$  west longitudes. The dataset is obtained from NODC World Ocean Database ([https://www.nodc.noaa.gov/OC5/WOD/pr\\_wod.html](https://www.nodc.noaa.gov/OC5/WOD/pr_wod.html)). Due to our focus on spatial modeling, we ignore the temporal component. After screening the data for quality control, we choose a random subset of about 1,000,800 spatial observations over the selected domain. From the selected observations, we randomly select  $10^6$  observations as training data and the remaining observations as test data. We replicate this setup ten times. The selected domain is large enough to allow considerable spatial variation in SST from north to south and provides an important first step in extending these models for analyzing global-scale SST database.

The SST data in the selected domain shows a clear decreasing trend in SST with increasing latitude (Figure 3). Based on this observation, we add latitude as a linear predictor in the univariate spatial regression model (1) to explain the long-range directional variability in the SST. The  $i$ th spatial location in SST data is  $\mathbf{s}_i = (\text{long}_i, \text{lat}_i)$ , where  $\text{long}_i$  and  $\text{lat}_i$  represents the  $i$ th longitude and latitude in training data. Thus the model in (1) for SST data is

$$y(\mathbf{s}_i) = \beta_0 + \beta_1 \text{lat}_i + w(\mathbf{s}_i) + \epsilon(\mathbf{s}_i), \quad \epsilon(\mathbf{s}_i) \sim N(0, \tau^2), \quad i = 1, \dots, 10^6. \quad (28)$$

We use the SST data at 800 test locations, denoted as  $\mathcal{S}^*$ , for comparing the performance of DISK and its competitors in terms of inference and prediction. The setup in (28) is identical to Simulation

2, except for the presence of  $\beta_1$ . We assign  $N(0, 100)$  prior to  $\beta_1$ , and the remaining priors and DISK competitors are identical to those in Simulation 2. For application of CMC (MPP), DISK (MPP), and SDP (MPP), we again follow the three-step strategy used in Simulation 1 but with  $k = 300$  and  $r = 400$ . Due to the lack of ground truth for estimating  $w_0(\mathbf{s}^*)$ , we compare the four methods in terms of their inference on  $\boldsymbol{\Omega}$  using 95% CIs and prediction of  $y(\mathbf{s}^*)$  for  $\mathbf{s}^* \in \mathcal{S}^*$  in terms of MSPE and the length and coverage of 95% posterior PIs.

DISK (MPP) outperforms CMC (MPP) and SDP (MPP) in predictions while closely matching the results of laGP, the current state-of-the-art method for modeling massive spatial data. The 50%, 2.5%, and 97.5% quantiles of the posterior distributions for  $\boldsymbol{\Omega}$ ,  $w(\mathbf{s}^*)$  and  $y(\mathbf{s}^*)$  for every  $\mathbf{s}^* \in \mathcal{S}^*$  are used for estimation and uncertainty quantification. CMC (MPP), SDP (MPP) and DISK (MPP) agree closely in their inference on  $\boldsymbol{\Omega}$ , but SDP (MPP) fails to provide any result for  $w(\mathbf{s}^*)$  or  $y(\mathbf{s}^*)$  due to the large size of  $\mathcal{S}^*$  (Table 5). For every  $\mathbf{s}^* \in \mathcal{S}^*$ , CMC's and DISK's estimates of  $w(\mathbf{s}^*)$  and  $y(\mathbf{s}^*)$  agree closely, but CMC severely underestimates uncertainty in  $w(\mathbf{s}^*)$  and  $y(\mathbf{s}^*)$  (Figures 3 and 4 and Table 5). The pointwise predictive coverages of laGP and DISK match their nominal levels; however, the 95% posterior PIs of DISK are wider than those of laGP because DISK accounts for uncertainty due to the error term (Figure 3 and Table 5). Our results in this section agree very closely with our results in Simulation 2, so we conclude that DISK (MPP) yields state-of-the-art predictive inference, spatial surface interpolation, and parameter estimation with 95% credible intervals. As a whole, SST data analysis reinforces our findings on DISK as a computationally efficient, flexible, and fully Bayesian inferential tool.

## 5 Discussion

This article presents a novel Bayesian approach for kriging with massive data using the divide-and-conquer technique. Distributed computation is the key in its ability to enhance the computational scalability of any spatial model, so we have called our approach Distributed Kriging (DISK). Our theoretical results shed light on the posterior convergence rate of the DISK posterior, as well as the bias-variance tradeoff phenomenon. When the number of subsets  $k$  is chosen to satisfy certain bounds depending on the analytic properties of the spatial surface, we have shown that the Bayes  $L_2$ -risk of the DISK posterior is nearly minimax optimal. We have confirmed this empirically via simulated and real data analyses, where DISK compares well with state-of-the-art methods.

Our theory has focused mostly on the estimation of  $w_0$ . Following the common practice, our theory assumes that the parameters  $\boldsymbol{\beta}$ ,  $\tau_0^2$ ,  $\sigma$ ,  $\phi$  are fixed. In practice, these parameters are also estimated under the unified Bayesian framework. It is therefore desirable, though technically much more complicated, to develop a more general theory that treats all these parameters as unknown.

The simplicity and generality of the DISK framework implies that it can be used to scale any spatial model. For example, recent applications have confirmed that the NNGP prior requires modifications if scalability is desired for tens of millions of locations [23]. In future, we aim to scale ordinary NNGP and other multiscale approaches to tens of millions of locations with the DISK



framework. Another important future work is to extend the DISK framework for scalable modeling of multiple correlated outcomes observed over massive number of locations.

This article focuses on developing the DISK framework for spatial modeling due to the motivating applications from massive geostatistical data. The DISK framework, however, is applicable to any mixed effects model where the random effects are assigned a GP prior, which includes Bayesian nonparametric regression using GP prior [58]. If we set  $\beta = 0$  in (1), univariate spatial regression with MPP prior reduces to nonparametric regression using the sparse GP prior obtained using the Fully Independent Training Conditional (FITC) approximation [66]. Our empirical investigations provide evidence that the DISK framework offers an approach for enhancing the scalability and accuracy of the FITC approximation if the covariates belong to a two dimensional space. We plan to explore more general applications in future with high dimensional covariates.

## Acknowledgment

We thank Professor David B. Dunson of Duke University for inspiring many questions that we have addressed in this work and Professor Sudipto Banerjee of UCLA for helpful conversations. Cheng Li's research is supported by the National University of Singapore start-up grant (R155000172133).

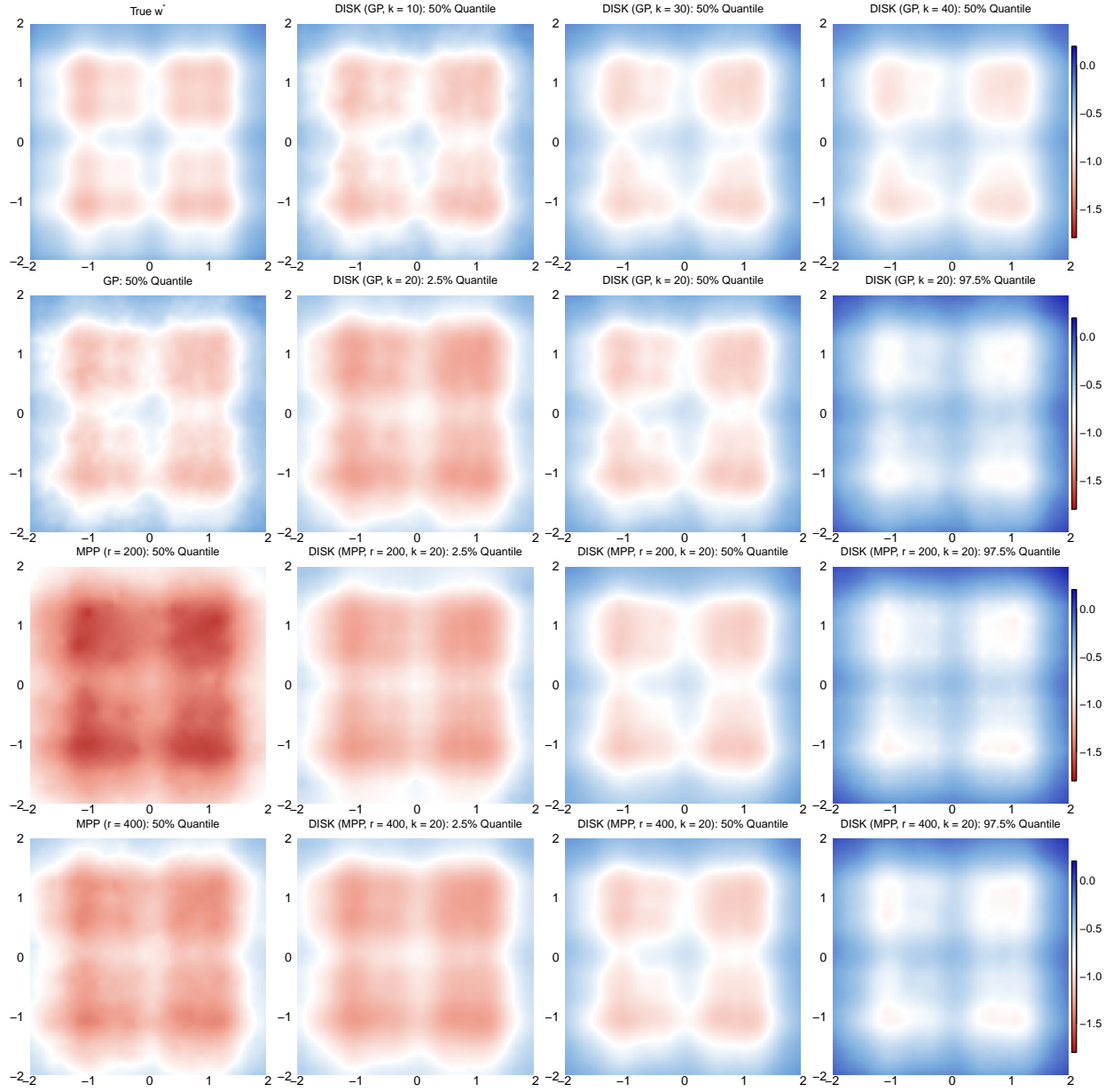


Figure 1: The spatial surface  $w_0$  at the locations in  $\mathcal{S}^*$  for all the competing full Bayesian methods (except NNGP) in Simulation 1. The 2.5%, 50%, and 97.5% quantile surfaces, respectively, represent pointwise quantiles of the posterior distribution for  $w(\mathbf{s}^*)$  for every  $\mathbf{s}^* \in \mathcal{S}^*$ , where the 50% quantile of  $w(\mathbf{s}^*)$  is the estimate of  $w_0(\mathbf{s}^*)$  and the 2.5% and 97.5% quantiles quantify uncertainty. The true spatial surface  $w_0(\mathbf{s}^*)$ ,  $\mathbf{s}^* \in \mathcal{S}^*$  is in the first row and column. The remaining entries in the first column are the estimates of  $w_0(\mathbf{s}^*)$ ,  $\mathbf{s}^* \in \mathcal{S}^*$  obtained using the full data posterior distributions with full-rank GP prior and MPP prior with  $r = 200, 400$ . The remaining entries in the first row are the estimates of  $w_0(\mathbf{s}^*)$ ,  $\mathbf{s}^* \in \mathcal{S}^*$  obtained using DISK with GP prior and  $k = 10, 30, 40$ , respectively. All other entries provide point estimates and quantify uncertainty in inference on  $w_0(\mathbf{s}^*)$ ,  $\mathbf{s}^* \in \mathcal{S}^*$  with  $k = 20$  and GP prior (second row), MPP prior with rank 200 (third row) and MPP prior with rank 400 (fourth row).

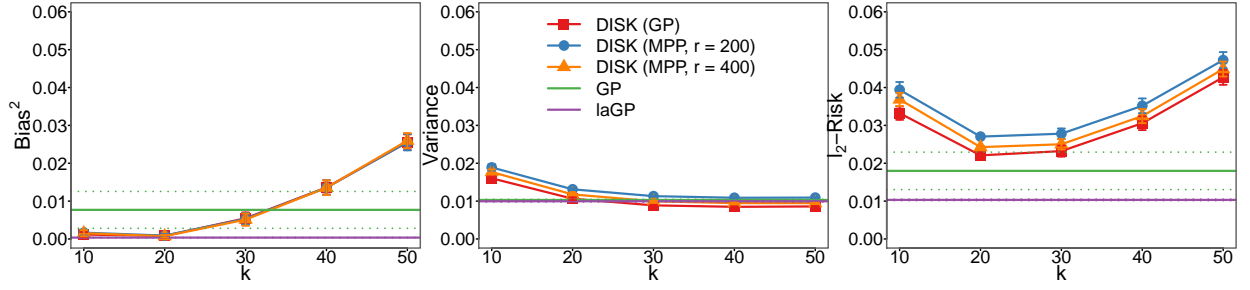


Figure 2: The empirical estimate of bias, variance, and Bayes  $L_2$ -risk in estimating the spatial surface  $w_0$  at the locations in  $\mathcal{S}^*$  in Simulation 1. The GP is the theoretical benchmark and laGP is the state-of-the-art method for estimation. The solid lines represent averaged values and the dotted lines and arrows represent one standard deviation error for the full-GP over 10 simulation replications.

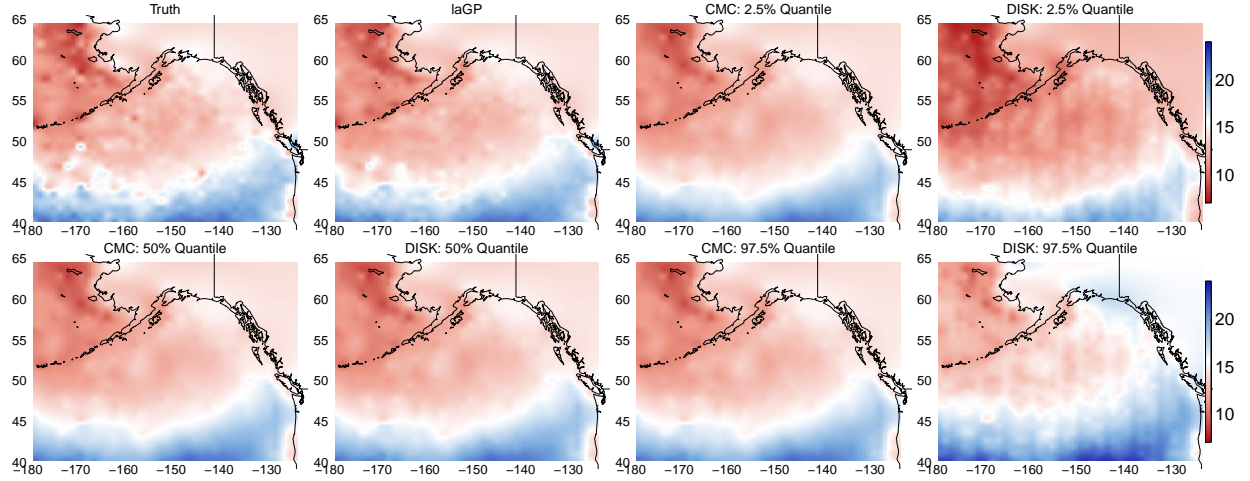


Figure 3: Predication of sea surface temperatures at the locations in  $\mathcal{S}^*$ . Negative longitude means degree west from Greenwich. CMC and DISK use MPP-based modeling with  $r = 400$  on  $k = 300$  subsets and laGP uses the ‘nn’ method. The 2.5%, 50%, and 97.5% quantile surfaces, respectively, represent pointwise quantiles of the posterior distribution for  $y(\mathbf{s}^*)$  for every  $\mathbf{s}^* \in \mathcal{S}^*$ .

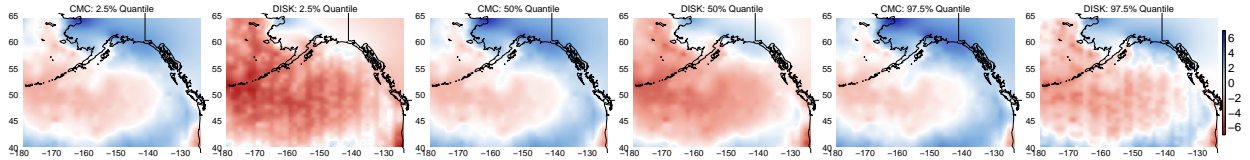


Figure 4: Interpolated spatial surface  $w$  at the locations in  $\mathcal{S}^*$ . Negative longitude means degree west from Greenwich. CMC and DISK use MPP-based modeling with  $r = 400$  on  $k = 300$  subsets. The 2.5%, 50%, and 97.5% quantile surfaces, respectively, represent pointwise quantiles of the posterior distribution for  $w(\mathbf{s}^*)$  for every  $\mathbf{s}^* \in \mathcal{S}^*$ .

Table 2: Parametric inference and prediction in Simulation 1. For parametric inference posterior medians are provided along with the 95% credible intervals (CIs) in the parentheses, where available. Similarly mean squared prediction errors (MSPEs) along with length and coverage of 95% predictive intervals (PIs) are presented, where available. The upper and lower quantiles of 95% CIs and PIs are averaged over 10 simulation replications, with the numbers in parentheses for the last three columns denoting standard deviations across replications; ‘-’ indicates that the parameter estimate or prediction is not provided by the software or the competitor

	$\beta$	$\sigma^2$	$\tau^2$	$\phi$	MSPE	95% PI Coverage	95% PI Length
Truth	1.00	-	0.01	-	-	-	-
laGP	-	-	-	-	0.010 (0.000)	0.94 (0.01)	0.39 (0.00)
LatticeKrig	-	0.01 (-, -)	-	0.08 (-, -)	0.010 (0.000)	0.95 (0.01)	0.39 (0.00)
GP	1.08 (0.50, 1.65)	0.12 (0.10, 0.14)	0.009 (0.009, 0.010)	0.115 (0.107, 0.135)	0.010 (0.000)	0.95 (0.01)	0.39 (0.00)
MPP ( $r = 200$ )	1.56 (0.99, 2.15)	0.15 (0.13, 0.18)	0.008 (0.007, 0.008)	0.119 (0.110, 0.133)	0.010 (0.000)	0.95 (0.01)	0.41 (0.00)
MPP ( $r = 200$ )	1.23 (0.61, 1.84)	0.16 (0.13, 0.19)	0.008 (0.008, 0.008)	0.120 (0.110, 0.148)	0.010 (0.000)	0.95 (0.01)	0.40 (0.00)
NNGP							
NN= 5	0.36 (0.36, 0.36)	0.29 (0.29, 0.29)	0.009 (0.009, 0.009)	0.123 (0.123, 0.123)	0.011 (0.000)	0.94 (0.01)	0.39 (0.02)
NN= 15	0.31 (0.31, 0.31)	0.17 (0.17, 0.17)	0.009 (0.009, 0.009)	0.113 (0.113, 0.113)	0.010 (0.000)	0.95 (0.01)	0.40 (0.01)
NN= 25	0.30 (0.30, 0.30)	0.16 (0.16, 0.16)	0.009 (0.009, 0.009)	0.112 (0.112, 0.112)	0.010 (0.000)	0.95 (0.01)	0.40 (0.01)
CMC (MPP)							
$r = 200, k = 10$	0.99 (0.74, 1.23)	0.23 (0.22, 0.25)	0.006 (0.005, 0.006)	0.112 (0.107, 0.119)	0.011 (0.000)	0.50 (0.01)	0.14 (0.00)
$r = 200, k = 20$	1.09 (0.89, 1.28)	0.29 (0.27, 0.31)	0.007 (0.006, 0.007)	0.109 (0.106, 0.114)	0.011 (0.000)	0.38 (0.01)	0.10 (0.00)
$r = 200, k = 30$	1.05 (0.89, 1.21)	0.30 (0.28, 0.32)	0.007 (0.007, 0.007)	0.111 (0.108, 0.115)	0.011 (0.000)	0.32 (0.01)	0.09 (0.00)
$r = 200, k = 40$	1.02 (0.88, 1.16)	0.31 (0.30, 0.33)	0.008 (0.007, 0.008)	0.108 (0.106, 0.112)	0.011 (0.000)	0.30 (0.01)	0.08 (0.00)
$r = 200, k = 50$	0.99 (0.86, 1.12)	0.32 (0.31, 0.34)	0.008 (0.008, 0.008)	0.109 (0.107, 0.114)	0.012 (0.000)	0.27 (0.01)	0.08 (0.00)
SDP (MPP)							
$r = 400, k = 10$	1.04 (0.77, 1.30)	0.26 (0.24, 0.28)	0.006 (0.006, 0.007)	0.108 (0.105, 0.114)	0.011 (0.000)	0.49 (0.01)	0.14 (0.00)
$r = 400, k = 20$	1.02 (0.82, 1.22)	0.29 (0.27, 0.32)	0.007 (0.007, 0.007)	0.112 (0.109, 0.119)	0.010 (0.000)	0.38 (0.01)	0.10 (0.00)
$r = 400, k = 30$	0.99 (0.83, 1.16)	0.30 (0.28, 0.32)	0.007 (0.007, 0.008)	0.115 (0.111, 0.121)	0.011 (0.000)	0.32 (0.01)	0.09 (0.00)
$r = 400, k = 40$	0.98 (0.83, 1.13)	0.32 (0.30, 0.33)	0.008 (0.007, 0.008)	0.112 (0.109, 0.116)	0.011 (0.000)	0.29 (0.01)	0.08 (0.00)
$r = 400, k = 50$	0.95 (0.83, 1.08)	0.33 (0.31, 0.34)	0.008 (0.008, 0.009)	0.111 (0.109, 0.115)	0.011 (0.000)	0.27 (0.01)	0.07 (0.00)
SDP (MPP)							
$r = 200, k = 10$	0.98 (0.75, 1.23)	0.23 (0.22, 0.25)	0.006 (0.005, 0.006)	0.112 (0.106, 0.118)	-	-	-
$r = 200, k = 20$	1.08 (0.89, 1.27)	0.29 (0.27, 0.31)	0.007 (0.006, 0.007)	0.109 (0.106, 0.113)	-	-	-
$r = 200, k = 30$	1.05 (0.89, 1.21)	0.30 (0.28, 0.32)	0.007 (0.007, 0.007)	0.111 (0.108, 0.115)	-	-	-
$r = 200, k = 40$	1.01 (0.87, 1.16)	0.31 (0.30, 0.33)	0.008 (0.007, 0.008)	0.108 (0.106, 0.111)	-	-	-
$r = 200, k = 50$	0.99 (0.86, 1.12)	0.33 (0.31, 0.34)	0.008 (0.008, 0.008)	0.110 (0.107, 0.112)	-	-	-
SDP (MPP)							
$r = 400, k = 10$	1.04 (0.79, 1.29)	0.26 (0.24, 0.28)	0.006 (0.006, 0.007)	0.109 (0.104, 0.113)	-	-	-
$r = 400, k = 20$	1.02 (0.83, 1.21)	0.30 (0.27, 0.32)	0.007 (0.007, 0.007)	0.113 (0.108, 0.118)	-	-	-
$r = 400, k = 30$	0.99 (0.84, 1.15)	0.31 (0.29, 0.33)	0.007 (0.007, 0.008)	0.115 (0.110, 0.120)	-	-	-
$r = 400, k = 40$	0.97 (0.83, 1.11)	0.32 (0.30, 0.34)	0.008 (0.007, 0.008)	0.112 (0.109, 0.116)	-	-	-
$r = 400, k = 50$	0.95 (0.82, 1.08)	0.33 (0.31, 0.35)	0.008 (0.008, 0.009)	0.112 (0.108, 0.115)	-	-	-
DISK (GP)							
$k = 10$	1.03 (0.80, 1.26)	0.21 (0.17, 0.24)	0.009 (0.008, 0.009)	0.124 (0.111, 0.147)	0.010 (0.000)	0.95 (0.01)	0.41 (0.00)
$k = 20$	0.98 (0.82, 1.15)	0.22 (0.17, 0.26)	0.008 (0.008, 0.009)	0.142 (0.121, 0.179)	0.010 (0.000)	0.96 (0.01)	0.42 (0.00)
$k = 30$	0.93 (0.80, 1.07)	0.20 (0.16, 0.24)	0.008 (0.008, 0.008)	0.171 (0.140, 0.219)	0.010 (0.000)	0.96 (0.00)	0.43 (0.00)
$k = 40$	0.88 (0.78, 1.00)	0.18 (0.15, 0.23)	0.008 (0.007, 0.008)	0.201 (0.162, 0.252)	0.010 (0.000)	0.97 (0.01)	0.44 (0.00)
$k = 50$	0.84 (0.75, 0.94)	0.17 (0.14, 0.21)	0.007 (0.007, 0.008)	0.231 (0.186, 0.285)	0.011 (0.000)	0.97 (0.00)	0.46 (0.00)
DISK (MPP)							
$r = 200, k = 10$	1.03 (0.80, 1.27)	0.21 (0.18, 0.24)	0.009 (0.008, 0.009)	0.120 (0.109, 0.144)	0.010 (0.000)	0.97 (0.01)	0.44 (0.00)
$r = 200, k = 20$	0.98 (0.82, 1.16)	0.22 (0.17, 0.26)	0.008 (0.008, 0.009)	0.140 (0.119, 0.177)	0.010 (0.000)	0.97 (0.01)	0.46 (0.00)
$r = 200, k = 30$	0.93 (0.80, 1.07)	0.20 (0.16, 0.25)	0.008 (0.008, 0.008)	0.170 (0.137, 0.217)	0.011 (0.000)	0.98 (0.00)	0.47 (0.00)
$r = 200, k = 40$	0.89 (0.78, 1.00)	0.18 (0.15, 0.23)	0.008 (0.007, 0.008)	0.201 (0.161, 0.252)	0.011 (0.000)	0.97 (0.01)	0.47 (0.02)
$r = 200, k = 50$	0.84 (0.75, 0.94)	0.17 (0.14, 0.21)	0.007 (0.007, 0.008)	0.232 (0.186, 0.286)	0.011 (0.000)	0.98 (0.00)	0.49 (0.00)
DISK (MPP)							
$r = 400, k = 10$	1.03 (0.80, 1.27)	0.21 (0.18, 0.24)	0.009 (0.008, 0.009)	0.119 (0.109, 0.143)	0.010 (0.000)	0.96 (0.01)	0.42 (0.00)
$r = 400, k = 20$	0.98 (0.82, 1.16)	0.22 (0.17, 0.26)	0.008 (0.008, 0.009)	0.140 (0.119, 0.181)	0.010 (0.000)	0.97 (0.01)	0.44 (0.00)
$r = 400, k = 30$	0.93 (0.80, 1.07)	0.20 (0.16, 0.25)	0.008 (0.008, 0.008)	0.169 (0.137, 0.217)	0.010 (0.000)	0.97 (0.01)	0.45 (0.00)
$r = 400, k = 40$	0.89 (0.78, 1.00)	0.18 (0.14, 0.23)	0.008 (0.007, 0.008)	0.200 (0.159, 0.254)	0.011 (0.000)	0.97 (0.01)	0.46 (0.00)
$r = 400, k = 50$	0.84 (0.75, 0.94)	0.17 (0.13, 0.20)	0.007 (0.007, 0.008)	0.232 (0.187, 0.287)	0.011 (0.000)	0.98 (0.00)	0.47 (0.00)

Table 3: Inference on the values of spatial surface at the locations in  $\mathcal{S}^*$  in Simulation 2. The numbers in parentheses are standard deviations over 10 simulation replications. The bias, variance, and  $L_2$ -risk in the estimation of  $w_0$  are defined in (27) and the coverage and credible intervals are calculated pointwise for the locations in  $\mathcal{S}^*$ .

	Bias <sup>2</sup>	Variance	$L_2$ -Risk	95% CI Coverage	95% CI Length
laGP	0.0002 (0.0000)	0.0100 (0.0000)	0.0102 (0.0000)	1.0000 (0.0000)	0.3905 (0.0006)
DISK (MPP) ( $r = 400, k = 500$ )	0.0002 (0.0000)	0.0030 (0.0000)	0.0061 (0.0000)	1.0000 (0.0000)	0.2132 (0.0002)
DISK (MPP) ( $r = 600, k = 500$ )	0.0001 (0.0000)	0.0026 (0.0000)	0.0052 (0.0000)	1.0000 (0.0000)	0.1977 (0.0002)

Table 4: Parametric inference and prediction in Simulation 2. For parametric inference posterior medians are provided along with The 95% credible intervals (CIs) in the parentheses, where available. Similarly mean squared prediction errors (MSPEs) along with length and coverage of 95% predictive intervals (PIs) are presented, where available. The upper and lower quantiles of 95% CIs and PIs are averaged over 10 simulation replications, with the numbers in parentheses for the last three columns denoting standard deviations across replications; ‘-’ indicates that the parameter estimate or prediction is not provided by the software or the competitor.

	$\beta$	$\sigma^2$	$\tau^2$	$\phi$
Truth	1.00	-	0.01	-
laGP	-	-	-	-
DISK (MPP) ( $r = 400, k = 500$ )	1.01 (0.98, 1.04)	0.1609 (0.1561, 0.1700)	0.00863 (0.00860, 0.00866)	0.134907 (0.131456, 0.138885)
DISK (MPP) ( $r = 600, k = 500$ )	1.01 (0.98, 1.04)	0.1607 (0.1560, 0.1700)	0.00863 (0.00860, 0.00866)	0.135020 (0.131545, 0.139009)
	MSPE	95% PI Coverage	95% PI Length	
laGP	0.0101 (0.0003)	0.9450 (0.0040)	0.3903 (0.0000)	
DISK (MPP) ( $r = 400, k = 500$ )	0.0099 (0.0003)	0.9624 (0.0030)	0.4177 (0.0000)	
DISK (MPP) ( $r = 600, k = 500$ )	0.0099 (0.0002)	0.9590 (0.0040)	0.4097 (0.0000)	

Table 5: Parametric inference and prediction in SST data. CMC, SDP, and DISK use MPP-based modeling with  $r = 400$  on  $k = 300$  subsets. For parametric inference posterior medians are provided along with The 95% credible intervals (CIs) in the parentheses, where available. Similarly mean squared prediction errors (MSPEs) along with length and coverage of 95% predictive intervals (PIs) are presented, where available. The upper and lower quantiles of 95% CIs and PIs are averaged over 10 simulation replications, with the numbers in parentheses for the last three columns denoting standard deviations across replications; ‘-’ indicates that the parameter estimate or prediction is not provided by the software or the competitor

	$\beta_0$	$\beta_1$	$\sigma^2$	$\tau^2$	$\phi$
laGP	-	-	-	-	-
CMC	31.78 (31.19, 32.37)	-0.35 (-0.36, -0.34)	12.22 (11.78, 12.69)	0.110 (0.108, 0.112)	0.021 (0.020, 0.022)
SDP	31.67 (31.45, 31.82)	-0.35 (-0.36, -0.34)	14.42 (13.29, 14.80)	0.110 (0.108, 0.112)	0.021 (0.020, 0.022)
DISK	32.34 (31.74, 32.95)	-0.32 (-0.33, -0.31)	11.83 (11.23, 12.45)	0.184 (0.182, 0.185)	0.039 (0.037, 0.041)
	MSPE	95% PI Coverage	95% PI Length		
laGP	0.25 (0.00)	0.95 (0.00)	1.35 (0.00)		
CMC	0.41 (0.00)	0.13 (0.00)	0.14 (0.00)		
SDP	-	-	-		
DISK	0.41 (0.00)	0.95 (0.00)	2.67 (0.00)		

# Supplementary Material for A Divide-and-Conquer Bayesian Approach to Large-Scale Kriging

## 1 Proof of Theorems in Section 3.5

### 1.1 Technical Lemmas

For notational convenience, we define two additional “Hilbert” norms  $\|\cdot\|_{\mathbb{H}_j}$  and  $\|\cdot\|_{\mathbb{H}}$ , which are rescaled versions of  $\|\cdot\|_{\mathcal{S}_j}$  and  $\|\cdot\|_{\mathcal{S}}$ . The inner products can also be defined accordingly.

$$\begin{aligned}\langle \mathbf{h}_{j1}, \mathbf{h}_{j2} \rangle_{\mathbb{H}_j} &= \mathbf{h}_{j1}^T \mathbf{A}_j^T \boldsymbol{\Sigma}_j^{-1} \mathbf{A}_j \mathbf{h}_{j2}, \quad \|\mathbf{h}_{j1}\|_{\mathbb{H}_j}^2 = \langle \mathbf{h}_{j1}, \mathbf{h}_{j1} \rangle_{\mathbb{H}_j}, \quad \mathbf{h}_{j1}, \mathbf{h}_{j2} \in \mathbb{R}^l, \quad \|\cdot\|_{\mathbb{H}_j} = \sqrt{m} \|\cdot\|_{\mathcal{S}_j}, \\ \langle \mathbf{h}_1, \mathbf{h}_2 \rangle_{\mathbb{H}} &= \mathbf{h}_1^T \mathbf{A}^T \boldsymbol{\Sigma}^{-1} \mathbf{A} \mathbf{h}_2, \quad \|\mathbf{h}_1\|_{\mathbb{H}}^2 = \langle \mathbf{h}_1, \mathbf{h}_1 \rangle_{\mathbb{H}}, \quad \mathbf{h}_1, \mathbf{h}_2 \in \mathbb{R}^l, \quad \|\cdot\|_{\mathbb{H}} = \sqrt{n} \|\cdot\|_{\mathcal{S}}.\end{aligned}$$

We first prove a series of technical lemmas under our model setup, similar to the lemmas in van der Vaart and van Zanten [73].

**Lemma 1.1** *Suppose that Assumption A.2 holds. Let  $\mathbf{y}_j \sim N_m(\mathbf{A}_j \boldsymbol{\theta}, \boldsymbol{\Sigma}_j)$ , where  $\boldsymbol{\theta} \in \mathbb{R}^l$  is such that  $\|\boldsymbol{\theta} - \boldsymbol{\theta}_1\|_{\mathbb{H}_j} \leq \|\boldsymbol{\theta}_0 - \boldsymbol{\theta}_1\|_{\mathbb{H}_j}/2$  for any  $\boldsymbol{\theta}_0, \boldsymbol{\theta}_1 \in \mathbb{R}^l$ . Then, there exists a test  $\phi(\mathbf{y}_j)$  such that  $\max(\mathbb{E}_{\boldsymbol{\theta}_0}\{\phi(\mathbf{y}_j)\}, \mathbb{E}_{\boldsymbol{\theta}}\{1 - \phi(\mathbf{y}_j)\}) \leq e^{-\|\boldsymbol{\theta}_0 - \boldsymbol{\theta}_1\|_{\mathbb{H}_j}^2/32} \leq e^{-H_l \|\boldsymbol{\theta}_1\|_{\mathbb{H}}^2/32}$ , where  $\mathbb{E}_{\boldsymbol{\theta}}$  is the expectation with respect to the measure  $N_m(\mathbf{y}_j \mid \mathbf{A}_j \boldsymbol{\theta}, \boldsymbol{\Sigma}_j)$ .*

**Proof** Choose  $\boldsymbol{\theta}_0 = \mathbf{0}$  for simplicity, and define the test function  $\phi(\mathbf{y}_j) = \mathbf{1}(\boldsymbol{\theta}_1^T \mathbf{A}_j^T \boldsymbol{\Sigma}_j^{-1} \mathbf{y}_j > D \|\boldsymbol{\theta}_1\|_{\mathbb{H}_j})$ . If  $\boldsymbol{\theta}_0 = \mathbf{0}$ , then  $\|\boldsymbol{\theta} - \boldsymbol{\theta}_1\|_{\mathbb{H}_j} \leq \|\boldsymbol{\theta}_1\|_{\mathbb{H}_j}/2$  and the triangular inequality gives  $\|\boldsymbol{\theta}_1\|_{\mathbb{H}_j}/2 \leq \|\boldsymbol{\theta}\|_{\mathbb{H}_j}$ . The type I error probability of  $\phi(\mathbf{y}_j)$  is

$$\mathbb{E}_{\boldsymbol{\theta}_0}\{\phi(\mathbf{y}_j)\} = \mathbb{P}_{\boldsymbol{\theta}_0}\left(\boldsymbol{\theta}_1^T \mathbf{A}_j^T \boldsymbol{\Sigma}_j^{-1} \mathbf{y}_j > D \|\boldsymbol{\theta}_1\|_{\mathbb{H}_j}\right). \quad (29)$$

Since  $\mathbf{y}_j \sim N_m(\mathbf{0}, \boldsymbol{\Sigma}_j)$ ,  $\boldsymbol{\theta}_1^T \mathbf{A}_j^T \boldsymbol{\Sigma}_j^{-1} \mathbf{y}_j \sim N_m(0, \boldsymbol{\theta}_1^T \mathbf{A}_j^T \boldsymbol{\Sigma}_j^{-1} \mathbf{A}_j \boldsymbol{\theta}_1) = N(0, \|\boldsymbol{\theta}_1\|_{\mathbb{H}_j}^2)$  and type I error probability in (29) is

$$\mathbb{E}_{\boldsymbol{\theta}_0}\{\phi(\mathbf{y}_j)\} = 1 - \mathbb{P}_{\boldsymbol{\theta}_0}\left(\frac{\boldsymbol{\theta}_1^T \mathbf{A}_j^T \boldsymbol{\Sigma}_j^{-1} \mathbf{y}_j - 0}{\|\boldsymbol{\theta}_1\|_{\mathbb{H}_j}} \leq D\right) = 1 - \Phi(D).$$

For  $\boldsymbol{\theta} \neq \boldsymbol{\theta}_0$ ,  $\boldsymbol{\theta}_1^T \mathbf{A}_j^T \boldsymbol{\Sigma}_j^{-1} \mathbf{y}_j \sim N(\boldsymbol{\theta}_1^T \mathbf{A}_j^T \boldsymbol{\Sigma}_j^{-1} \mathbf{A}_j \boldsymbol{\theta}, \boldsymbol{\theta}_1^T \mathbf{A}_j^T \boldsymbol{\Sigma}_j^{-1} \mathbf{A}_j \boldsymbol{\theta}_1) = N(\langle \boldsymbol{\theta}_1, \boldsymbol{\theta} \rangle_{\mathbb{H}_j}, \|\boldsymbol{\theta}_1\|_{\mathbb{H}_j}^2)$  and

$$\begin{aligned}\mathbb{E}_{\boldsymbol{\theta}}\{1 - \phi(\mathbf{y}_j)\} &= \mathbb{P}_{\boldsymbol{\theta}}\left(\boldsymbol{\theta}_1^T \mathbf{A}_j^T \boldsymbol{\Sigma}_j^{-1} \mathbf{y}_j < D \|\boldsymbol{\theta}_1\|_{\mathbb{H}_j}\right) = \mathbb{P}_{\boldsymbol{\theta}}\left(\frac{\boldsymbol{\theta}_1^T \mathbf{A}_j^T \boldsymbol{\Sigma}_j^{-1} \mathbf{y}_j - \langle \boldsymbol{\theta}_1, \boldsymbol{\theta} \rangle_{\mathbb{H}_j}}{\|\boldsymbol{\theta}_1\|_{\mathbb{H}_j}} < D - \frac{\langle \boldsymbol{\theta}_1, \boldsymbol{\theta} \rangle_{\mathbb{H}_j}}{\|\boldsymbol{\theta}_1\|_{\mathbb{H}_j}}\right) \\ &= \Phi\left(D - \frac{\langle \boldsymbol{\theta}_1, \boldsymbol{\theta} \rangle_{\mathbb{H}_j}}{\|\boldsymbol{\theta}_1\|_{\mathbb{H}_j}}\right).\end{aligned} \quad (30)$$

To find an upper bound for  $\mathbb{E}_{\boldsymbol{\theta}}\{1 - \phi(\mathbf{y}_j)\}$ , notice that

$$\langle \boldsymbol{\theta}_1, \boldsymbol{\theta} \rangle_{\mathbb{H}_j} = \frac{\|\boldsymbol{\theta}_1\|_{\mathbb{H}_j}^2 + \|\boldsymbol{\theta}\|_{\mathbb{H}_j}^2 - \|\boldsymbol{\theta} - \boldsymbol{\theta}_1\|_{\mathbb{H}_j}^2}{2} \geq \frac{\|\boldsymbol{\theta}_1\|_{\mathbb{H}_j}^2 + \|\boldsymbol{\theta}_1\|_{\mathbb{H}_j}^2/4 - \|\boldsymbol{\theta}_1\|_{\mathbb{H}_j}^2/4}{2} = \frac{\|\boldsymbol{\theta}_1\|_{\mathbb{H}_j}^2}{2}. \quad (31)$$

Substituting (31) in (30) implies that  $\mathbb{E}_{\boldsymbol{\theta}}\{1 - \phi(\mathbf{y}_j)\} \leq \Phi\left(D - \frac{\|\boldsymbol{\theta}_1\|_{\mathbb{H}_j}}{2}\right)$ . Under 0-1 loss, an upper bound on the risk of the decision rule based on  $\phi$  is

$$1 - \Phi(D) + \Phi\left(D - \frac{\|\boldsymbol{\theta}_1\|_{\mathbb{H}_j}}{2}\right) = \Phi(-D) + \Phi\left(D - \frac{\|\boldsymbol{\theta}_1\|_{\mathbb{H}_j}}{2}\right),$$

which attains its minimum at  $D = \|\boldsymbol{\theta}_1\|_{\mathbb{H}_j}/4$ . Substituting this in the upper bounds for Type I and II error probabilities and using  $\Phi(-x) \leq \exp(-x^2/2)$ , we get

$$\Phi(-\|\boldsymbol{\theta}_1\|_{\mathbb{H}_j}/4) \leq e^{-(\|\boldsymbol{\theta}_1\|_{\mathbb{H}_j}/4)^2/2} = e^{-\|\boldsymbol{\theta}_1\|_{\mathbb{H}_j}^2/32} \leq e^{-H_l\|\boldsymbol{\theta}_1\|_{\mathbb{H}}^2/32}. \quad (32)$$

■

Define,  $D(\epsilon, \boldsymbol{\Theta}, \|\cdot\|_{\mathbb{H}_j})$  is the maximal number of points that can be placed inside the set  $\boldsymbol{\Theta} \subset \mathbb{R}^l$  such that  $\|\boldsymbol{\theta}_0 - \boldsymbol{\theta}_1\|_{\mathbb{H}_j} > \epsilon$  for any two different points  $\boldsymbol{\theta}_0$  and  $\boldsymbol{\theta}_1$  in  $\boldsymbol{\Theta}$ .

**Lemma 1.2** *Suppose that Assumptions A.1 and A.2 hold. Let  $\mathbf{y}_j \sim N_m(\mathbf{A}_j \boldsymbol{\theta}, \boldsymbol{\Sigma}_j)$  for any  $\boldsymbol{\theta} \in \mathbb{R}^l$ . Then, there exists a test  $\phi(\mathbf{y}_j)$  such that for every  $r > 1$  and every  $i \geq 1$ ,*

$$\begin{aligned} \mathbb{E}_{\boldsymbol{\theta}_0}\{\phi(\mathbf{y}_j)\} &\leq 33 D(r/2, \boldsymbol{\Theta}, \|\cdot\|_{\mathbb{H}_j}) e^{-r^2/32}, \\ \sup_{\{\boldsymbol{\theta} \in \boldsymbol{\Theta} : \|\boldsymbol{\theta} - \boldsymbol{\theta}_0\|_{\mathbb{H}_j} \geq ir\}} \mathbb{E}_{\boldsymbol{\theta}}\{1 - \phi(\mathbf{y}_j)\} &\leq e^{-i^2 r^2/32}; \end{aligned}$$

and

$$\begin{aligned} \mathbb{E}_{\boldsymbol{\theta}_0}\{\phi(\mathbf{y}_j)\} &\leq 33 D(\sqrt{k}H_l^{-1}r/2, \boldsymbol{\Theta}, \|\cdot\|_{\mathbb{H}}) e^{-r^2/32}, \\ \sup_{\{\boldsymbol{\theta} \in \boldsymbol{\Theta} : \|\boldsymbol{\theta} - \boldsymbol{\theta}_0\|_{\mathbb{H}} \geq ir\sqrt{k}H_l^{-1}\}} \mathbb{E}_{\boldsymbol{\theta}}\{1 - \phi(\mathbf{y}_j)\} &\leq e^{-i^2 r^2/32}. \end{aligned}$$

**Proof** Partition  $\boldsymbol{\Theta}$  into disjoint shells defined as  $E_{i,r} = \{\boldsymbol{\theta} : ir \leq \|\boldsymbol{\theta} - \boldsymbol{\theta}_0\|_{\mathbb{H}_j} \leq (i+1)r\}$  ( $i = 0, 1, \dots$ ). For any  $i \geq 1$ , if  $\boldsymbol{\Theta}_i = D(ir/2, E_{i,r}, \|\cdot\|_{\mathbb{H}_j})$ , then  $\|\boldsymbol{\theta}_{ia} - \boldsymbol{\theta}_{ib}\|_{\mathbb{H}_j} > ir/2$  for any  $\boldsymbol{\theta}_{ia}, \boldsymbol{\theta}_{ib} \in \boldsymbol{\Theta}_i$ . Furthermore, for any  $\boldsymbol{\theta} \in E_{i,r}$ , there is some  $\boldsymbol{\theta}_{i1} \in \boldsymbol{\Theta}_i$  such that  $\|\boldsymbol{\theta} - \boldsymbol{\theta}_{i1}\|_{\mathbb{H}_j} \leq ir/2 \leq \|\boldsymbol{\theta}_{i1} - \boldsymbol{\theta}_0\|_{\mathbb{H}_j}/2$ ; therefore, Lemma 1.1 implies that there exists a test  $\phi_i^*(\mathbf{y}_j)$  such that  $\max\{\mathbb{E}_{\boldsymbol{\theta}_0}\{\phi_i^*(\mathbf{y}_j)\}, \mathbb{E}_{\boldsymbol{\theta}}\{1 - \phi_i^*(\mathbf{y}_j)\}\} \leq e^{-\|\boldsymbol{\theta}_0 - \boldsymbol{\theta}_{i1}\|_{\mathbb{H}_j}^2/32}$ . Define the test  $\phi_i(\mathbf{y}_j) = \sup_{\boldsymbol{\theta}_{i1} \in \boldsymbol{\Theta}_i} \phi_i^*(\mathbf{y}_j)$ , so the

union bound implies that

$$\begin{aligned}\mathbb{E}_{\boldsymbol{\theta}_0}\{\phi_i(\mathbf{y}_j)\} &\leq \sum_{\boldsymbol{\theta}_{i1} \in \boldsymbol{\Theta}_i} e^{-\|\boldsymbol{\theta}_0 - \boldsymbol{\theta}_{i1}\|_{\mathbb{H}_j}^2/32} \leq D(ir/2, E_{i,r}, \|\cdot\|_{\mathbb{H}_j}) e^{-i^2 r^2/32}, \\ \sup_{\boldsymbol{\theta} \in E_{i,r}} \mathbb{E}_{\boldsymbol{\theta}}\{1 - \phi_i(\mathbf{y}_j)\} &\leq e^{\sup_{\boldsymbol{\theta}_{i1} \in \boldsymbol{\Theta}_i} (-\|\boldsymbol{\theta}_0 - \boldsymbol{\theta}_{i1}\|_{\mathbb{H}_j}^2/32)} \leq e^{-i^2 r^2/32}.\end{aligned}$$

Define  $\phi(\mathbf{y}_j) = \sup_{i \geq 1} \phi_i(\mathbf{y}_j)$ . Again, union bound implies that

$$\begin{aligned}\mathbb{E}_{\boldsymbol{\theta}_0}\{\phi(\mathbf{y}_j)\} &\leq \sum_{i \geq 1} D(ir/2, E_{i,r}, \|\cdot\|_{\mathbb{H}_j}) e^{-i^2 r^2/32} \leq D(r/2, \boldsymbol{\Theta}, \|\cdot\|_{\mathbb{H}_j}) e^{-r^2/32} (1 - e^{-1/32})^{-1} \\ &\leq 33D(r/2, \boldsymbol{\Theta}, \|\cdot\|_{\mathbb{H}_j}) e^{-r^2/32}, \\ \sup_{\{\boldsymbol{\theta} \in \boldsymbol{\Theta} : \|\boldsymbol{\theta} - \boldsymbol{\theta}_0\|_{\mathbb{H}_j} \geq ir\}} \mathbb{E}_{\boldsymbol{\theta}}\{1 - \phi(\mathbf{y}_j)\} &\leq e^{-i^2 r^2/32},\end{aligned}$$

for any  $r > 1$  and every  $i \geq 1$ . Since  $H_l \|\cdot\|_{\mathbb{H}} \leq \sqrt{k} \|\cdot\|_{\mathbb{H}_j} \leq H_u \|\cdot\|_{\mathbb{H}}$  according to Assumption A.2, we have

$$\begin{aligned}\mathbb{E}_{\boldsymbol{\theta}_0}\{\phi(\mathbf{y}_j)\} &\leq 33D(\sqrt{k}H_l^{-1}r/2, \boldsymbol{\Theta}, \|\cdot\|_{\mathbb{H}}) e^{-r^2/32}, \\ \sup_{\{\boldsymbol{\theta} \in \boldsymbol{\Theta} : \|\boldsymbol{\theta} - \boldsymbol{\theta}_0\|_{\mathbb{H}} \geq irH_l^{-1}\sqrt{k}\}} \mathbb{E}_{\boldsymbol{\theta}}\{1 - \phi(\mathbf{y}_j)\} &\leq e^{-i^2 r^2/32}.\end{aligned}$$

■

**Lemma 1.3** *Let  $p_{m,\boldsymbol{\theta}}(\mathbf{y}_j)$  be the pdf of  $\mathbf{y}_j \sim N_m(\mathbf{A}_j \boldsymbol{\theta}, \boldsymbol{\Sigma}_j)$  for any  $\boldsymbol{\theta} \in \mathbb{R}^l$ . Then, for any probability distribution  $\Pi$  on  $\mathbb{R}^l$  and  $x > 0$ ,*

$$\mathbb{P}_{\boldsymbol{\theta}_0} \left\{ \mathbf{y}_j : \int \left( \frac{p_{m,\boldsymbol{\theta}}}{p_{m,\boldsymbol{\theta}_0}} \right) (\mathbf{y}_j) d\Pi(\boldsymbol{\theta}) \leq e^{-\sigma_{0j}^2/2 - \|\boldsymbol{\mu}_0\|_{\mathbb{H}_j} x} \right\} \leq e^{-x^2/2}, \quad (33)$$

where  $\boldsymbol{\mu}_0 = \int (\boldsymbol{\theta} - \boldsymbol{\theta}_0) d\Pi(\boldsymbol{\theta})$  and  $\sigma_{0j}^2 = \int \|\boldsymbol{\theta} - \boldsymbol{\theta}_0\|_{\mathbb{H}_j}^2 d\Pi(\boldsymbol{\theta})$ . Consequently, for any probability distribution  $\Pi$  on  $\mathbb{R}^l$  and any  $r > 1$

$$\mathbb{P}_{\boldsymbol{\theta}_0} \left\{ \mathbf{y}_j : \int \left( \frac{p_{m,\boldsymbol{\theta}}}{p_{m,\boldsymbol{\theta}_0}} \right) (\mathbf{y}_j) d\Pi(\boldsymbol{\theta}) \geq e^{-r^2} \Pi \left( \boldsymbol{\theta} : \|\boldsymbol{\theta} - \boldsymbol{\theta}_0\|_{\mathbb{H}_j}^2 < r^2 \right) \right\} \geq 1 - e^{-r^2/8}. \quad (34)$$

**Proof** The pdf of  $\mathbf{y}_j$  implies that

$$\begin{aligned}&\log \left( \frac{p_{m,\boldsymbol{\theta}}}{p_{m,\boldsymbol{\theta}_0}} \right) (\mathbf{y}_j) \\ &= \frac{1}{2} \left\{ (\mathbf{y}_j - \mathbf{A}_j \boldsymbol{\theta}_0)^T \boldsymbol{\Sigma}_j^{-1} (\mathbf{y}_j - \mathbf{A}_j \boldsymbol{\theta}_0) - (\mathbf{y}_j - \mathbf{A}_j \boldsymbol{\theta})^T \boldsymbol{\Sigma}_j^{-1} (\mathbf{y}_j - \mathbf{A}_j \boldsymbol{\theta}_j) \right\} \\ &= \frac{1}{2} \left\{ \|\boldsymbol{\theta}_0\|_{\mathbb{H}_j}^2 - \|\boldsymbol{\theta}\|_{\mathbb{H}_j}^2 - 2\boldsymbol{\theta}_0^T \mathbf{A}_j^T \boldsymbol{\Sigma}_j^{-1} \mathbf{y}_j + 2\boldsymbol{\theta}^T \mathbf{A}_j^T \boldsymbol{\Sigma}_j^{-1} \mathbf{y}_j \right\}\end{aligned}$$



$$\begin{aligned}
&= \frac{1}{2} \left\{ 2\|\boldsymbol{\theta}_0\|_{\mathbb{H}_j}^2 - 2\langle \boldsymbol{\theta}_0, \boldsymbol{\theta} \rangle_{\mathbb{H}_j} + 2\mathbf{y}_j^T \boldsymbol{\Sigma}_j^{-1} \mathbf{A}_j(\boldsymbol{\theta} - \boldsymbol{\theta}_0) - \left( \|\boldsymbol{\theta}\|_{\mathbb{H}_j}^2 + \|\boldsymbol{\theta}_0\|_{\mathbb{H}_j}^2 - 2\langle \boldsymbol{\theta}_0, \boldsymbol{\theta} \rangle_{\mathbb{H}_j} \right) \right\} \\
&= \langle \boldsymbol{\theta}_0, \boldsymbol{\theta}_0 - \boldsymbol{\theta} \rangle_{\mathbb{H}_j} + \mathbf{y}_j^T \boldsymbol{\Sigma}_j^{-1} \mathbf{A}_j(\boldsymbol{\theta} - \boldsymbol{\theta}_0) - \frac{1}{2} \|\boldsymbol{\theta} - \boldsymbol{\theta}_0\|_{\mathbb{H}_j}^2.
\end{aligned} \tag{35}$$

Integrating with respect to  $\Pi$  on both sides and using the definitions of  $\boldsymbol{\mu}_0$  and  $\sigma_{0j}^2$ ,

$$\begin{aligned}
\int \log \left( \frac{p_{m,\boldsymbol{\theta}}}{p_{m,\boldsymbol{\theta}_0}} \right) (\mathbf{y}_j) d\Pi(\boldsymbol{\theta}) &= -\langle \boldsymbol{\theta}_0, \boldsymbol{\mu}_0 \rangle_{\mathbb{H}_j} + \mathbf{y}_j^T \boldsymbol{\Sigma}_j^{-1} \mathbf{A}_j \boldsymbol{\mu}_0 - \sigma_{0j}^2/2 \\
&= \boldsymbol{\mu}_0^T \mathbf{A}_j^T \boldsymbol{\Sigma}_j^{-1} (\mathbf{y}_j - \mathbf{A}_j \boldsymbol{\theta}_0) - \sigma_{0j}^2/2.
\end{aligned}$$

If  $\mathbf{y}_j \sim N_m(\mathbf{A}_j \boldsymbol{\theta}_0, \boldsymbol{\Sigma}_j)$ , then  $\boldsymbol{\mu}_0^T \mathbf{A}_j^T \boldsymbol{\Sigma}_j^{-1} (\mathbf{y}_j - \mathbf{A}_j \boldsymbol{\theta}_0) \sim N_m(0, \|\boldsymbol{\mu}_0\|_{\mathbb{H}_j}^2)$  and

$$\boldsymbol{\mu}_0^T \mathbf{A}_j^T \boldsymbol{\Sigma}_j^{-1} (\mathbf{y}_j - \mathbf{A}_j \boldsymbol{\theta}_0) - \sigma_{0j}^2/2 \sim N(-\sigma_{0j}^2/2, \|\boldsymbol{\mu}_0\|_{\mathbb{H}_j}^2).$$

An application of Jensen's inequality implies that

$$\begin{aligned}
&\mathbb{P}_{\boldsymbol{\theta}_0} \left\{ \int \left( \frac{p_{m,\boldsymbol{\theta}}}{p_{m,\boldsymbol{\theta}_0}} \right) (\mathbf{y}_j) d\Pi(\boldsymbol{\theta}) \leq e^{-\sigma_{0j}^2/2 - \|\boldsymbol{\mu}_0\|_{\mathbb{H}_j} x} \right\} \\
&\leq \mathbb{P}_{\boldsymbol{\theta}_0} \left( \int \log \left( \frac{p_{m,\boldsymbol{\theta}}}{p_{m,\boldsymbol{\theta}_0}} \right) (\mathbf{y}_j) d\Pi(\boldsymbol{\theta}) \leq -\sigma_{0j}^2/2 - \|\boldsymbol{\mu}_0\|_{\mathbb{H}_j} x \right) \\
&= \mathbb{P}_{\boldsymbol{\theta}_0} \left( \frac{\int \log \left( \frac{p_{m,\boldsymbol{\theta}}}{p_{m,\boldsymbol{\theta}_0}} \right) (\mathbf{y}_j) d\Pi(\boldsymbol{\theta}) + \sigma_{0j}^2/2}{\|\boldsymbol{\mu}_0\|_{\mathbb{H}_j}} \leq \frac{-\sigma_{0j}^2/2 - \|\boldsymbol{\mu}_0\|_{\mathbb{H}_j} x + \sigma_{0j}^2/2}{\|\boldsymbol{\mu}_0\|_{\mathbb{H}_j}} \right) = \Phi(-x) \leq e^{-x^2/2}.
\end{aligned}$$

Suppose the integration in (33) is restricted to the set  $\tilde{\Theta} = \{\boldsymbol{\theta} : \|\boldsymbol{\theta} - \boldsymbol{\theta}_0\|_{\mathbb{H}_j} \leq r\}$ . The prior  $\Pi$  in (33) can be renormalized to the truncated prior  $\tilde{\Pi} = \Pi/\Pi(\tilde{\Theta})$ . Using (33) for  $\tilde{\Pi}$  implies that

$$\mathbb{P}_{\boldsymbol{\theta}_0} \left\{ \{\Pi(\tilde{\Theta})\}^{-1} \int_{\tilde{\Theta}} \left( \frac{p_{m,\boldsymbol{\theta}}}{p_{m,\boldsymbol{\theta}_0}} \right) (\mathbf{y}_j) d\Pi(\boldsymbol{\theta}) \leq e^{-\sigma_{0j}^2/2 - \|\boldsymbol{\mu}_0\|_{\mathbb{H}_j} x} \right\} \leq e^{-x^2/2}. \tag{36}$$

On the other hand,

$$\begin{aligned}
\|\boldsymbol{\mu}_0\|_{\mathbb{H}_j}^2 &= \left\| \int_{\tilde{\Theta}} (\boldsymbol{\theta} - \boldsymbol{\theta}_0) d\tilde{\Pi}(\boldsymbol{\theta}) \right\|_{\mathbb{H}_j}^2 \stackrel{(i)}{\leq} \int_{\tilde{\Theta}} \|\boldsymbol{\theta} - \boldsymbol{\theta}_0\|_{\mathbb{H}_j}^2 d\tilde{\Pi}(\boldsymbol{\theta}) \leq r^2 \tilde{\Pi}(\tilde{\Theta}) = r^2, \\
\sigma_{0j}^2 &= \int_{\tilde{\Theta}} \|\boldsymbol{\theta} - \boldsymbol{\theta}_0\|_{\mathbb{H}_j}^2 d\tilde{\Pi}(\boldsymbol{\theta}) \leq r^2 \tilde{\Pi}(\tilde{\Theta}) = r^2,
\end{aligned} \tag{37}$$

where (i) follows from Jensen's inequality. Substituting (37) in (36) and setting  $x = r/2$ ,

$$e^{-\sigma_{0j}^2/2 - \|\boldsymbol{\mu}_0\|_{\mathbb{H}_j} r/2} \geq e^{-r^2/2 - r^2/2} = e^{-r^2} \tag{38}$$

and

$$\mathbb{P}_{\boldsymbol{\theta}_0} \left\{ \int \left( \frac{p_{m,\boldsymbol{\theta}}}{p_{m,\boldsymbol{\theta}_0}} \right) (\mathbf{y}_j) d\Pi(\boldsymbol{\theta}) \leq e^{-r^2} \Pi(\boldsymbol{\theta} : \|\boldsymbol{\theta} - \boldsymbol{\theta}_0\|_{\mathbb{H}_j} \leq r) \right\}$$

$$\leq \mathbb{P}_{\theta_0} \left\{ \int \left( \frac{p_{m,\theta}}{p_{m,\theta_0}} \right) (\mathbf{y}_j) d\Pi(\theta) \leq e^{-\sigma_{0j}^2/2 - \|\mu_0\|_{\mathbb{H}_j} r/2} \Pi(\theta : \|\theta - \theta_0\|_{\mathbb{H}_j} \leq r) \right\} \leq e^{-r^2/8}. \quad (39)$$

■

## 1.2 Proofs of Theorems 3.1 and 3.2

### 1.2.1 Proof of Theorem 3.1

We now prove the main result for the  $j$ th subset posterior distribution. For clarity of notation, in the rest of the proof, we use  $\mathbb{P}_{m,w_0}$  to denote the expectation  $\mathbb{E}_{0|\mathcal{S}_j, \mathcal{S}^*}$  in Theorem 3.1, and  $\mathbb{P}_{m,w}$  to denote the expectation under a possibly different space varying function  $w$ . Let  $\underline{r} = 1 + (8H_l)^{-1} + H_l^{-2} + 1/(1 - H_l^2/8)$ , and let  $r$  be any number such that  $r > \underline{r} > 1$ . Define  $\mathcal{W}_r = \{w : \|\mathbf{w}^* - \mathbf{w}_0^*\|_{\mathcal{S}} > 8r\epsilon_m\}$ . For any event  $\mathcal{A}$  and any test  $\phi(\mathbf{y}_j)$ ,

$$\begin{aligned} & \mathbb{P}_{m,w_0} \{ \Pi_m(\mathcal{W}_r | \mathbf{y}_j) \} = \mathbb{P}_{m,w_0} \{ \Pi_m(\mathcal{W}_r | \mathbf{y}_j) (\mathbf{1}_{\mathcal{A}^c} + \mathbf{1}_{\mathcal{A}}) \} \\ &= \mathbb{P}_{m,w_0} \{ \Pi_m(\mathcal{W}_r | \mathbf{y}_j) \mathbf{1}_{\mathcal{A}^c} \} + \mathbb{P}_{m,w_0} \{ \Pi_m(\mathcal{W}_r | \mathbf{y}_j) \mathbf{1}_{\mathcal{A}} \} \\ &\leq \mathbb{P}_{m,w_0} (\mathcal{A}^c) + \mathbb{P}_{m,w_0} \{ \Pi_m(\mathcal{W}_r | \mathbf{y}_j) \mathbf{1}_{\mathcal{A}} \} \\ &= \mathbb{P}_{m,w_0} (\mathcal{A}^c) + \mathbb{P}_{m,w_0} \{ \Pi_m(\mathcal{W}_r | \mathbf{y}_j) \mathbf{1}_{\mathcal{A}} \phi(\mathbf{y}_j) \} + \mathbb{P}_{m,w_0} [ \Pi_m(\mathcal{W}_r | \mathbf{y}_j) \mathbf{1}_{\mathcal{A}} \{1 - \phi(\mathbf{y}_j)\} ] \\ &\leq \mathbb{P}_{m,w_0} (\mathcal{A}^c) + \mathbb{P}_{m,w_0} \{ \phi(\mathbf{y}_j) \} + \mathbb{P}_{m,w_0} [ \Pi_m(\mathcal{W}_r | \mathbf{y}_j) \mathbf{1}_{\mathcal{A}} \{1 - \phi(\mathbf{y}_j)\} ] \\ &\leq \mathbb{P}_{m,w_0} (\mathcal{A}^c) + \mathbb{P}_{m,w_0} \{ \phi(\mathbf{y}_j) \} + \mathbb{P}_{m,w_0} \{ \Pi_m(\mathcal{F}_r^c | \mathbf{y}_j) \mathbf{1}_{\mathcal{A}} \} + \mathbb{P}_{m,w_0} [ \Pi_m(\mathcal{W}_r \cap \mathcal{F}_r | \mathbf{y}_j) \mathbf{1}_{\mathcal{A}} \{1 - \phi(\mathbf{y}_j)\} ] \\ &\equiv A_1 + A_2 + A_3 + A_4. \end{aligned} \quad (40)$$

We find upper bound  $A_1, A_2, A_3$  and  $A_4$ , respectively.

#### Bounding $A_1$

Use (34) in Lemma 1.3 to define

$$\mathcal{A} = \left\{ \mathbf{y}_j : \int \left( \frac{p_{m,w}}{p_{m,w_0}} \right) (\mathbf{y}_j) d\Pi(w) \geq e^{-m\epsilon_m^2 r^2} \Pi(w : \|\mathbf{w}^* - \mathbf{w}_0^*\|_{\mathbb{H}_j} < \sqrt{m}\epsilon_m r) \right\}. \quad (41)$$

Since  $\sqrt{m}\epsilon_m > 1$  by Assumption A.3, setting  $r^2$  to be  $m\epsilon_m^2 r^2$  in (34) implies that

$$\begin{aligned} A_1 &= \mathbb{P}_{m,w_0} (\mathcal{A}^c) = \mathbb{P}_{m,w_0} \left\{ \mathbf{y}_j : \int \left( \frac{p_{m,w}}{p_{m,w_0}} \right) (\mathbf{y}_j) d\Pi(w) < e^{-m\epsilon_m^2 r^2} \Pi(w : \|\mathbf{w}^* - \mathbf{w}_0^*\|_{\mathbb{H}_j}^2 < m\epsilon_m^2 r^2) \right\} \\ &\leq e^{-m\epsilon_m^2 r^2/8}. \end{aligned}$$

#### Bounding $A_2$

Let  $\Theta = \{\mathbf{w}^* = \{w(\mathbf{s}_1^*), \dots, w(\mathbf{s}_l^*)\}^T : w \in \mathcal{F}_r\} \subset \mathbb{R}^l$  and  $\theta_0 = \mathbf{w}_0^* = \{w_0(\mathbf{s}_1^*), \dots, w_0(\mathbf{s}_l^*)\}^T$ . Set  $r$  to be  $8H_l\sqrt{m}\epsilon_m r$  in Lemma 1.2 and use the test  $\phi(\mathbf{y}_j)$  defined for every  $8H_l\sqrt{m}\epsilon_m r > 8H_l\underline{r} > 1$

and every integer  $i \geq 1$  such that

$$\begin{aligned} \mathbb{P}_{m,w_0}\{\phi(\mathbf{y}_j)\} &\leq 33D(4\sqrt{mk}\epsilon_m r, \boldsymbol{\Theta}, \|\cdot\|_{\mathbb{H}})e^{-2m\epsilon_m^2 H_l^2 r^2} \\ \sup_{\{w: \mathbf{w}^* = w(\mathbf{s}^*) \in \boldsymbol{\Theta}, \|\mathbf{w}^* - \mathbf{w}_0^*\|_{\mathbb{H}} \geq 8i\sqrt{mk}\epsilon_m r\}} \mathbb{P}_{m,w}\{1 - \phi(\mathbf{y}_j)\} &\leq e^{-2i^2 m\epsilon_m^2 H_l^2 r^2}. \end{aligned} \quad (42)$$

Noting that  $A_2 = \mathbb{P}_{m,w_0}\{\phi(\mathbf{y}_j)\} = \mathbb{P}_{m,w_0}\{\phi(\mathbf{y}_j)\} \leq 33D(4\sqrt{mk}\epsilon_m r, \boldsymbol{\Theta}, \|\cdot\|_{\mathbb{H}})e^{-2m\epsilon_m^2 H_l^2 r^2}$  gives

$$\begin{aligned} A_2 &\stackrel{(i)}{\leq} 33D(4\epsilon_m r, \boldsymbol{\Theta}, \|\cdot\|_{\mathcal{S}})e^{-2m\epsilon_m^2 H_l^2 r^2} \stackrel{(ii)}{\leq} 33D(\epsilon_m, \boldsymbol{\Theta}, \|\cdot\|_{\mathcal{S}})e^{-2m\epsilon_m^2 H_l^2 r^2} \\ &\stackrel{(iii)}{\leq} 33e^{m\epsilon_m^2 H_l^2 r^2} e^{-2m\epsilon_m^2 H_l^2 r^2} = 33e^{-m\epsilon_m^2 H_l^2 r^2}, \end{aligned}$$

where (i) follows from the definitions of  $\|\cdot\|_{\mathbb{H}_j}$  and  $\|\cdot\|_{\mathcal{S}_j}$  norms, (ii) follows from the property of covering number because  $4r > 1$ , and (iii) follows from Assumption A.3.

### Bounding $A_3$

If the event  $\mathcal{A}$  occurs, then

$$\begin{aligned} \int \left( \frac{p_{m,w}}{p_{m,w_0}} \right) (\mathbf{y}_j) d\Pi(w) &\geq e^{-m\epsilon_m^2 r^2} \Pi(w : \|\mathbf{w}^* - \mathbf{w}_0^*\|_{\mathbb{H}_j} < \sqrt{m}\epsilon_m r) \\ &\geq e^{-m\epsilon_m^2 r^2} \Pi\left(w : \frac{\|\mathbf{w}^* - \mathbf{w}_0^*\|_{\mathbb{H}}}{\sqrt{mk}} < H_u^{-1}\epsilon_m r\right) \\ &= e^{-m\epsilon_m^2 r^2} \Pi(w : \|\mathbf{w}^* - \mathbf{w}_0^*\|_{\mathcal{S}} < H_u^{-1}\epsilon_m r) \\ &\geq e^{-m\epsilon_m^2 r^2} \Pi(w : \|\mathbf{w}^* - \mathbf{w}_0^*\|_{\mathcal{S}} < H_u^{-1}\epsilon_m) \\ &\geq e^{-m\epsilon_m^2 r^2 - m\epsilon_m^2} = e^{-m\epsilon_m^2 (r^2 + 1)}, \end{aligned}$$

where the last inequality follows from Assumption A.4. Assuming that the event  $\mathcal{A}$  occurs, the posterior probability of any event  $\mathcal{B} \subset \boldsymbol{\Theta}$  implied by the  $j$ th subset posterior of  $\mathbf{w}^*$  is bounded by

$$\Pi_m(\mathcal{B} | \mathbf{y}_j) \leq e^{m\epsilon_m^2 (r^2 + 1)} \int_{\mathcal{B}} \left( \frac{p_{m,w}}{p_{m,w_0}} \right) (\mathbf{y}_j) d\Pi(w). \quad (43)$$

Substituting  $\mathcal{B} = \mathcal{F}_r^c$  in (43) implies that

$$\begin{aligned} A_3 &= \mathbb{P}_{m,w_0}\{\Pi_m(\mathcal{F}_r^c | \mathbf{y}_j) \mathbf{1}_{\mathcal{A}}\} \leq e^{m\epsilon_m^2 (r^2 + 1)} \mathbb{P}_{m,w_0}\left\{\int_{\mathcal{F}_r^c} \left( \frac{p_{m,w}}{p_{m,w_0}} \right) (\mathbf{y}_j) d\Pi(w)\right\} \\ &= e^{m\epsilon_m^2 (r^2 + 1)} \int_{\mathcal{F}_r^c} \mathbb{P}_{m,w_0}\left\{\left( \frac{p_{m,w}}{p_{m,w_0}} \right) (\mathbf{y}_j)\right\} d\Pi(w) \leq e^{mk\epsilon_m^2 (r^2 + 1)} \int_{\mathcal{F}_r^c} d\Pi(w) \\ &= e^{m\epsilon_m^2 (r^2 + 1)} \Pi(\mathcal{F}_r^c) \stackrel{(i)}{\leq} e^{m\epsilon_m^2 (r^2 + 1)} e^{-2m\epsilon_m^2 r^2} = e^{-m\epsilon_m^2 (r^2 - 1)}, \end{aligned}$$

where (i) follows from Assumption A.3.

### Bounding $A_4$

With a little abuse of notation, let  $E_{i,r} = \{w \in \mathcal{F}_r : 8i\epsilon_m r \leq \|\mathbf{w}^* - \mathbf{w}_0^*\|_{\mathbb{B}} \leq 8(i+1)\epsilon_m r\}$  for  $i \geq 1$ , then

$$\begin{aligned}
A_4 &\leq e^{m\epsilon_m^2(r^2+1)} \sum_{i \geq 1} \mathbb{P}_{m,w_0} \int_{E_{i,r}} \left( \frac{p_{m,w}}{p_{m,w_0}} \right) (\mathbf{y}_j) \{1 - \phi(\mathbf{y}_j)\} d\Pi(w) \\
&= e^{m\epsilon_m^2(r^2+1)} \sum_{i \geq 1} \int_{E_{i,r}} \left[ \mathbb{P}_{m,w_0} \left( \frac{p_{m,w}}{p_{m,w_0}} \right) (\mathbf{y}_j) \{1 - \phi(\mathbf{y}_j)\} \right] d\Pi(w) \\
&= e^{m\epsilon_m^2(r^2+1)} \sum_{i \geq 1} \int_{E_{i,r}} \mathbb{P}_{m,w} \{1 - \phi(\mathbf{y}_j)\} d\Pi(w) \\
&\leq e^{m\epsilon_m^2(r^2+1)} \sum_{i \geq 1} \int_{E_{i,r}} \sup_{\{w \in \mathcal{F}_r : \|\mathbf{w}^* - \mathbf{w}_0^*\|_{\mathbb{H}} \geq 8i\sqrt{mk}\epsilon_m r\}} \mathbb{P}_{m,w} \{1 - \phi(\mathbf{y}_j)\} d\Pi(w) \\
&\stackrel{(i)}{\leq} e^{m\epsilon_m^2(r^2+1)} \sum_{i \geq 1} \int_{E_{i,r}} e^{-2i^2 m \epsilon_m^2 H_l^2 r^2} d\Pi(w) \leq e^{m\epsilon_m^2(r^2+1)} \sum_{i \geq 1} e^{-2i^2 m \epsilon_m^2 H_l^2 r^2} \\
&\stackrel{(ii)}{\leq} e^{-m\epsilon_m^2(r^2-1)} \left( 1 + \sum_{i \geq 1} e^{-2i} \right) = e^{-m\epsilon_m^2(r^2-1)} (1 - e^{-2})^{-1} \stackrel{(iii)}{\leq} 2e^{-m\epsilon_m^2(r^2-1)},
\end{aligned}$$

where (i) follows from (42), (ii) follows since  $r > \underline{r} > H_l^{-2} > 1$  so that  $m\epsilon_m^2 H_l^2 r^2 > 1$ , and (iii) follows because  $1/(1 - e^{-2}) < 2$ .

We use the upper bounds for  $A_1, A_2, A_3$  and  $A_4$  to obtain a general upper bound for the risk of  $j$ th subset posterior distribution. The expectation of the posterior risk can be bounded as

$$\begin{aligned}
&\mathbb{P}_{m,w_0} \left\{ \int \|\mathbf{w}^* - \mathbf{w}_0^*\|_{\mathcal{S}}^2 d\Pi_m(w \mid \mathbf{y}_j) \right\} = \mathbb{P}_{m,w_0} \left\{ \int_0^\infty \Pi_m(\|\mathbf{w}^* - \mathbf{w}_0^*\|_{\mathcal{S}}^2 > t \mid \mathbf{y}_j) dt \right\} \\
&= \mathbb{P}_{m,w_0} \left\{ \int_0^{(8\epsilon_m \underline{r})^2} \Pi_m(\|\mathbf{w}^* - \mathbf{w}_0^*\|_{\mathcal{S}}^2 > t \mid \mathbf{y}_j) dt \right\} + \mathbb{P}_{m,w_0} \left\{ \int_{(8\epsilon_m \underline{r})^2}^\infty \Pi_m(\|\mathbf{w}^* - \mathbf{w}_0^*\|_{\mathcal{S}}^2 > t \mid \mathbf{y}_j) dt \right\} \\
&\stackrel{(i)}{\leq} 64\underline{r}^2 \epsilon_m^2 + 128\epsilon_m^2 \mathbb{P}_{m,w_0} \left\{ \int_{\underline{r}}^\infty r \Pi_m(\|\mathbf{w}^* - \mathbf{w}_0^*\|_{\mathcal{S}} > 8r\epsilon_m \mid \mathbf{y}_j) dr \right\} \\
&\leq 64\underline{r}^2 \epsilon_m^2 + 128\epsilon_m^2 \mathbb{P}_{m,w_0} \left\{ \int_{\underline{r}}^\infty r (A_1 + A_2 + A_3 + A_4) dr \right\} \\
&\leq 64\underline{r}^2 \epsilon_m^2 + 128\epsilon_m^2 \mathbb{P}_{m,w_0} \left\{ \int_{\underline{r}}^\infty r \left( e^{-m\epsilon_m^2 r^2/8} + 33e^{-m\epsilon_m^2 H_l^2 r^2} + e^{-m\epsilon_m^2(r^2-1)} + 2e^{-m\epsilon_m^2(r^2-1)} \right) dr \right\} \\
&\stackrel{(ii)}{\leq} 64\underline{r}^2 \epsilon_m^2 + 128\epsilon_m^2 \mathbb{P}_{m,w_0} \left\{ \int_{\underline{r}}^\infty r \left( e^{-m\epsilon_m^2 H_l^2 r^2/8} + 33e^{-m\epsilon_m^2 H_l^2 r^2/8} + e^{-m\epsilon_m^2 H_l^2 r^2/8} + 2e^{-m\epsilon_m^2 H_l^2 r^2/8} \right) dr \right\} \\
&\stackrel{(iii)}{\leq} 64\underline{r}^2 \epsilon_m^2 + 128\epsilon_m^2 \cdot 37 \cdot \frac{8}{m\epsilon_m^2 H_l^2} \int_0^\infty z e^{-z^2} dz \\
&\stackrel{(iv)}{\leq} \left( 64\underline{r}^2 + 128 \cdot 37 \cdot \frac{8}{2m\epsilon_m^2 H_l^2} \right) \epsilon_m^2 \stackrel{(v)}{<} \left\{ 64 \left( 1 + \frac{1}{8H_l} + \frac{1}{H_l^2} + \frac{1}{1 - H_l^2/8} \right)^2 + \frac{2^{15}}{H_l^2} \right\} \epsilon_m^2 \equiv c(H_l) \epsilon_m^2.
\end{aligned}$$

In the display above, (i) is because  $\Pi_m(\|\mathbf{w}^* - \mathbf{w}_0^*\|_S^2 > t \mid \mathbf{y}_j) \leq 1$  and we use a change of variable  $t = (8r\epsilon_m)^2$ . (ii) follows because  $1/8 > H_l^2/8$ ,  $H_l^2 > H_l^2/8$ , and  $r^2 - 1 = H_l^2 r^2/8 + (1 - H_l^2/8)r^2 - 1 > H_l^2 r^2/8 + (1 - H_l^2/8)\{\underline{r}^2 - 1/(1 - H_l^2/8)\} > H_l^2 r^2/8$ . For (iii) we use a change of variable  $z = \sqrt{m\epsilon_m^2 H_l^2/8} \cdot r$ . (iv) follows from  $\int_0^\infty z e^{-z^2} dz = 1/2$ . (v) follows from  $m\epsilon_m^2 \geq 1$  and the definition of  $\underline{r}$ . Finally, Assumption A.5 implies that

$$\mathbb{P}_{m,w_0} \left\{ \int \|\mathbf{w}^* - \mathbf{w}_0^*\|_2^2 d\Pi_m(w \mid \mathbf{y}_j) \right\} \leq C_u^2 \mathbb{P}_{m,w_0} \left\{ \int \|\mathbf{w}^* - \mathbf{w}_0^*\|_S^2 d\Pi_m(w \mid \mathbf{y}_j) \right\} \leq C_u^2 c(H_l) \epsilon_m^2.$$

This has proved Theorem 3.1.

### 1.2.2 Proof of Theorem 3.2

We now use the bound in Theorem 3.1 to obtain an upper bound on the DISK pseudo posterior distribution. First, we note that

$$W_2^2 \{ \bar{\Pi}(\cdot \mid \mathbf{y}_1, \dots, \mathbf{y}_k), \delta_{\mathbf{w}_0^*} \} = \int \|\mathbf{w}^* - \mathbf{w}_0^*\|_2^2 d\bar{\Pi}(w \mid \mathbf{y}_1, \dots, \mathbf{y}_k).$$

Second, Lemma 1.7 in Srivastava et al. [68] implies that

$$W_2^2 \{ \bar{\Pi}(\cdot \mid \mathbf{y}_1, \dots, \mathbf{y}_k), \delta_{\mathbf{w}_0^*} \} \leq \frac{1}{k} \sum_{j=1}^k W_2^2 \{ \Pi_m(\cdot \mid \mathbf{y}_j), \delta_{\mathbf{w}_0^*} \} = \frac{1}{k} \sum_{j=1}^k \int \|\mathbf{w}^* - \mathbf{w}_0^*\|_2^2 d\Pi_m(w \mid \mathbf{y}_j).$$

Therefore, Theorem 3.1 implies that

$$\begin{aligned} \mathbb{E}_{0|\mathcal{S}, \mathcal{S}^*} \int \|\mathbf{w}^* - \mathbf{w}_0^*\|_2^2 d\bar{\Pi}(w \mid \mathbf{y}_1, \dots, \mathbf{y}_k) &\leq \frac{1}{k} \sum_{j=1}^k \mathbb{E}_{0|\mathcal{S}_j, \mathcal{S}^*} \int \|\mathbf{w}^* - \mathbf{w}_0^*\|_2^2 d\Pi_m(w \mid \mathbf{y}_j) \\ &\leq \frac{l}{k} \sum_{j=1}^k C_u^2 c(H_l) \epsilon_m^2 = C_u^2 c(H_l) \epsilon_m^2, \end{aligned}$$

which has proved Theorem 3.2.

## 2 Proof of Theorems in Section 3.6

Recall that the spatial regression model with a GP prior considered in Section 3 is

$$y(\mathbf{s}_i) = w(\mathbf{s}_i) + \epsilon(\mathbf{s}_i), \quad \epsilon(\mathbf{s}_i) \sim N(0, \tau_0^2), \quad i = 1, \dots, n, \quad w(\cdot) \sim \text{GP}\{0, C_\alpha(\cdot, \cdot)\}. \quad (44)$$

Writing this model for the  $n$  locations in  $\mathcal{S}$  gives

$$\mathbf{y} = \mathbf{w}_0 + \boldsymbol{\epsilon}, \quad \boldsymbol{\epsilon} \mid \mathcal{S} \sim N(\mathbf{0}, \tau_0^2 \mathbf{I}), \quad \mathbf{y} \mid \mathcal{S} \sim N(\mathbf{w}_0, \tau_0^2 \mathbf{I}), \quad (45)$$

where  $\mathbf{w}_0 = \{w_0(\mathbf{s}_1), \dots, w_0(\mathbf{s}_n)\}$  and  $\boldsymbol{\epsilon} = \{\epsilon(\mathbf{s}_1), \dots, \epsilon(\mathbf{s}_n)\}$  are the true value of the residual spatial surface and white noise realized at the locations in  $\mathcal{S}$ . Let  $\mathbf{s} \in \mathcal{D}$  be a location,  $w_0(\mathbf{s})$  be the true value of the residual spatial surface,  $\mathbb{E}_{\mathbf{s}^*}$ ,  $\mathbb{E}_0$ ,  $\mathbb{E}_{\mathcal{S}}$ , and  $\mathbb{E}_{0|\mathcal{S}}$  respectively be the expectations with respect to the distributions of  $\mathbf{s}^*$ ,  $(\mathcal{S}, \mathbf{y})$ ,  $\mathcal{S}$ , and  $\mathbf{y}$  given  $\mathcal{S}$ . If  $\bar{w}(\mathbf{s}^*)$  is a random variable that follows the DISK posterior for estimating  $w_0(\mathbf{s}^*)$ , then  $\bar{w}(\mathbf{s}^*)$  has the density  $N(\bar{m}, \bar{v})$ , where

$$\bar{m} = \frac{1}{k} \sum_{j=1}^k \mathbf{c}_{j,*}^T (\mathbf{C}_{j,j} + \frac{\tau_0^2}{k} \mathbf{I})^{-1} \mathbf{y}_j, \quad \bar{v}^{1/2} = \frac{1}{k} \sum_{j=1}^k v_j^{1/2}, \quad v_j = c_{*,*} - \mathbf{c}_{j,*}^T (\mathbf{C}_{j,j} + \frac{\tau_0^2}{k} \mathbf{I})^{-1} \mathbf{c}_{j,*}, \quad (46)$$

$c_{*,*} = \text{cov}\{w(\mathbf{s}^*), w(\mathbf{s}^*)\}$ , and  $\mathbf{c}_{j,*}^T = [\text{cov}\{w(\mathbf{s}_{j1}), w(\mathbf{s}^*)\}, \dots, \text{cov}\{w(\mathbf{s}_{jm}), w(\mathbf{s}^*)\}]$ . The Bayes  $L_2$ -risk in estimating  $w_0$  using the DISK posterior is defined as

$$\mathbb{E}_0 [\mathbb{E}_{\mathbf{s}^*} \{\bar{w}(\mathbf{s}^*) - w_0(\mathbf{s}^*)\}^2] \stackrel{(i)}{=} \mathbb{E}_{\mathcal{S}} \int_{\mathcal{D}} \mathbb{E}_{0|\mathcal{S}} \{\bar{w}(\mathbf{s}^*) - w_0(\mathbf{s}^*)\}^2 \mathbb{P}_{\mathbf{s}}(d\mathbf{s}^*), \quad (47)$$

where (i) follows from Fubini's theorem. Using bias-variance decomposition,

$$\begin{aligned} \mathbb{E}_{0|\mathcal{S}} \{\bar{w}(\mathbf{s}^*) - w_0(\mathbf{s}^*)\}^2 &= \mathbb{E}_{0|\mathcal{S}} [\bar{w}(\mathbf{s}^*) - \mathbb{E}_{0|\mathcal{S}} \{\bar{w}(\mathbf{s}^*)\} + \mathbb{E}_{0|\mathcal{S}} \{\bar{w}(\mathbf{s}^*)\} - w_0(\mathbf{s}^*)]^2 \\ &= [\mathbb{E}_{0|\mathcal{S}} \{\bar{w}(\mathbf{s}^*)\} - w_0(\mathbf{s}^*)]^2 + \mathbb{E}_{0|\mathcal{S}} [\bar{w}(\mathbf{s}^*) - \mathbb{E}_{0|\mathcal{S}} \{\bar{w}(\mathbf{s}^*)\}]^2 \\ &\equiv \text{bias}_{0|\mathcal{S}}^2 \{\bar{w}(\mathbf{s}^*)\} + \text{var}_{0|\mathcal{S}} \{\bar{w}(\mathbf{s}^*)\}. \end{aligned}$$

If  $\mathbf{c}_j^T(\cdot) = [\text{cov}\{w(\cdot), w(\mathbf{s}_{j1})\}, \dots, \text{cov}\{w(\cdot), w(\mathbf{s}_{jm})\}] = \{C_{\alpha}(\mathbf{s}_{j1}, \cdot), \dots, C_{\alpha}(\mathbf{s}_{jm}, \cdot)\}$ ,  $\mathbf{c}^T(\cdot) = \{\mathbf{c}_1^T(\cdot), \dots, \mathbf{c}_k^T(\cdot)\}$ ,  $\mathbf{w}_{0j}^T = \{w_0(\mathbf{s}_{j1}), \dots, w_0(\mathbf{s}_{jm})\}$ , and  $\mathbf{w}_0^T = \{\mathbf{w}_{01}^T, \dots, \mathbf{w}_{0k}^T\}$ , then the distribution of  $\bar{w}(\mathbf{s}^*)$  in (46) implies that

$$\mathbb{E}_{0|\mathcal{S}} \{\bar{w}(\mathbf{s}^*)\} = \frac{1}{k} \sum_{j=1}^k \mathbf{c}(\mathbf{s}^*) \left( \mathbf{C}_{j,j} + \frac{\tau_0^2}{k} \mathbf{I} \right)^{-1} \mathbf{w}_{0j} = \mathbf{c}^T(\mathbf{s}^*) (k \mathbf{L} + \tau_0^2 \mathbf{I})^{-1} \mathbf{w}_0,$$

$$\text{var}_{0|\mathcal{S}} \{\bar{w}(\mathbf{s}^*)\} = \text{var}_{0|\mathcal{S}} [\mathbb{E}\{\bar{w}(\mathbf{s}^*) \mid \mathbf{y}\}] + \mathbb{E}_{0|\mathcal{S}} [\text{var}\{\bar{w}(\mathbf{s}^*) \mid \mathbf{y}\}] = \tau_0^2 \mathbf{c}^T(\mathbf{s}^*) (k \mathbf{L} + \tau_0^2 \mathbf{I})^{-2} \mathbf{c}(\mathbf{s}^*) + \bar{v}(\mathbf{s}^*),$$

where  $\mathbf{L}$  is a block-diagonal matrix with  $\mathbf{C}_{1,1}, \dots, \mathbf{C}_{k,k}$  along the diagonal; therefore, the Bayes  $L_2$ -risk in (47) is

$$\mathbb{E}_{\mathbf{s}^*} \mathbb{E}_{\mathcal{S}} \{\mathbf{c}_*^T (k \mathbf{L} + \tau_0^2 \mathbf{I})^{-1} \mathbf{w}_0 - w_0(\mathbf{s}^*)\}^2 + \tau_0^2 \mathbb{E}_{\mathbf{s}^*} \mathbb{E}_{\mathcal{S}} \{\mathbf{c}_*^T (k \mathbf{L} + \tau_0^2 \mathbf{I})^{-2} \mathbf{c}_*\} + \mathbb{E}_{\mathbf{s}^*} \mathbb{E}_{\mathcal{S}} \bar{v}(\mathbf{s}^*). \quad (48)$$

## 2.1 Proof of Theorem 3.4

The next three sections find upper bounds for each of the three terms in (48). The conclusion of Theorem 3.4 follows directly by combining the three upper bounds.

### 2.1.1 An upper bound for the squared bias

Consider the squared-bias term in (48). For ease of presentation, assume that  $\{\mathbf{s}_1, \dots, \mathbf{s}_n\}$  are relabeled to  $\{\mathbf{s}_{11}, \dots, \mathbf{s}_{1m}, \dots, \mathbf{s}_{k1}, \dots, \mathbf{s}_{km}\}$  corresponding to the  $k$  subsets. Define  $\xi_{\mathbf{s}_{ji}} = C_{\alpha}(\mathbf{s}_{ji}, \cdot)$ ,

$$\begin{aligned} \mathbf{w}_0^T &= (\langle w_0, \xi_{\mathbf{s}_{11}} \rangle_{\mathbb{H}}, \dots, \langle w_0, \xi_{\mathbf{s}_{1m}} \rangle_{\mathbb{H}}, \dots, \langle w_0, \xi_{\mathbf{s}_{k1}} \rangle_{\mathbb{H}}, \dots, \langle w_0, \xi_{\mathbf{s}_{km}} \rangle_{\mathbb{H}}) \equiv \{\mathbf{w}_{01}^T, \dots, \mathbf{w}_{0k}^T\}, \\ \mathbf{c}^T(\cdot) &= (\xi_{\mathbf{s}_{11}}, \dots, \xi_{\mathbf{s}_{1m}}, \dots, \xi_{\mathbf{s}_{k1}}, \dots, \xi_{\mathbf{s}_{km}}) = \{\mathbf{c}_1^T(\cdot), \dots, \mathbf{c}_k^T(\cdot)\} \equiv \{\mathbf{c}_1^T, \dots, \mathbf{c}_k^T\}. \end{aligned} \quad (49)$$

The following lemma provides an upper bound on the squared bias of the DISK posterior.

**Lemma 2.1** *If Assumptions B.1–B.3 in the main paper hold, then*

$$\begin{aligned} \mathbb{E}_{\mathbf{s}^*} \mathbb{E}_{\mathcal{S}} \{ \mathbf{c}_*^T (k \mathbf{L} + \tau_0^2 \mathbf{I})^{-1} \mathbf{w}_0 - w_0(\mathbf{s}^*) \}^2 \leq \\ \frac{8\tau_0^2}{n} \|w_0\|_{\mathbb{H}}^2 + \|w_0\|_{\mathbb{H}}^2 \inf_{d \in \mathbb{N}} \left[ \frac{8n}{\tau_0^2} \rho^4 \text{tr}(C_{\alpha}) \text{tr}(C_{\alpha}^d) + \mu_1 \left\{ \frac{Ab(m, d, r) \rho^2 \gamma(\frac{\tau_0^2}{n})}{\sqrt{m}} \right\}^r \right]. \end{aligned}$$

**Proof** This is an extension of Lemma 6 in Zhang et al. [84] for the DISK posterior and it is proved following similar arguments.

Based on the term  $\mathbf{w}_0^T (k \mathbf{L} + \tau_0^2 \mathbf{I})^{-1} \mathbf{c}$  in (48), define  $\Delta_j$  ( $j = 1, \dots, k$ ) and  $\Delta$  as

$$\begin{aligned} \Delta_j(\cdot) &= \mathbf{y}_j^T (\mathbf{C}_{j,j} + \frac{\tau_0^2}{k} \mathbf{I})^{-1} \mathbf{c}_j(\cdot) - w_0(\cdot) \equiv \tilde{w}_j(\cdot) - w_0(\cdot), \\ \Delta(\cdot) &= \mathbf{y}^T (k \mathbf{L} + \tau_0^2 \mathbf{I})^{-1} \mathbf{c}(\cdot) - w_0(\cdot) = \frac{1}{k} \sum_{j=1}^k \{ \tilde{w}_j(\cdot) - w_0(\cdot) \} = \frac{1}{k} \sum_{j=1}^k \Delta_j(\cdot) \end{aligned} \quad (50)$$

so that  $\mathbb{E}_{0|\mathcal{S}}(\Delta) = \mathbf{w}_0^T (k \mathbf{L} + \tau_0^2 \mathbf{I})^{-1} \mathbf{c}(\cdot) - w_0(\cdot) = k^{-1} \sum_{j=1}^k \mathbb{E}_{0|\mathcal{S}}(\Delta_j)$  and  $\mathbb{E}_{\mathcal{S}} \|\mathbb{E}_{0|\mathcal{S}}(\Delta)\|_2^2$  yields the bias term in (48). Jensen's inequality implies that  $\|\mathbb{E}_{0|\mathcal{S}}(\Delta)\|_2^2 \leq k^{-1} \sum_{j=1}^k \|\mathbb{E}_{0|\mathcal{S}}(\Delta_j)\|_2^2$ , so we only need to find upper bounds for  $\|\mathbb{E}_{0|\mathcal{S}}(\Delta_j)\|_2^2$  ( $j = 1, \dots, k$ ).

The optimization problem below has  $\tilde{w}_j(\cdot)$  defined in (50) as its solution,

$$\text{argmin}_{w \in \mathcal{H}} \sum_{i=1}^m \frac{\{w(\mathbf{s}_{ji}) - y(\mathbf{s}_{ji})\}^2}{2\tau_0^2/k} + \frac{1}{2} \|w\|_{\mathbb{H}}^2, \quad j = 1, \dots, k. \quad (51)$$

Differentiating (51) and taking expectations with respect to  $\mathbb{E}_{0|\mathcal{S}}$  implies that

$$\sum_{i=1}^m \mathbb{E}_{0|\mathcal{S}} \{ \tilde{w}_j(\mathbf{s}_{ji}) - y(\mathbf{s}_{ji}) \} \xi_{\mathbf{s}_{ji}} + \frac{\tau_0^2}{k} \mathbb{E}_{0|\mathcal{S}} \tilde{w}_j(\cdot) = \sum_{i=1}^m \langle \mathbb{E}_{0|\mathcal{S}}(\Delta_j), \xi_{\mathbf{s}_{ji}} \rangle_{\mathbb{H}} \xi_{\mathbf{s}_{ji}} + \frac{\tau_0^2}{k} \mathbb{E}_{0|\mathcal{S}}(\tilde{w}_j) = 0, \quad (52)$$

where the last inequality follows because  $y(\mathbf{s}_{ji}) = \langle w_0, \xi_{\mathbf{s}_{ji}} \rangle_{\mathbb{H}} + \langle \epsilon, \xi_{\mathbf{s}_{ji}} \rangle_{\mathbb{H}}$  and  $\langle \mathbb{E}_{0|\mathcal{S}}(\epsilon), \xi_{\mathbf{s}_{ji}} \rangle_{\mathbb{H}} = 0$ . Using (50),  $\Delta_j = \tilde{w}_j - w_0$ ,  $\mathbb{E}_{0|\mathcal{S}}(\tilde{w}_j) = \mathbb{E}_{0|\mathcal{S}}(\Delta_j) + w_0$ , and dividing by  $m$  in (52), we obtain that

$$\frac{1}{m} \sum_{i=1}^m \langle \mathbb{E}_{0|\mathcal{S}}(\Delta_j), \xi_{\mathbf{s}_{ji}} \rangle_{\mathbb{H}} \xi_{\mathbf{s}_{ji}} + \frac{\tau_0^2}{km} \mathbb{E}_{0|\mathcal{S}}(\Delta_j) = -\frac{\tau_0^2}{km} w_0. \quad (53)$$

If we define the  $j$ th sample covariance operator as  $\hat{\Sigma}_j = \frac{1}{m} \sum_{i=1}^m \xi_{\mathbf{s}_{ji}} \otimes \xi_{\mathbf{s}_{ji}}$ , then (53) reduces to

$$\left( \hat{\Sigma}_j + \frac{\tau_0^2}{km} \mathbf{I} \right) \mathbb{E}_{0|\mathcal{S}}(\Delta_j) = -\frac{\tau_0^2}{km} w_0 \implies \|\mathbb{E}_{0|\mathcal{S}}(\Delta_j)\|_{\mathbb{H}} \leq \|w_0\|_{\mathbb{H}}, \quad j = 1, \dots, k, \quad (54)$$

where the last inequality follows because  $\hat{\Sigma}_j$  is a positive semi-definite matrix.

The rest of the proof finds an upper bound for  $\|\mathbb{E}_{0|\mathcal{S}}(\Delta_j)\|_2^2$ . We now reduce this problem to a finite dimensional one indexed by a fixed  $d \in \mathbb{N}$ . Let  $\boldsymbol{\delta}_j = (\delta_{j1}, \dots, \delta_{jd}, \delta_{j(d+1)}, \dots, \delta_{j\infty}) \in L_2(\mathbb{N})$  such that

$$\mathbb{E}_{0|\mathcal{S}}(\Delta_j) = \sum_{i=1}^{\infty} \delta_{ji} \phi_i, \quad \delta_{ji} = \langle \mathbb{E}_{0|\mathcal{S}}(\Delta_j), \phi_i \rangle_{L^2(\mathbb{P})}, \quad \|\mathbb{E}_{0|\mathcal{S}}(\Delta_j)\|_2^2 = \sum_{i=1}^{\infty} \delta_{ji}^2, \quad j = 1, \dots, k. \quad (55)$$

Define the vectors  $\boldsymbol{\delta}_j^\downarrow$  as  $(\delta_{j1}, \dots, \delta_{jd})$  and  $\boldsymbol{\delta}_j^\uparrow$  as  $(\delta_{j(d+1)}, \dots, \delta_{j\infty})$ , so  $\|\mathbb{E}_{0|\mathcal{S}}(\Delta_j)\|_2^2 = \|\boldsymbol{\delta}_j^\downarrow\|_2^2 + \|\boldsymbol{\delta}_j^\uparrow\|_2^2$  and we upper bound  $\|\mathbb{E}_{0|\mathcal{S}}(\Delta_j)\|_2^2$  by separately upper bounding  $\|\boldsymbol{\delta}_j^\downarrow\|_2^2$  and  $\|\boldsymbol{\delta}_j^\uparrow\|_2^2$ . Using the expansion  $C_{\boldsymbol{\alpha}}(\mathbf{s}, \mathbf{s}') = \sum_{j=1}^{\infty} \mu_j \phi_j(\mathbf{s}) \phi_j(\mathbf{s}')$  for any  $\mathbf{s}, \mathbf{s}' \in \mathcal{D}$ , we have the following upper bound for  $\|\boldsymbol{\delta}_j^\uparrow\|_2^2$ :

$$\|\boldsymbol{\delta}_j^\uparrow\|_2^2 = \frac{\mu_{d+1}}{\mu_{d+1}} \sum_{i=d+1}^{\infty} \delta_{ji}^2 \leq \mu_{d+1} \sum_{i=d+1}^{\infty} \frac{\delta_{ji}^2}{\mu_i} \stackrel{(i)}{\leq} \mu_{d+1} \|\mathbb{E}_{0|\mathcal{S}}(\Delta_j)\|_{\mathbb{H}}^2 \stackrel{(ii)}{\leq} \mu_{d+1} \|w_0\|_{\mathbb{H}}^2, \quad (56)$$

where (i) follows because  $\|\mathbb{E}_{0|\mathcal{S}}(\Delta_j)\|_{\mathbb{H}}^2 = \sum_{i=1}^{\infty} \delta_{ji}^2 / \mu_i$  and (ii) follows from (54).

We then derive an upper bound for  $\|\boldsymbol{\delta}_j^\downarrow\|_2^2$ . Let  $\mathbf{M} = \text{diag}(\mu_1, \dots, \mu_d) \in \mathbb{R}^{d \times d}$ ,  $\boldsymbol{\Phi}^j \in \mathbb{R}^{m \times d}$  be a matrix such that

$$\boldsymbol{\Phi}_{ih}^j = \phi_h(\mathbf{s}_{ji}), \quad i = 1, \dots, m, \quad h = 1, \dots, d, \quad j = 1, \dots, k, \quad (57)$$

$w_0 = \sum_{i=1}^{\infty} \theta_i \phi_i$ , and the tail error vector  $\mathbf{v}_j = (v_{j1}, \dots, v_{jm})^T \in \mathbb{R}^m$  ( $j = 1, \dots, k$ ) such that

$$v_{ji} = \sum_{h=d+1}^{\infty} \delta_{jh} \phi_h(\mathbf{s}_{ji}), \quad i = 1, \dots, m.$$

For any  $g \in \{1, \dots, d\}$ , taking the  $\mathbb{H}$ -inner product with respect  $\phi_g$  in (54) yields

$$\left\langle \left( \frac{1}{m} \sum_{i=1}^m \xi_{\mathbf{s}_{ji}} \otimes \xi_{\mathbf{s}_{ji}} + \frac{\tau_0^2}{km} \mathbf{I} \right) \mathbb{E}_{0|\mathcal{S}}(\Delta_j), \phi_g \right\rangle_{\mathbb{H}} = -\frac{\tau_0^2}{km} \langle w_0, \phi_g \rangle_{\mathbb{H}} = -\frac{\tau_0^2}{km} \frac{\theta_g}{\mu_g}, \quad j = 1, \dots, k. \quad (58)$$

Expanding the left hand side in (58), we obtain that

$$\frac{1}{m} \sum_{i=1}^m \langle \phi_g, \xi_{\mathbf{s}_{ji}} \rangle_{\mathbb{H}} \mathbb{E}_{0|\mathcal{S}} \{ \Delta_j(\mathbf{s}_{ji}) \} + \frac{\tau_0^2}{km} \langle \phi_g, \mathbb{E}_{0|\mathcal{S}}(\Delta_j) \rangle_{\mathbb{H}} = \frac{1}{m} \sum_{i=1}^m \phi_g(\mathbf{s}_{ji}) \mathbb{E}_{0|\mathcal{S}} \{ \Delta_j(\mathbf{s}_{ji}) \} + \frac{\tau_0^2}{km} \frac{\delta_{jg}}{\mu_g}.$$



The term  $\frac{1}{m} \sum_{i=1}^m \phi_g(\mathbf{s}_{ji}) \mathbb{E}_{0|\mathcal{S}} \{\Delta_j(\mathbf{s}_{ji})\}$  on the right hand side is

$$\begin{aligned} &= \frac{1}{m} \sum_{i=1}^m \mathbf{\Phi}_{ig}^j \sum_{h=1}^d \delta_{jh} \phi_h(\mathbf{s}_{ji}) + \frac{1}{m} \sum_{i=1}^m \mathbf{\Phi}_{ig}^j \sum_{h=d+1}^{\infty} \delta_{jh} \phi_h(\mathbf{s}_{ji}) = \frac{1}{m} \sum_{h=1}^d \delta_{jh} \sum_{i=1}^m \mathbf{\Phi}_{ig}^j \mathbf{\Phi}_{ih}^j + \frac{1}{m} \sum_{i=1}^m \mathbf{\Phi}_{ig}^j v_{ji} \\ &= \frac{1}{m} \sum_{h=1}^d \delta_{jh} \left( \mathbf{\Phi}^{jT} \mathbf{\Phi}^j \right)_{gh} + \frac{1}{m} \sum_{i=1}^m \left( \mathbf{\Phi}^{jT} v_j \right)_g = \frac{1}{m} \left( \mathbf{\Phi}^{jT} \mathbf{\Phi}^j \boldsymbol{\delta}^\downarrow \right)_g + \frac{1}{m} \left( \mathbf{\Phi}^{jT} \mathbf{v}_j \right)_g. \end{aligned} \quad (59)$$

Substitute (59) in (58) for  $g = 1, \dots, d$  to obtain that

$$\begin{aligned} \frac{1}{m} \mathbf{\Phi}^{jT} \mathbf{\Phi}^j \boldsymbol{\delta}_j^\downarrow + \frac{1}{m} \mathbf{\Phi}^{jT} \mathbf{v}_j + \frac{\tau_0^2}{km} \mathbf{M}^{-1} \boldsymbol{\delta}_j^\downarrow &= -\frac{\tau_0^2}{km} \mathbf{M}^{-1} \boldsymbol{\theta}^\downarrow \\ \left( \frac{1}{m} \mathbf{\Phi}^{jT} \mathbf{\Phi}^j + \frac{\tau_0^2}{km} \mathbf{M}^{-1} \right) \boldsymbol{\delta}_j^\downarrow &= -\frac{\tau_0^2}{km} \mathbf{M}^{-1} \boldsymbol{\theta}^\downarrow - \frac{1}{m} \mathbf{\Phi}^{jT} \mathbf{v}_j. \end{aligned} \quad (60)$$

The proof is completed by showing that the right hand side expression in (60) gives an upper bound for  $\|\boldsymbol{\delta}_j^\downarrow\|_2^2$ . Define  $\mathbf{Q} = \left( \mathbf{I} + \frac{\tau_0^2}{km} \mathbf{M}^{-1} \right)^{1/2}$ , then

$$\frac{1}{m} \mathbf{\Phi}^{jT} \mathbf{\Phi}^j + \frac{\tau_0^2}{km} \mathbf{M}^{-1} = \mathbf{I} + \frac{\tau_0^2}{km} \mathbf{M}^{-1} + \frac{1}{m} \mathbf{\Phi}^{jT} \mathbf{\Phi}^j - \mathbf{I} = \mathbf{Q} \left\{ \mathbf{I} + \mathbf{Q}^{-1} \left( \frac{1}{m} \mathbf{\Phi}^{jT} \mathbf{\Phi}^j - \mathbf{I} \right) \mathbf{Q}^{-1} \right\} \mathbf{Q}$$

and using this in (60) gives

$$\left\{ \mathbf{I} + \mathbf{Q}^{-1} \left( \frac{1}{m} \mathbf{\Phi}^{jT} \mathbf{\Phi}^j - \mathbf{I} \right) \mathbf{Q}^{-1} \right\} \mathbf{Q} \boldsymbol{\delta}_j^\downarrow = -\frac{\tau_0^2}{km} \mathbf{Q}^{-1} \mathbf{M}^{-1} \boldsymbol{\theta}^\downarrow - \frac{1}{m} \mathbf{Q}^{-1} \mathbf{\Phi}^{jT} \mathbf{v}_j. \quad (61)$$

Define the event  $\mathbb{P}$ -measureable event

$$\mathcal{E}_1 = \left\{ s_{\max} \left\{ \mathbf{Q}^{-1} \left( \frac{1}{m} \mathbf{\Phi}^{jT} \mathbf{\Phi}^j - \mathbf{I} \right) \mathbf{Q}^{-1} \right\} \leq 1/2 \right\},$$

where  $s_{\max}(\mathbf{A})$  is the maximum eigenvalue of the square matrix  $\mathbf{A}$ . We have that  $\mathbf{I} + \mathbf{Q}^{-1} \left( \frac{1}{m} \mathbf{\Phi}^{jT} \mathbf{\Phi}^j - \mathbf{I} \right) \mathbf{Q}^{-1} \succeq (1/2) \mathbf{I}$  whenever  $\mathcal{E}_1$  occurs. Furthermore, when  $\mathcal{E}_1$  occurs, (61) implies that

$$\begin{aligned} \|\boldsymbol{\delta}_j^\downarrow\|_2^2 &\leq \|\mathbf{Q} \boldsymbol{\delta}_j^\downarrow\|_2^2 \leq 4 \left\| \frac{\tau_0^2}{km} \mathbf{Q}^{-1} \mathbf{M}^{-1} \boldsymbol{\theta}^\downarrow + \frac{1}{m} \mathbf{Q}^{-1} \mathbf{\Phi}^{jT} \mathbf{v}_j \right\|_2^2 \\ &\leq 8 \left\| \frac{\tau_0^2}{km} \mathbf{Q}^{-1} \mathbf{M}^{-1} \boldsymbol{\theta}^\downarrow \right\|_2^2 + 8 \left\| \frac{1}{m} \mathbf{Q}^{-1} \mathbf{\Phi}^{jT} \mathbf{v}_j \right\|_2^2, \end{aligned}$$

where the last inequality follows because  $(a+b)^2 \leq 2a^2 + 2b^2$  for any  $a, b \in \mathbb{R}$ .

Since  $\mathcal{E}_1$  is  $\mathbb{P}$ -measureable,  $\mathbb{E}_{\mathcal{S}} \left( \|\boldsymbol{\delta}_j^\downarrow\|_2^2 \right) = \mathbb{E}_{\mathcal{S}} \left\{ \|\boldsymbol{\delta}_j^\downarrow\|_2^2 \mathbf{1}(\mathcal{E}_1) \right\} + \mathbb{E}_{\mathcal{S}} \left\{ \|\boldsymbol{\delta}_j^\downarrow\|_2^2 \mathbf{1}(\mathcal{E}_1^c) \right\}$  and the previous display gives

$$\mathbb{E}_{\mathcal{S}} \left\{ \|\boldsymbol{\delta}_j^\downarrow\|_2^2 \mathbf{1}(\mathcal{E}_1) \right\} \leq 8 \left\| \frac{\tau_0^2}{km} \mathbf{Q}^{-1} \mathbf{M}^{-1} \boldsymbol{\theta}^\downarrow \right\|_2^2 + 8 \mathbb{E}_{\mathcal{S}} \left\| \frac{1}{m} \mathbf{Q}^{-1} \mathbf{\Phi}^{jT} \mathbf{v}_j \right\|_2^2. \quad (62)$$

From Lemma 10 in Zhang et al. [84], we have that

$$\left\| \frac{\tau_0^2}{km} \mathbf{Q}^{-1} \mathbf{M}^{-1} \boldsymbol{\theta}^\downarrow \right\|_2^2 \leq \frac{\tau_0^2}{km} \|w_0\|_{\mathbb{H}}^2, \quad \mathbb{E}_{\mathcal{S}} \left\| \frac{1}{m} \mathbf{Q}^{-1} \boldsymbol{\Phi}^{j^T} \mathbf{v}_j \right\|_2^2 \leq \frac{km}{\tau_0^2} \rho^4 \text{tr}(C_{\boldsymbol{\alpha}}) \text{tr}(C_{\boldsymbol{\alpha}}^d) \|w_0\|_{\mathbb{H}}^2. \quad (63)$$

Also from Lemma 10 in Zhang et al. [84], we have that under our assumptions there exists an universal constant  $A$  such that

$$\mathbb{P}(\mathcal{E}_1^c) \leq \left\{ A \max \left( \sqrt{\max(r, \log d)}, \frac{\max(r, \log d)}{m^{1/2-1/r}} \right) \frac{\rho^2 \gamma(\frac{\tau_0^2}{km})}{\sqrt{m}} \right\}^r = \left\{ \frac{Ab(m, d, r) \rho^2 \gamma(\frac{\tau_0^2}{km})}{\sqrt{m}} \right\}^r. \quad (64)$$

Since  $\mu_1 \geq \mu_2 \geq \dots \geq 0$ , the optimality condition in (54) implies that

$$\|\mathbb{E}_{0|\mathcal{S}}(\Delta_j)\|_2^2 = \frac{\mu_1}{\mu_1} \sum_{i=1}^{\infty} \delta_{ji} \phi_i \leq \mu_1 \sum_{i=1}^{\infty} \frac{\delta_{ji}}{\mu_i} \phi_i = \mu_1 \|\mathbb{E}_{0|\mathcal{S}}(\Delta_j)\|_{\mathbb{H}}^2 \leq \mu_1 \|w_0\|_{\mathbb{H}}^2. \quad (65)$$

Using the shorthand (64) and (65), we obtain that

$$\mathbb{E}_{\mathcal{S}} \left\{ \|\boldsymbol{\delta}_j^\downarrow\|_2^2 \mathbf{1}(\mathcal{E}_1^c) \right\} \leq \mathbb{E}_{\mathcal{S}} \left\{ \|\mathbb{E}_{0|\mathcal{S}}(\Delta_j)\|_2^2 \mathbf{1}(\mathcal{E}_1^c) \right\} \leq \mathbb{P}(\mathcal{E}_1^c) \mu_1 \|w_0\|_{\mathbb{H}}^2. \quad (66)$$

Combining (62) and (66) gives

$$\mathbb{E}_{\mathcal{S}}(\|\boldsymbol{\delta}_j\|_2^2) \leq \frac{8\tau_0^2}{km} \|w_0\|_{\mathbb{H}}^2 + \frac{8km}{\tau_0^2} \rho^4 \text{tr}(C_{\boldsymbol{\alpha}}) \text{tr}(C_{\boldsymbol{\alpha}}^d) \|w_0\|_{\mathbb{H}}^2 + \left\{ \frac{Ab(m, d, r) \rho^2 \gamma(\frac{\tau_0^2}{km})}{\sqrt{m}} \right\}^r \mu_1 \|w_0\|_{\mathbb{H}}^2. \quad (67)$$

Finally, we use that  $\|\mathbb{E}_{0|\mathcal{S}}(\Delta)\|_2^2 \leq k^{-1} \sum_{j=1}^k \|\mathbb{E}_{0|\mathcal{S}}(\Delta_j)\|_2^2 = k^{-1} \sum_{j=1}^k \|\boldsymbol{\delta}_j\|_2^2$  to obtain that

$$\begin{aligned} \mathbb{E}_{\mathcal{S}}(\|\mathbb{E}_{0|\mathcal{S}}(\Delta)\|_2^2) &\leq \frac{8\tau_0^2}{km} \|w_0\|_{\mathbb{H}}^2 + \frac{8km}{\tau_0^2} \rho^4 \text{tr}(C_{\boldsymbol{\alpha}}) \text{tr}(C_{\boldsymbol{\alpha}}^d) \|w_0\|_{\mathbb{H}}^2 + \left\{ \frac{Ab(m, d, r) \rho^2 \gamma(\frac{\tau_0^2}{km})}{\sqrt{m}} \right\}^r \mu_1 \|w_0\|_{\mathbb{H}}^2 \\ &= \left[ \frac{8\tau_0^2}{n} + \frac{8n}{\tau_0^2} \rho^4 \text{tr}(C_{\boldsymbol{\alpha}}) \text{tr}(C_{\boldsymbol{\alpha}}^d) + \mu_1 \left\{ \frac{Ab(m, d, r) \rho^2 \gamma(\frac{\tau_0^2}{n})}{\sqrt{m}} \right\}^r \right] \|w_0\|_{\mathbb{H}}^2, \end{aligned} \quad (68)$$

where we have replaced  $km$  by  $n$  in the last equality. Taking the infimum over  $d \in \mathbb{N}$  leads to the proof. ■

### 2.1.2 An upper bound for the first variance term

The following lemma provides an upper bound the first part of the variance term in (48).

**Lemma 2.2** *If Assumptions B.1–B.3 in the main paper hold, then*

$$\tau_0^2 \mathbb{E}_{\mathcal{S}} \mathbb{E}_{0|\mathcal{S}} \left\{ \mathbf{c}^T (k \mathbf{L} + \tau_0^2 \mathbf{I})^{-2} \mathbf{c} \right\} \leq$$

$$\frac{2n+4\|w_0\|_{\mathbb{H}}^2}{k} \inf_{d \in \mathbb{N}} \left[ \mu_{d+1} + 12 \frac{n}{\tau_0^2} \rho^4 \text{tr}(C_{\alpha}) \text{tr}(C_{\alpha}^d) + \left\{ \frac{Ab(m, d, r) \rho^2 \gamma(\frac{\tau_0^2}{n})}{\sqrt{m}} \right\}^r \right] + \frac{12}{k} \frac{\tau_0^2}{n} \|w_0\|_{\mathbb{H}}^2 + 12 \frac{\tau_0^2}{n} \gamma\left(\frac{\tau_0^2}{n}\right).$$

**Proof** This is an extension of Lemma 7 in Zhang et al. [84] for the DISK posterior and it is proved using similar arguments.

Continuing from (50), we start by finding an upper bound for  $\mathbb{E}_{0|S} \|\Delta_j\|_{\mathbb{H}}^2$ , which is required later to upper bound  $\mathbb{E}_0 \|\Delta_j\|_{\mathbb{H}}^2$ . From (50) we have

$$\mathbb{E}_{0|S} \|\Delta_j\|_{\mathbb{H}}^2 \leq 2 \mathbb{E}_{0|S} \|\tilde{w}_j\|_{\mathbb{H}}^2 + 2\|w_0\|_{\mathbb{H}}^2. \quad (69)$$

An upper bound for  $\mathbb{E}_{0|S} \|\tilde{w}_j\|_{\mathbb{H}}^2$  gives the desired bound. Using the objective in (51),

$$\frac{1}{2} \|\tilde{w}_j\|_{\mathbb{H}}^2 \stackrel{(i)}{\leq} \sum_{i=1}^m \frac{\{\tilde{w}_j(\mathbf{s}_{ji}) - y(\mathbf{s}_{ji})\}^2}{2\tau_0^2/k} + \frac{1}{2} \|\tilde{w}_j\|_{\mathbb{H}}^2 \stackrel{(ii)}{\leq} \sum_{i=1}^m \frac{\{w_0(\mathbf{s}_{ji}) - y(\mathbf{s}_{ji})\}^2}{2\tau_0^2/k} + \frac{1}{2} \|w_0\|_{\mathbb{H}}^2, \quad (70)$$

where (i) follows because the term inside the summation is non-negative and (ii) follows because  $\tilde{w}_j$  minimizes the objective. Since  $w(\mathbf{s}_{ji}) - y(\mathbf{s}_{ji}) = -\epsilon(\mathbf{s}_{ji})$  and  $\mathbb{E}_{0|S} \{\epsilon^2(\mathbf{s}_{ji})\} \leq \tau_0^2$  by Assumption B2, (70) reduces to

$$\mathbb{E}_{0|S} \|\tilde{w}_j\|_{\mathbb{H}}^2 \leq \frac{k}{\tau_0^2} \sum_{i=1}^m \mathbb{E}_{0|S} \{\epsilon(\mathbf{s}_{ji})\}^2 + \|w_0\|_{\mathbb{H}}^2 \leq km + \|w_0\|_{\mathbb{H}}^2. \quad (71)$$

Substituting (71) in (69) gives

$$\mathbb{E}_{0|S} \|\Delta_j\|_{\mathbb{H}}^2 \leq 2km + 4\|w_0\|_{\mathbb{H}}^2. \quad (72)$$

First notice that

$$\tau_0^2 \mathbb{E}_{0|S} \left\{ \mathbf{c}^T (k\mathbf{L} + \tau_0^2 \mathbf{I})^{-2} \mathbf{c} \right\} = \frac{1}{k^2} \sum_{j=1}^k \tau_0^2 \mathbb{E}_{0|S} \left\{ \mathbf{c}_j^T \left( \mathbf{C}_{j,j} + \frac{\tau_0^2}{k} \mathbf{I} \right)^{-2} \mathbf{c}_j \right\}. \quad (73)$$

and from (48) we have

$$\begin{aligned} \tau_0^2 \mathbb{E}_{0|S} \left\{ \mathbf{c}_j^T \left( \mathbf{C}_{j,j} + \frac{\tau_0^2}{k} \mathbf{I} \right)^{-2} \mathbf{c}_j \right\} &= \text{var}_{0|S} \left\{ \mathbf{c}_j^T \left( \mathbf{C}_{j,j} + \frac{\tau_0^2}{k} \mathbf{I} \right)^{-1} \mathbf{y}_j \right\} \\ &\leq \mathbb{E}_{0|S} \left\{ \mathbf{c}_j^T \left( \mathbf{C}_{j,j} + \frac{\tau_0^2}{k} \mathbf{I} \right)^{-1} \mathbf{y}_j - w_0 \right\}^2 = \mathbb{E}_{0|S} \|\Delta_j\|_2^2. \end{aligned} \quad (74)$$

Substituting (74) to (73) leads to

$$\tau_0^2 \mathbb{E}_{0|\mathcal{S}} \{ \mathbf{c}^T (k \mathbf{L} + \tau_0^2 \mathbf{I})^{-2} \mathbf{c} \} \leq \frac{1}{k^2} \sum_{j=1}^k \tau_0^2 \mathbb{E}_{0|\mathcal{S}} \|\Delta_j\|_2^2. \quad (75)$$

We then find an upper bound for  $\mathbb{E}_{0|\mathcal{S}} \|\Delta_j\|_2^2$  by following similar steps to the proof of Lemma 2.1. Let  $\boldsymbol{\delta}_j \in L_2(\mathbb{N})$  be the expansion of  $\Delta_j$  in the basis  $\{\phi_i\}_{i=1}^\infty$ , so that  $\Delta_j = \sum_{i=1}^\infty \delta_{ji} \phi_i$  (the  $\boldsymbol{\delta}_j$  sequence here is different from the one in the previous section). Similar to Section 2.1.1, choose a fixed  $d \in \mathbb{N}$  and truncate  $\Delta_j$  by defining  $\Delta_j^\downarrow$ ,  $\Delta_j^\uparrow$ ,  $\boldsymbol{\delta}_j^\downarrow$ , and  $\boldsymbol{\delta}_j^\uparrow$  as

$$\Delta_j^\downarrow = \sum_{i=1}^d \delta_{ji} \phi_i, \quad \Delta_j^\uparrow = \sum_{i=d+1}^\infty \delta_{ji} \phi_i = \Delta_j - \Delta_j^\downarrow, \quad \boldsymbol{\delta}_j^\downarrow = (\delta_{j1}, \dots, \delta_{jd}), \quad \boldsymbol{\delta}_j^\uparrow = (\delta_{j(d+1)}, \dots, \delta_{j\infty}).$$

The orthonormality of  $\{\phi_i\}_{i=1}^\infty$  implies that

$$\mathbb{E}_{\mathcal{S}} \mathbb{E}_{0|\mathcal{S}} \|\Delta_j\|_2^2 = \mathbb{E}_{\mathcal{S}} \mathbb{E}_{0|\mathcal{S}} \|\Delta_j^\downarrow\|_2^2 + \mathbb{E}_{\mathcal{S}} \mathbb{E}_{0|\mathcal{S}} \|\Delta_j^\uparrow\|_2^2 = \mathbb{E}_{\mathcal{S}} \mathbb{E}_{0|\mathcal{S}} \|\boldsymbol{\delta}_j^\downarrow\|_2^2 + \mathbb{E}_{\mathcal{S}} \mathbb{E}_{0|\mathcal{S}} \|\boldsymbol{\delta}_j^\uparrow\|_2^2. \quad (76)$$

First, the upper bound for  $\mathbb{E}_{0|\mathcal{S}} \|\boldsymbol{\delta}_j^\uparrow\|_2^2$  follows from (56),

$$\begin{aligned} \mathbb{E}_{0|\mathcal{S}} \|\Delta_j^\uparrow\|_2^2 &= \sum_{i=d+1}^\infty \mathbb{E}_{0|\mathcal{S}}(\delta_{ji}^2) = \mu_{d+1} \sum_{i=d+1}^\infty \frac{\mathbb{E}_{0|\mathcal{S}}(\delta_{ji}^2)}{\mu_{d+1}} \leq \mu_{d+1} \sum_{i=d+1}^\infty \frac{\mathbb{E}_{0|\mathcal{S}}(\delta_{ji}^2)}{\mu_i} \\ &= \mu_{d+1} \mathbb{E}_{0|\mathcal{S}} \|\Delta_j^\uparrow\|_{\mathbb{H}}^2 \leq \mu_{d+1} \mathbb{E}_{0|\mathcal{S}} \|\Delta_j\|_{\mathbb{H}}^2, \end{aligned}$$

and using (72),

$$\mathbb{E}_{0|\mathcal{S}} \|\Delta_j^\uparrow\|_2^2 \leq \mu_{d+1} (2km + 4\|w_0\|_{\mathbb{H}}^2). \quad (77)$$

We now find an upper bound for  $\mathbb{E}_{\mathcal{S}} \mathbb{E}_{0|\mathcal{S}} \|\Delta_j^\downarrow\|_2^2$ . Following Section 2.1.1, define the error vector  $\mathbf{v}_j = (v_{j1}, \dots, v_{jm})^T \in \mathbb{R}^m$  with  $v_{ji} = \sum_{h=d+1}^\infty \delta_{ji} \phi_h(\mathbf{s}_{ji})$  ( $i = 1, \dots, m$ ), and  $\mathbf{M} = \text{diag}(\mu_1, \dots, \mu_d)$ . From (51) and (52),  $\tilde{w}_j(\cdot)$  in (50) satisfies

$$\frac{1}{m} \sum_{i=1}^m \langle \xi_{\mathbf{s}_{ji}}, \tilde{w}_j - w_0 - \epsilon \rangle_{\mathbb{H}} \xi_{\mathbf{s}_{ji}} + \frac{\tau_0^2}{km} \tilde{w}_j = 0. \quad (78)$$

For any  $g \in \{1, \dots, d\}$ , taking the  $\mathbb{H}$ -inner product with respect  $\phi_g$  in (78) to obtain that

$$\begin{aligned} \frac{1}{m} \sum_{i=1}^m \langle \xi_{\mathbf{s}_{ji}}, \Delta_j - \epsilon \rangle_{\mathbb{H}} \langle \xi_{\mathbf{s}_{ji}}, \phi_g \rangle_{\mathbb{H}} + \frac{\tau_0^2}{km} \langle \Delta_j + w_0, \phi_g \rangle_{\mathbb{H}} = \\ \frac{1}{m} \sum_{i=1}^m \{ \Delta_j(\mathbf{s}_{ji}) - \epsilon(\mathbf{s}_{ji}) \} \phi_g(\mathbf{s}_{ji}) + \frac{\tau_0^2}{km} \frac{\delta_{jg}}{\mu_g} + \frac{\tau_0^2}{km} \frac{\theta_g}{\mu_g} = 0, \end{aligned}$$

$$\begin{aligned}
& \frac{1}{m} \sum_{i=1}^m \left\{ \sum_{h=1}^d \delta_{jh} \phi_h(\mathbf{s}_{ji}) + \sum_{h=d+1}^{\infty} \delta_{jh} \phi_h(\mathbf{s}_{ji}) - \epsilon(\mathbf{s}_{ji}) \right\} \phi_g(\mathbf{s}_{ji}) + \frac{\tau_0^2}{km} \frac{\delta_{jg}}{\mu_g} = -\frac{\tau_0^2}{km} \frac{\theta_g}{\mu_g}, \\
& \frac{1}{m} \sum_{h=1}^d \left\{ \sum_{i=1}^m \phi_h(\mathbf{s}_{ji}) \phi_g(\mathbf{s}_{ji}) \right\} \delta_{jh} + \frac{1}{m} \sum_{i=1}^m \{v_{ji} - \epsilon(\mathbf{s}_{ji})\} \phi_g(\mathbf{s}_{ji}) + \frac{\tau_0^2}{km} \frac{\delta_{jg}}{\mu_g} = -\frac{\tau_0^2}{km} \frac{\theta_g}{\mu_g}, \\
& \frac{1}{m} \left( \mathbf{\Phi}^{jT} \mathbf{\Phi}^j \boldsymbol{\delta}_j^\downarrow \right)_g + \frac{1}{m} \left\{ \mathbf{\Phi}^{jT} (\mathbf{v}_j - \boldsymbol{\epsilon}_j) \right\}_g + \frac{\tau_0^2}{km} (\mathbf{M}^{-1} \boldsymbol{\delta}_j^\downarrow)_g = -\frac{\tau_0^2}{km} (\mathbf{M}^{-1} \boldsymbol{\theta}^\downarrow)_g.
\end{aligned}$$

Writing this equation in the matrix form yields,

$$\left( \frac{1}{m} \mathbf{\Phi}^{jT} \mathbf{\Phi}^j + \frac{\tau_0^2}{km} \mathbf{M}^{-1} \right) \boldsymbol{\delta}_j^\downarrow = -\frac{\tau_0^2}{km} \mathbf{M}^{-1} \boldsymbol{\theta}^\downarrow - \frac{1}{m} \mathbf{\Phi}^{jT} \mathbf{v}_j + \frac{1}{m} \mathbf{\Phi}^{jT} \boldsymbol{\epsilon}_j. \quad (79)$$

Following Section 2.1.1, by defining  $\mathbf{Q} = (\mathbf{I} + \frac{\tau_0^2}{km} \mathbf{M}^{-1})^{1/2}$ , (79) reduces to

$$\left\{ \mathbf{I} + \mathbf{Q}^{-1} \left( \frac{1}{m} \mathbf{\Phi}^{jT} \mathbf{\Phi}^j - \mathbf{I} \right) \mathbf{Q}^{-1} \right\} \mathbf{Q} \boldsymbol{\delta}_j^\downarrow = -\frac{\tau_0^2}{km} \mathbf{Q}^{-1} \mathbf{M}^{-1} \boldsymbol{\theta}^\downarrow - \frac{1}{m} \mathbf{Q}^{-1} \mathbf{\Phi}^{jT} \mathbf{v}_j + \frac{1}{m} \mathbf{Q}^{-1} \mathbf{\Phi}^{jT} \boldsymbol{\epsilon}_j. \quad (80)$$

Again, following Section 2.1.1 and Lemma 10 in Zhang et al. [84], define the  $\mathbb{P}$ -measureable event

$$\mathcal{E}_1 = \left\{ \text{smax} \left\{ \mathbf{Q}^{-1} \left( \frac{1}{m} \mathbf{\Phi}^{jT} \mathbf{\Phi}^j - \mathbf{I} \right) \mathbf{Q}^{-1} \right\} \leq 1/2 \right\}.$$

We have that  $\mathbf{I} + \mathbf{Q}^{-1} \left( \frac{1}{m} \mathbf{\Phi}^{jT} \mathbf{\Phi}^j - \mathbf{I} \right) \mathbf{Q}^{-1} \succeq (1/2) \mathbf{I}$  whenever  $\mathcal{E}_1$  holds. Furthermore, when  $\mathcal{E}_1$  occurs, (80) implies that

$$\begin{aligned}
\|\Delta_j^\downarrow\|_2^2 & \leq \|\mathbf{Q} \boldsymbol{\delta}_j^\downarrow\|_2^2 \leq 4 \left\| -\frac{\tau_0^2}{km} \mathbf{Q}^{-1} \mathbf{M}^{-1} \boldsymbol{\theta}^\downarrow - \frac{1}{m} \mathbf{Q}^{-1} \mathbf{\Phi}^{jT} \mathbf{v}_j + \frac{1}{m} \mathbf{Q}^{-1} \mathbf{\Phi}^{jT} \boldsymbol{\epsilon}_j \right\|_2^2 \\
& \leq 12 \left\| \frac{\tau_0^2}{km} \mathbf{Q}^{-1} \mathbf{M}^{-1} \boldsymbol{\theta}^\downarrow \right\|_2^2 + 12 \left\| \frac{1}{m} \mathbf{Q}^{-1} \mathbf{\Phi}^{jT} \mathbf{v}_j \right\|_2^2 + 12 \left\| \frac{1}{m} \mathbf{Q}^{-1} \mathbf{\Phi}^{jT} \boldsymbol{\epsilon}_j \right\|_2^2,
\end{aligned}$$

where the last inequality follows because  $(a + b + c)^2 \leq 3a^2 + 3b^2 + 3c^2$  for any  $a, b, c \in \mathbb{R}$ . Since  $\mathcal{E}_1$  is  $\mathbb{P}$ -measureable,  $\mathbb{E}_{0|S} (\|\Delta_j^\downarrow\|_2^2) = \mathbb{E}_{0|S} \left\{ \|\Delta_j^\downarrow\|_2^2 \mathbf{1}(\mathcal{E}_1) \right\} + \mathbb{E}_{0|S} \left\{ \|\Delta_j^\downarrow\|_2^2 \mathbf{1}(\mathcal{E}_1^c) \right\}$ . If the event  $\mathcal{E}_1$  occurs, then the upper bounds for the first term and the last two terms in the last inequality are implied by Lemmas 10 and 7 of Zhang et al. [84], respectively, and we have that

$$\begin{aligned}
& \left\| \frac{\tau_0^2}{km} \mathbf{Q}^{-1} \mathbf{M}^{-1} \boldsymbol{\theta}^\downarrow \right\|_2^2 \leq \frac{\tau_0^2}{km} \|w_0\|_{\mathbb{H}}^2, \\
& \mathbb{E}_S \left\| \frac{1}{m} \mathbf{Q}^{-1} \mathbf{\Phi}^{jT} \mathbf{v}_j \right\|_2^2 \leq \frac{km}{\tau_0^2} \rho^4 \text{tr}(C_\alpha) \text{tr}(C_\alpha^d) (2km + 4\|w_0\|_{\mathbb{H}}^2), \\
& \mathbb{E}_S \mathbb{E}_{0|S} \left\| \frac{1}{m} \mathbf{Q}^{-1} \mathbf{\Phi}^{jT} \boldsymbol{\epsilon}_j \right\|_2^2 \leq \frac{1}{m^2} \sum_{h=1}^d \sum_{i=1}^m \frac{1}{1 + \frac{\tau_0^2}{km} \frac{1}{\mu_h}} \mathbb{E}_S \mathbb{E}_{0|S} \left\{ \phi_h^2(\mathbf{s}_{ji}) \epsilon^2(\mathbf{s}_{ji}) \right\}. \quad (81)
\end{aligned}$$

Since the error  $\epsilon(\cdot)$  and  $w(\cdot)$  are independent,

$$\mathbb{E}_{\mathcal{S}} \mathbb{E}_{0|\mathcal{S}} \{ \phi_h^2(\mathbf{s}_{ji}) \epsilon^2(\mathbf{s}_{ji}) \} = \mathbb{E}_{\mathcal{S}} \{ \phi_h^2(\mathbf{s}_{ji}) \} \mathbb{E}_{0|\mathcal{S}} \{ \epsilon^2(\mathbf{s}_{ji}) \} \leq \tau_0^2$$

and the last inequality in (81) simplifies to

$$\mathbb{E}_{\mathcal{S}} \mathbb{E}_{0|\mathcal{S}} \left\| \frac{1}{m} \mathbf{Q}^{-1} \mathbf{\Phi}^j \epsilon_j \right\|_2^2 \leq \frac{\tau_0^2}{m} \sum_{h=1}^d \frac{1}{1 + \frac{\tau_0^2}{km} \frac{1}{\mu_h}} \leq \frac{\tau_0^2}{m} \gamma \left( \frac{\tau_0^2}{km} \right).$$

Hence when the event  $\mathcal{E}_1$  occurs,

$$\begin{aligned} & \mathbb{E}_{\mathcal{S}} \mathbb{E}_{0|\mathcal{S}} \left\{ \|\Delta_j^\downarrow\|_2^2 \mathbf{1}(\mathcal{E}_1) \right\} \leq \\ & 12 \frac{\tau_0^2}{km} \|w_0\|_{\mathbb{H}}^2 + 12 \frac{km}{\tau_0^2} \rho^4 \text{tr}(C_{\alpha}) \text{tr}(C_{\alpha}^d) (2km + 4\|w_0\|_{\mathbb{H}}^2) + 12 \frac{\tau_0^2}{m} \gamma \left( \frac{\tau_0^2}{km} \right). \end{aligned} \quad (82)$$

If the event  $\mathcal{E}_1$  does not occur, then

$$\begin{aligned} \mathbb{E}_{\mathcal{S}} \mathbb{E}_{0|\mathcal{S}} \left\{ \|\Delta_j^\downarrow\|_2^2 \mathbf{1}(\mathcal{E}_1^c) \right\} & \leq \mathbb{E}_{\mathcal{S}} \left\{ \mathbf{1}(\mathcal{E}_1^c) \mathbb{E}_{0|\mathcal{S}} \|\Delta_j^\downarrow\|_2^2 \right\} \stackrel{(i)}{\leq} \mathbb{P}(\mathcal{E}_1^c) (2km + 4\|w_0\|_{\mathbb{H}}^2) \\ & \stackrel{(ii)}{=} \left\{ \frac{Ab(m, d, r) \rho^2 \gamma \left( \frac{\tau_0^2}{km} \right)}{\sqrt{m}} \right\}^r (2km + 4\|w_0\|_{\mathbb{H}}^2), \end{aligned} \quad (83)$$

where (i) follows from (72) and (ii) follows from (64). Substituting (82), (83), and (77) in (76) implies that

$$\begin{aligned} \mathbb{E}_{\mathcal{S}} \mathbb{E}_{0|\mathcal{S}} \left\{ \|\Delta_j\|_2^2 \right\} & \leq \left[ \mu_{d+1} + 12 \frac{km}{\tau_0^2} \rho^4 \text{tr}(C_{\alpha}) \text{tr}(C_{\alpha}^d) + \left\{ \frac{Ab(m, d, r) \rho^2 \gamma \left( \frac{\tau_0^2}{km} \right)}{\sqrt{m}} \right\}^r \right] (2km + 4\|w_0\|_{\mathbb{H}}^2) + \\ & 12 \frac{\tau_0^2}{km} \|w_0\|_{\mathbb{H}}^2 + 12 \frac{\tau_0^2}{m} \gamma \left( \frac{\tau_0^2}{km} \right). \end{aligned} \quad (84)$$

Therefore, substituting (84) in (75) implies that

$$\begin{aligned} & \tau_0^2 \mathbb{E}_{\mathcal{S}} \mathbb{E}_{0|\mathcal{S}} \left\{ \mathbf{c}^T (k \mathbf{L} + \tau_0^2 \mathbf{I})^{-2} \mathbf{c} \right\} \leq \\ & \frac{2n + 4\|w_0\|_{\mathbb{H}}^2}{k} \left[ \mu_{d+1} + 12 \frac{n}{\tau_0^2} \rho^4 \text{tr}(C_{\alpha}) \text{tr}(C_{\alpha}^d) + \left\{ \frac{Ab(m, d, r) \rho^2 \gamma \left( \frac{\tau_0^2}{n} \right)}{\sqrt{m}} \right\}^r \right] + \\ & \frac{12}{k} \frac{\tau_0^2}{n} \|w_0\|_{\mathbb{H}}^2 + 12 \frac{\tau_0^2}{n} \gamma \left( \frac{\tau_0^2}{n} \right). \end{aligned} \quad (85)$$

where we have replace  $km$  by  $n$ . Taking the infimum over  $d \in \mathbb{N}$  leads to the proof. ■

### 2.1.3 An upper bound for the second variance term

The following lemma provides an upper bound the second part of the variance term in (48).

**Lemma 2.3** *If Assumptions B.1–B.3 in the main paper hold, then*

$$\mathbb{E}_{\mathbf{s}^*} \mathbb{E}_{\mathcal{S}} \bar{v}(\mathbf{s}^*) \leq 2 \frac{\tau_0^2}{n} \gamma \left( \frac{\tau_0^2}{n} \right) + \inf_{d \in \mathbb{N}} \left[ \text{tr}(C_{\alpha}^d) + \text{tr}(C_{\alpha}) \left\{ \frac{Ab(m, d, r) \rho^2 \gamma(\frac{\tau_0^2}{n})}{\sqrt{m}} \right\}^r \right].$$

**Proof** First we have the following relation between  $\bar{v}$  and the subset variance  $v_j$ :

$$\bar{v}(\mathbf{s}^*) = \left( \frac{1}{k} \sum_{j=1}^k v_j^{1/2}(\mathbf{s}^*) \right)^2 \leq \frac{1}{k} \sum_{j=1}^k v_j(\mathbf{s}^*) = \frac{1}{k} \sum_{j=1}^k \left\{ C_{\alpha}(\mathbf{s}^*, \mathbf{s}^*) - \mathbf{c}_j^T(\mathbf{s}^*) \left( \mathbf{C}_{j,j} + \frac{\tau_0^2}{k} \mathbf{I} \right)^{-1} \mathbf{c}_j(\mathbf{s}^*) \right\}. \quad (86)$$

Since  $C_{\alpha}(\mathbf{s}, \mathbf{s}') = \sum_{i=1}^{\infty} \mu_i \phi_i(\mathbf{s}) \phi_i(\mathbf{s}')$  for  $\mathbf{s}, \mathbf{s}' \in \mathcal{D}$ , we have

$$C_{\alpha}(\mathbf{s}^*, \mathbf{s}^*) = \sum_{a=1}^{\infty} \mu_a \phi_a^2(\mathbf{s}^*), \quad \{\mathbf{c}_j(\mathbf{s}^*)\}_i = \sum_{a=1}^{\infty} \mu_a \phi_a(\mathbf{s}_{ji}) \phi_a(\mathbf{s}^*), \quad i = 1, \dots, m.$$

These together with the orthogonality property of  $\{\phi_i\}_{i=1}^{\infty}$  imply that

$$\begin{aligned} \mathbb{E}_{\mathbf{s}^*} \mathbb{E}_{\mathcal{S}} \{v_j(\mathbf{s}^*)\} &= \sum_{a=1}^{\infty} \mu_a \mathbb{E}_{\mathbf{s}^*} \phi_a^2(\mathbf{s}^*) \\ &\quad - \sum_{i=1}^m \sum_{i'=1}^m \sum_{a=1}^{\infty} \sum_{b=1}^{\infty} \mu_a \mu_b \left\{ \left( \mathbf{C}_{j,j} + \frac{\tau_0^2}{k} \mathbf{I} \right)^{-1} \right\}_{i'i''} \mathbb{E}_{\mathcal{S}} [\phi_a(\mathbf{s}_{ji}) \phi_b(\mathbf{s}_{ji'}) \mathbb{E}_{\mathbf{s}^*} \{\phi_a(\mathbf{s}^*) \phi_b(\mathbf{s}^*)\}] \\ &= \text{tr}(C_{\alpha}) - \mathbb{E}_{\mathcal{S}} \sum_{i=1}^m \sum_{i'=1}^m \sum_{a=1}^{\infty} \mu_a^2 \left\{ \left( \mathbf{C}_{j,j} + \frac{\tau_0^2}{k} \mathbf{I} \right)^{-1} \right\}_{ii'} \phi_a(\mathbf{s}_{ji}) \phi_a(\mathbf{s}_{ji'}) \\ &= \sum_{a=1}^d \mu_a - \mathbb{E}_{\mathcal{S}} \sum_{a=1}^d \mu_a^2 \left[ \sum_{i=1}^m \sum_{i'=1}^m \left\{ \left( \mathbf{C}_{j,j} + \frac{\tau_0^2}{k} \mathbf{I} \right)^{-1} \right\}_{ii'} \phi_a(\mathbf{s}_{ji}) \phi_a(\mathbf{s}_{ji'}) \right] + \\ &\quad \text{tr}(C_{\alpha}^d) - \mathbb{E}_{\mathcal{S}} \sum_{a=d+1}^{\infty} \mu_a^2 \left[ \sum_{i=1}^m \sum_{i'=1}^m \left\{ \left( \mathbf{C}_{j,j} + \frac{\tau_0^2}{k} \mathbf{I} \right)^{-1} \right\}_{i'i''} \phi_a(\mathbf{s}_{ji}) \phi_a(\mathbf{s}_{ji'}) \right] \\ &\stackrel{(i)}{\leq} \mathbb{E}_{\mathcal{S}} \sum_{a=1}^d \left\{ \mu_a - \mu_a^2 \phi_a^{jT} (\mathbf{C}_{j,j} + \frac{\tau_0^2}{k} \mathbf{I})^{-1} \phi_a^j \right\} + \text{tr}(C_{\alpha}^d), \end{aligned} \quad (87)$$

where  $i$ ath element of the matrix  $\Phi^j$  (defined in the proof of Lemma 2.1) is  $\phi_a(\mathbf{s}_{ji})$ ,  $\phi_a^j$  is the  $a$ th column of  $\Phi^j$ , and (i) follows because  $(\mathbf{C}_{j,j} + \frac{\tau_0^2}{k} \mathbf{I})$  is a positive definite matrix and  $\phi_a^{jT} (\mathbf{C}_{j,j} + \frac{\tau_0^2}{k} \mathbf{I})^{-1} \phi_a^j \geq 0$ .

Let  $\mathbf{M} = \text{diag}(\mu_1, \dots, \mu_d)$  and  $\mathbf{Q} = \left( \mathbf{I} + \frac{\tau_0^2}{km} \mathbf{M}^{-1} \right)^{1/2}$  as defined in the proofs of Lemmas 2.1

and 2.2. Define a  $d \times d$  matrix  $\mathbf{B} \equiv \mathbf{M} - \mathbf{M} \Phi^{jT} \left( \mathbf{C}_{j,j} + \frac{\tau_0^2}{k} \mathbf{I} \right)^{-1} \Phi^j \mathbf{M}$ , so that from (87),

$$\text{tr}(\mathbf{B}) = \sum_{a=1}^d \left\{ \mu_a - \mu_a^2 \phi_a^{jT} \left( \mathbf{C}_{j,j} + \frac{\tau_0^2}{k} \mathbf{I} \right)^{-1} \phi_a^j \right\}, \quad \mathbb{E}_{\mathbf{s}^*} \mathbb{E}_{\mathcal{S}} \{v_j(\mathbf{s}^*)\} \leq \mathbb{E}_{\mathcal{S}} \text{tr}(\mathbf{B}) + \text{tr}(C_{\alpha}^d). \quad (88)$$

Let

$$\begin{aligned} \mathbf{C}_{j,j} &= \Phi^j \mathbf{M} \Phi^{jT} + \Phi^{j\uparrow} \mathbf{M}^{\uparrow} \Phi^{j\uparrow T} \equiv \Phi^j \mathbf{M} \Phi^{jT} + \mathbf{C}_{j,j}^{\uparrow}, \\ \mathbf{M}^{\uparrow} &= \text{diag}(\mu_{d+1}, \dots, \mu_{\infty}), \quad \Phi^{j\uparrow} = [\phi_{d+1}^j, \dots, \phi_{\infty}^j], \end{aligned}$$

then the Woodbury formula [38] and the definition of  $\mathbf{Q}$  imply that

$$\begin{aligned} \mathbf{B} &= \left\{ \mathbf{M}^{-1} + \Phi^{jT} \left( \mathbf{C}_{j,j}^{\uparrow} + \frac{\tau_0^2}{k} \mathbf{I} \right)^{-1} \Phi^j \right\}^{-1} = \frac{\tau_0^2}{km} \left\{ \mathbf{I} + \frac{\tau_0^2}{km} \mathbf{M}^{-1} + \frac{1}{m} \Phi^{jT} \left( \frac{k}{\tau_0^2} \mathbf{C}_{j,j}^{\uparrow} + \mathbf{I} \right)^{-1} \Phi^j - \mathbf{I} \right\}^{-1} \\ &= \frac{\tau_0^2}{km} \mathbf{Q}^{-2} \left[ \mathbf{I} + \mathbf{Q}^{-1} \left\{ \frac{1}{m} \Phi^{jT} \left( \frac{k}{\tau_0^2} \mathbf{C}_{j,j}^{\uparrow} + \mathbf{I} \right)^{-1} \Phi^j - \mathbf{I} \right\} \mathbf{Q}^{-1} \right]^{-1}. \end{aligned} \quad (89)$$

Analogous to Lemma 10 in [84], define the event

$$\mathcal{E}_2 = \left\{ \text{smax} \left[ \mathbf{Q}^{-1} \left\{ \frac{1}{m} \Phi^{jT} \left( \frac{k}{\tau_0^2} \mathbf{C}_{j,j}^{\uparrow} + \mathbf{I} \right)^{-1} \Phi^j - \mathbf{I} \right\} \mathbf{Q}^{-1} \right] \leq \frac{1}{2} \right\}.$$

Since  $\frac{k}{\tau_0^2} \mathbf{C}_{j,j}^{\uparrow}$  is a positive semi-definite matrix,  $\left( \frac{k}{\tau_0^2} \mathbf{C}_{j,j}^{\uparrow} + \mathbf{I} \right)^{-1} \preceq \mathbf{I}$  and

$$\begin{aligned} \mathbf{Q}^{-1} \left( \frac{1}{m} \Phi^{jT} \Phi^j - \mathbf{I} \right) \mathbf{Q}^{-1} - \mathbf{Q}^{-1} \left\{ \frac{1}{m} \Phi^{jT} \left( \frac{k}{\tau_0^2} \mathbf{C}_{j,j}^{\uparrow} + \mathbf{I} \right)^{-1} \Phi^j - \mathbf{I} \right\} \mathbf{Q}^{-1} &\succeq \mathbf{0}, \\ \implies \mathcal{E}_2^c &\subseteq \mathcal{E}_1^c, \end{aligned} \quad (90)$$

where  $\mathcal{E}_1$  is the event defined in Lemma 10 of [84] and in (61). Using the upper bound for  $\mathbb{P}(\mathcal{E}_1^c)$  given in (64), our assumptions and (90) imply that

$$\mathbb{P}(\mathcal{E}_2^c) \leq \mathbb{P}(\mathcal{E}_1^c) \leq \left\{ \frac{Ab(m, d, r) \rho^2 \gamma \left( \frac{\tau_0^2}{km} \right)}{\sqrt{m}} \right\}^r. \quad (91)$$

If event  $\mathcal{E}_2$  occurs, then from (89)

$$\frac{1}{2} \mathbf{I} \preceq \left[ \mathbf{I} + \mathbf{Q}^{-1} \left\{ \frac{1}{m} \Phi^{jT} \left( \frac{k}{\tau_0^2} \mathbf{C}_{j,j}^{\uparrow} + \mathbf{I} \right)^{-1} \Phi^j - \mathbf{I} \right\} \mathbf{Q}^{-1} \right] \implies \mathbf{B} \preceq 2 \frac{\tau_0^2}{km} \mathbf{Q}^{-2}. \quad (92)$$

which implies that

$$\mathbb{E}_{\mathcal{S}} \text{tr}(\mathbf{B}) \leq \mathbb{E}_{\mathcal{S}} \{ \text{tr}(\mathbf{B}) \mathbf{1}(\mathcal{E}_2) \} + \mathbb{E}_{\mathcal{S}} \{ \text{tr}(\mathbf{B}) \mathbf{1}(\mathcal{E}_2^c) \}$$



$$\begin{aligned}
&\stackrel{(i)}{\leq} 2 \frac{\tau_0^2}{km} \operatorname{tr}(\mathbf{Q}^{-2}) + \operatorname{tr}(C_\alpha) \mathbb{P}(\mathcal{E}_2^c) \\
&\leq 2 \frac{\tau_0^2}{km} \gamma\left(\frac{\tau_0^2}{km}\right) + \operatorname{tr}(C_\alpha) \mathbb{P}(\mathcal{E}_2^c),
\end{aligned} \tag{93}$$

where (i) follows from (92), and the fact that  $\operatorname{tr}(\mathbf{B}) \leq \sum_{a=1}^d \mu_a \leq \operatorname{tr}(C_\alpha)$ .

(87), (91), and (93) together yield

$$\begin{aligned}
\mathbb{E}_{\mathbf{s}^*} \mathbb{E}_{\mathcal{S}} \{\bar{v}_j(\mathbf{s}^*)\} &\leq \mathbb{E}_{\mathcal{S}} \operatorname{tr}(\mathbf{B}) + \operatorname{tr}(C_\alpha^d) \\
&\leq 2 \frac{\tau_0^2}{n} \gamma\left(\frac{\tau_0^2}{n}\right) + \operatorname{tr}(C_\alpha) \left\{ \frac{Ab(m, d, r) \rho^2 \gamma(\frac{\tau_0^2}{n})}{\sqrt{m}} \right\}^r + \operatorname{tr}(C_\alpha^d),
\end{aligned} \tag{94}$$

where we have replaced  $km$  by  $n$  and used the upperbound for  $\mathbb{P}(\mathcal{E}_2^c)$  in (64). Since the righthand side of (94) does not depend on  $j$ , a further upper bound for (86) is given by

$$\begin{aligned}
\mathbb{E}_{\mathbf{s}^*} \mathbb{E}_{\mathcal{S}} \{\bar{v}(\mathbf{s}^*)\} &\leq \frac{1}{k} \sum_{j=1}^k \mathbb{E}_{\mathbf{s}^*} \mathbb{E}_{\mathcal{S}} \{\bar{v}_j(\mathbf{s}^*)\} \\
&\leq 2 \frac{\tau_0^2}{n} \gamma\left(\frac{\tau_0^2}{n}\right) + \operatorname{tr}(C_\alpha) \left\{ \frac{Ab(m, d, r) \rho^2 \gamma(\frac{\tau_0^2}{n})}{\sqrt{m}} \right\}^r + \operatorname{tr}(C_\alpha^d).
\end{aligned} \tag{95}$$

Taking the infimum over  $d \in \mathbb{N}$  leads to the proof. ■

## 2.2 Proof of Theorem 3.5

(i) Since  $d^*$  is a constant integer and  $k = o(n)$ , we can take  $m$  sufficiently large such that  $n \geq m > \max(d^*, e^r)$ . In the upper bounds of Theorem 3.4, we choose  $d = n$  in every infimum. This implies  $\operatorname{tr}(C_\alpha^d) = 0$ ,  $\mu_{d+1} = 0$ , and  $b(m, d, r) \leq \log n$ . Also notice that in this case,  $\gamma(a) \leq d^*$  for any  $a > 0$ . Then, Theorem 3.4 implies that

$$\begin{aligned}
\mathbb{E}_{\mathbf{s}^*} \mathbb{E}_{\mathcal{S}} \mathbb{E}_{0|\mathcal{S}} \{\bar{w}(\mathbf{s}^*) - w_0(\mathbf{s}^*)\}^2 &\leq (8\|w_0\|_{\mathbb{H}}^2 + 12k^{-1}\|w_0\|_{\mathbb{H}}^2 + 14d^*) \frac{\tau_0^2}{n} \\
&\quad + \left\{ \mu_1\|w_0\|_{\mathbb{H}}^2 + \operatorname{tr}(C_\alpha) + \frac{4\|w_0\|_{\mathbb{H}}^2}{k} + \frac{2n}{k} \right\} \left( \frac{A\rho^2 d^* \log n}{\sqrt{n/k}} \right)^r \\
&\leq O(n^{-1}) + \{1 + o(1)\} \frac{2(A\rho^2 d^* \log n)^r k^{r/2-1}}{n^{r/2-1}} \\
&= O(n^{-1}),
\end{aligned} \tag{96}$$

where the last equality follows from the condition on  $k$ .

(ii) In the upper bounds of Theorem 3.4, we choose  $d = n^2$  in every infimum for sufficiently large

$n$  such that  $\log d = 2 \log n > r$ . Then

$$\begin{aligned}
\mu_{d+1} &\leq c_{1\mu} \exp(-c_{2\mu} n^2) = O(n^{-4}), \\
\text{tr}(C_{\alpha}^d) &= \sum_{i=n^2+1}^{\infty} \mu_i \leq \sum_{i=n^2+1}^{\infty} c_{1\mu} \exp(-c_{2\mu} i^2) \leq c_{1\mu} \int_{n^2}^{\infty} c_{1\mu} \exp(-c_{2\mu} z^2) dz \\
&\leq \int_{n^2}^{\infty} c_{1\mu} \exp(-c_{2\mu} z) dz = \frac{c_{1\mu}}{c_{2\mu}} \exp(-c_{2\mu} n^2) = O(n^{-4}), \\
b(m, d, r) &\leq \max\left(\sqrt{\log d}, \frac{\log d}{m^{1/2-1/r}}\right) \leq \log d \leq 2 \log n.
\end{aligned} \tag{97}$$

For sufficiently large  $n$ ,  $\gamma(\tau_0^2/n)$  can be bounded as

$$\begin{aligned}
\gamma(\tau_0^2/n) &= \sum_{i=1}^{\infty} \frac{\mu_i}{\mu_i + \frac{\tau_0^2}{n}} = \sum_{i=1}^{\lfloor \sqrt{\log n/c_{2\mu}} \rfloor + 1} \frac{\mu_i}{\mu_i + \frac{\tau_0^2}{n}} + \sum_{i=\lfloor \sqrt{\log n/c_{2\mu}} \rfloor + 2}^{\infty} \frac{\mu_i}{\mu_i + \frac{\tau_0^2}{n}} \\
&\leq \sqrt{\log n/c_{2\mu}} + 1 + \frac{n}{\tau_0^2} \sum_{i=\lfloor \sqrt{\log n/c_{2\mu}} \rfloor + 1}^{\infty} c_{1\mu} \exp(-c_{2\mu} i^2) \\
&\leq \sqrt{\log n/c_{2\mu}} + 1 + \frac{n}{\tau_0^2} \int_{\sqrt{\log n/c_{2\mu}}}^{\infty} c_{1\mu} \exp(-c_{2\mu} z^2) dz \\
&= \sqrt{\log n/c_{2\mu}} + 1 + \frac{nc_{1\mu}}{\tau_0^2 \sqrt{2c_{2\mu}}} \int_{\sqrt{2 \log n}}^{\infty} \exp(-u^2/2) du \\
&\stackrel{(i)}{\leq} \sqrt{\log n/c_{2\mu}} + 1 + \frac{nc_{1\mu}}{2\tau_0^2 \sqrt{c_{2\mu} \log n}} \exp(-\log n) \\
&= \sqrt{\log n/c_{2\mu}} + 1 + \frac{c_{1\mu}}{2\tau_0^2 \sqrt{c_{2\mu} \log n}} = O\left(\sqrt{\log n}\right),
\end{aligned} \tag{98}$$

where (i) follows from the normal tail probability bound  $\int_x^{\infty} e^{-u^2/2} du \leq e^{-x^2/2}/x$  for large  $x > 0$ ; therefore, from (97), (98), and the bounds in Theorem 3.4, we obtain that

$$\begin{aligned}
\mathbb{E}_{\mathbf{s}^*} \mathbb{E}_{\mathcal{S}} \mathbb{E}_{0|\mathcal{S}} \{\bar{w}(\mathbf{s}^*) - w_0(\mathbf{s}^*)\}^2 &\leq O(n^{-1}) + 14 \frac{\tau_0^2}{n} \gamma\left(\frac{\tau_0^2}{n}\right) + \{1 + o(1)\} \frac{2n}{k} \left\{ \frac{Ab(m, d, r) \rho^2 \gamma(\frac{\tau_0^2}{n})}{\sqrt{m}} \right\}^r \\
&\leq O(n^{-1}) + O\left(\sqrt{\log n}/n\right) + O(1) \cdot \frac{n}{k} \left\{ \frac{\sqrt{\log n} \cdot \log n}{\sqrt{n/k}} \right\}^r \\
&\leq O\left(\sqrt{\log n}/n\right) + O(1) \cdot \frac{k^{\frac{r}{2}-1} (\log n)^{\frac{3r}{2}}}{n^{\frac{r}{2}-1}} \\
&= O\left(\sqrt{\log n}/n\right),
\end{aligned}$$

where the last equality follows from the condition on  $k$ .

(iii) In the upper bounds of Theorem 3.4, we choose  $d = \lfloor n^{3/(2\nu-1)} \rfloor$  in every infimum for sufficiently

large  $n$  such that  $\log d \geq \log \left( n^{\frac{3}{2\nu-1}} - 1 \right) > r$ . Then

$$\begin{aligned}
\mu_{d+1} &\leq c_\mu n^{-6\nu/(2\nu-1)} \leq c_\mu n^{-3}, \\
\text{tr} \left( C_\alpha^d \right) &= \sum_{i=d+1}^{\infty} \mu_i \leq \sum_{i=d+1}^{\infty} c_\mu i^{-2\nu} \leq c_\mu \int_d^{\infty} \frac{1}{z^{2\nu}} dz \\
&= \frac{c_\mu}{2\nu-1} d^{-(2\nu-1)} \leq \frac{c_\mu}{2\nu-1} n^{-6\nu/(2\nu-1)} \leq \frac{c_\mu}{2\nu-1} n^{-3}, \\
b(m, d, r) &\leq \max \left( \sqrt{\log d}, \frac{\log d}{m^{1/2-1/r}} \right) \leq \log d \leq \frac{3}{2\nu-1} \log n.
\end{aligned} \tag{99}$$

$\gamma(\tau_0^2/n)$  can be bounded as

$$\begin{aligned}
\gamma(\tau_0^2/n) &= \sum_{i=1}^{\infty} \frac{1}{1 + \frac{\tau_0^2}{n\mu_i}} \leq \sum_{i=1}^{\infty} \frac{1}{1 + \frac{\tau_0^2 i^{2\nu}}{c_\mu n}} \\
&\leq n^{1/(2\nu)} + 1 + \frac{c_\mu n}{\tau_0^2} \sum_{i=\lfloor n^{1/(2\nu)} \rfloor + 2}^{\infty} \frac{1}{i^{2\nu}} \\
&\leq n^{1/(2\nu)} + 1 + \frac{c_\mu n}{\tau_0^2} \int_{n^{1/(2\nu)}}^{\infty} \frac{1}{z^{2\nu}} dz \\
&\leq n^{1/(2\nu)} + 1 + \frac{c_\mu n}{\tau_0^2 (2\nu-1) n^{(2\nu-1)/(2\nu)}} = \left( 2 + \frac{c_\mu}{\tau_0^2 (2\nu-1)} \right) n^{1/(2\nu)}.
\end{aligned} \tag{100}$$

From (99), (100), and the bounds in Theorem 3.4, we obtain that

$$\begin{aligned}
\mathbb{E}_{\mathbf{s}^*} \mathbb{E}_{\mathcal{S}} \mathbb{E}_{0|S} \{ \bar{w}(\mathbf{s}^*) - w_0(\mathbf{s}^*) \}^2 &\leq O(n^{-1}) + 14 \frac{\tau_0^2}{n} \gamma \left( \frac{\tau_0^2}{n} \right) + \{1 + o(1)\} \frac{2n}{k} \left\{ \frac{Ab(m, d, r) \rho^2 \gamma(\frac{\tau_0^2}{n})}{\sqrt{m}} \right\}^r \\
&\leq O(n^{-1}) + \frac{14\tau_0^2 \left( 2 + \frac{c_\mu}{\tau_0^2 (2\nu-1)} \right) n^{1/(2\nu)}}{n} + \{1 + o(1)\} \frac{2n}{k} \left\{ \frac{3A\rho^2 \left( 2 + \frac{c_\mu}{\tau_0^2 (2\nu-1)} \right) n^{1/(2\nu)} \log n}{(2\nu-1)\sqrt{n/k}} \right\}^r \\
&\leq O(n^{-1}) + O \left( n^{-\frac{2\nu-1}{2\nu}} \right) + O(1) \cdot \frac{k^{\frac{r}{2}-1} (\log n)^r}{n^{\frac{r}{2}-1-\frac{r}{2\nu}}} \\
&= O \left( n^{-\frac{2\nu-1}{2\nu}} \right),
\end{aligned}$$

where the last equality follows from the condition on  $k$ .

### 3 Sampling from the subset posterior distributions using a full-rank GP prior

Recall the univariate spatial regression model for the data observed at the  $i$ th location in subset  $j$  using a GP prior is

$$y(\mathbf{s}_{ji}) = \mathbf{x}(\mathbf{s}_{ji})^T \boldsymbol{\beta} + w(\mathbf{s}_{ji}) + \epsilon(\mathbf{s}_{ji}), \quad j = 1, \dots, k, \quad i = 1, \dots, m. \tag{101}$$

For the simulations and real data analysis, we assume that  $C_{\alpha}(\mathbf{s}_{ji}, \mathbf{s}_{ji'}) = \sigma^2 \rho(\mathbf{s}_{ji}, \mathbf{s}_{ji'}; \phi)$  and  $D_{\alpha}(\mathbf{s}_{ji}, \mathbf{s}_{ji'}) = \mathbf{1}(i = i')\tau^2$ , where  $\sigma^2, \phi, \tau^2$  are positive scalars,  $\rho(\cdot, \cdot)$  is a known positive definite correlation function, and  $\mathbf{1}(i = i') = 1$  if  $i = i'$  and 0 otherwise. This implies that  $\alpha = (\sigma^2, \tau^2, \phi)$ . The model in (101) is completed by putting priors on the unknown parameters. The priors distributions on  $\beta$  and  $\alpha$  have the following forms:

$$\beta \sim N(\mu_{\beta}, \Sigma_{\beta}), \quad \sigma^2 \sim \text{IG}(a_{\sigma}, b_{\sigma}), \quad \tau^2 \sim \text{IG}(a_{\tau}, b_{\tau}), \quad \phi \sim \text{U}(a_{\phi}, b_{\phi}), \quad (102)$$

where  $\mu_{\beta}, \Sigma_{\beta}, a_{\sigma}, b_{\sigma}, a_{\tau}, b_{\tau}, a_{\phi}$ , and  $b_{\phi}$  are constants,  $N$  represents the multivariate Gaussian distribution of appropriate dimension,  $\text{IG}(a, b)$  represents the Inverse-Gamma distribution with mean  $a/(b+1)$  and variance  $b/\{(a-1)^2(a-2)\}$  for  $a > 2$ , and  $\text{U}(a, b)$  represents the uniform distribution on the interval  $[a, b]$ . The spatial process  $w(\cdot)$  is assigned a GP prior as

$$w(\cdot) \mid \sigma^2, \phi \sim \text{GP}\{0, C_{\alpha}(\cdot, \cdot)\}, \quad C_{\alpha}(\cdot, \cdot) = \sigma^2 \rho(\cdot, \cdot; \phi). \quad (103)$$

The training data  $\{\mathbf{x}(\mathbf{s}_{j1}), y(\mathbf{s}_{j1})\}, \dots, \{\mathbf{x}(\mathbf{s}_{jm}), y(\mathbf{s}_{jm})\}$  are observed at the  $m$  spatial locations and  $\mathcal{S}_j = \{\mathbf{s}_{j1}, \dots, \mathbf{s}_{jm}\}$  contains the locations in subset  $j$ .

Consider the setup for predictions and inferences on subset  $j$ . Let  $\mathcal{S}^* = \{\mathbf{s}_1^*, \dots, \mathbf{s}_l^*\}$  be the set of locations such that  $\mathcal{S}^* \cap \mathcal{S}_j = \emptyset$ . If  $\mathbf{w}_j^T = \{w(\mathbf{s}_{j1}), \dots, w(\mathbf{s}_{jm})\}$  and  $\epsilon_j^T = \{\epsilon(\mathbf{s}_{j1}), \dots, \epsilon(\mathbf{s}_{jm})\}$ , then (101) implies that  $\mathbf{w}_j$  apriori follows  $N\{\mathbf{0}, \mathbf{C}_{j,j}(\alpha)\}$ , where  $\mathbf{C}_{j,j}(\alpha)$  is the block of  $\mathbf{C}(\alpha)$  that corresponds to the locations in  $\mathcal{S}_j$ , and  $\epsilon_j$  follows  $N(\mathbf{0}, \tau^2 \mathbf{I})$ , where  $\mathbf{I}$  is the identity matrix of appropriate dimension. Given the training data on subset  $j$ , our goal is to predict  $\mathbf{y}_j^* = \{y(\mathbf{s}_1^*), \dots, y(\mathbf{s}_l^*)\}$  and to perform posterior inference on  $\mathbf{w}_j^* = \{w(\mathbf{s}_1), \dots, w(\mathbf{s}_l)\}$ ,  $\beta_j$ , and  $\alpha_j$ , where the subscript  $j$  denotes that the predictions and inferences condition only on subset  $j$ . Standard Markov chain Monte Carlo (MCMC) algorithms exist to achieve this goal [4], but conditioning only on subset  $j$  ignores the information contained in the other  $(k-1)$  subsets, resulting in greater posterior uncertainty compared to the full data posterior distribution.

Stochastic approximation is an approach for proper uncertainty quantification that modifies the likelihood used for sampling from the subset posterior distributions for predictions and inferences. The likelihoods for  $\beta$ ,  $\alpha$ , and  $\mathbf{w}_j$  are raised to the power of  $k$  to compensate for the data in the other  $(k-1)$  subsets. First, consider stochastic approximation for the likelihood of  $\beta$  and  $\alpha$ . Integrating out  $\mathbf{w}_j$  in (101) gives

$$\mathbf{y}_j = \mathbf{X}_j \beta + \boldsymbol{\eta}_j, \quad \boldsymbol{\eta}_j \sim N\{\mathbf{0}, \mathbf{C}_{j,j}(\alpha) + \tau^2 \mathbf{I}\}, \quad (104)$$

where  $\mathbf{X}_j = [\mathbf{x}(\mathbf{s}_{j1}) : \dots : \mathbf{x}(\mathbf{s}_{jm})]^T \in \mathbb{R}^{m \times p}$  is the design matrix for subset  $j$ . The likelihood of  $\beta$  and  $\alpha$  given  $\mathbf{y}_j$ ,  $\mathbf{X}_j$  after stochastic approximation is

$$\{l_j(\beta, \alpha)\}^k = (2\pi)^{-mk/2} |\mathbf{C}_{j,j}(\alpha) + \tau^2 \mathbf{I}|^{-k/2} e^{-\frac{k}{2}(\mathbf{y}_j - \mathbf{X}_j \beta)^T \{\mathbf{C}_{j,j}(\alpha) + \tau^2 \mathbf{I}\}^{-1} (\mathbf{y}_j - \mathbf{X}_j \beta)}. \quad (105)$$

The prior distribution for  $\beta$  in (102), the pseudo likelihood in (105), and Bayes rule implies that

the density of the  $j$ th subset posterior distribution for  $\beta$  given the rest is

$$\beta \mid \text{rest} \propto e^{-\frac{1}{2}(\mathbf{y}_j - \mathbf{X}_j \beta)^T [k^{-1}\{\mathbf{C}_{j,j}(\alpha) + \tau^2 \mathbf{I}\}]^{-1}(\mathbf{y}_j - \mathbf{X}_j \beta)} e^{-\frac{1}{2}(\beta - \mu_\beta)^T \Sigma_\beta^{-1}(\beta - \mu_\beta)}.$$

This implies that the complete conditional distribution of  $\beta_j$  has density  $N(\mathbf{m}_{j\beta}, \mathbf{V}_{j\beta})$ , where

$$\mathbf{V}_{j\beta} = \left[ k \mathbf{X}_j^T \{\mathbf{C}_{j,j}(\alpha) + \tau^2 \mathbf{I}\}^{-1} \mathbf{X}_j + \Sigma_\beta^{-1} \right]^{-1}, \quad \mathbf{m}_{j\beta} = \mathbf{V}_{j\beta} \left[ k \mathbf{X}_j^T \{\mathbf{C}_{j,j}(\alpha) + \tau^2 \mathbf{I}\}^{-1} \mathbf{y}_j + \Sigma_\beta^{-1} \mu_\beta \right]. \quad (106)$$

If the density of the prior distribution for  $\alpha$  is assumed to be  $\pi(\sigma^2)\pi(\tau^2)\pi(\phi)$ , where the prior densities  $\pi(\sigma^2)$ ,  $\pi(\tau^2)$ , and  $\pi(\phi)$  are defined in (102), then the pseudo likelihood in (105), and Bayes rule implies that the density of the  $j$ th subset posterior distribution for  $\alpha$  given the rest is

$$\alpha \mid \text{rest} \propto |\mathbf{C}_{j,j}(\alpha) + \tau^2 \mathbf{I}|^{-k/2} e^{-\frac{1}{2}(\mathbf{y}_j - \mathbf{X}_j \beta)^T [k^{-1}\{\mathbf{C}_{j,j}(\alpha) + \tau^2 \mathbf{I}\}]^{-1}(\mathbf{y}_j - \mathbf{X}_j \beta)} (\sigma^2)^{-a_\sigma - 1} e^{-b_\sigma/\sigma^2} (\tau^2)^{-a_\tau - 1} e^{-b_\tau/\tau^2} (b_\phi - a_\phi)^{-1}. \quad (107)$$

This density does not have a standard form, so we use a Metropolis-Hastings step with a normal random walk proposal and sample  $\alpha_j$  using the `metrop` function in the R package `mcmc` [56].

Second, we derive the posterior predictive distribution of  $\mathbf{w}_j^*$  given the rest. The GP prior on  $(\mathbf{w}_j, \mathbf{w}_j^*)$  implies that the density of  $\mathbf{w}_j^*$  given  $\mathbf{w}_j$  is

$$\mathbf{w}_j^* \mid \mathbf{w}_j \sim N \left\{ \mathbf{C}_{*,j}(\alpha) \mathbf{C}_{j,j}^{-1}(\alpha) \mathbf{w}_j, \mathbf{C}_{*,*}(\alpha) - \mathbf{C}_{*,j}(\alpha) \mathbf{C}_{j,j}^{-1}(\alpha) \mathbf{C}_{j,*}(\alpha) \right\}, \quad (108)$$

where  $\text{cov}(\mathbf{w}_j^*, \mathbf{w}_j^*) = \mathbf{C}_{*,*}(\alpha)$ ,  $\text{cov}(\mathbf{w}_j^*, \mathbf{w}_j) = \mathbf{C}_{*,j}(\alpha)$ , and  $\text{cov}(\mathbf{w}_j, \mathbf{w}_j^*) = \mathbf{C}_{j,*}(\alpha)$ . Given  $\alpha$ ,  $\beta$ ,  $\mathbf{y}_j$ , and  $\mathbf{X}_j$ , (101) implies that the likelihood of  $\mathbf{w}_j$  after stochastic approximation is

$$\{l_j(\mathbf{w}_j)\}^k = (2\pi)^{-mk/2} |\tau^2 \mathbf{I}|^{-k/2} e^{-\frac{k}{2\tau^2}(\mathbf{y}_j - \mathbf{X}_j \beta - \mathbf{w}_j)^T (\mathbf{y}_j - \mathbf{X}_j \beta - \mathbf{w}_j)}. \quad (109)$$

The GP prior on  $\mathbf{w}_j$ , the pseudo likelihood in (109), and Bayes rule implies that the density of the subset posterior distribution for  $\mathbf{w}_j$  given the rest is

$$\mathbf{w}_j \mid \text{rest} \propto e^{-\frac{1}{2\tau^2/k}(\mathbf{y}_j - \mathbf{X}_j \beta - \mathbf{w}_j)^T (\mathbf{y}_j - \mathbf{X}_j \beta - \mathbf{w}_j)} e^{-\frac{1}{2} \mathbf{w}_j^T \mathbf{C}_{j,j}^{-1}(\alpha) \mathbf{w}_j}.$$

This implies that the complete conditional distribution of  $\mathbf{w}_j$  has density  $N(\mathbf{m}_{\mathbf{w}_j}, \mathbf{V}_{\mathbf{w}_j})$ , where

$$\mathbf{V}_{\mathbf{w}_j} = \left\{ \mathbf{C}_{j,j}^{-1}(\alpha) + \frac{k}{\tau^2} \mathbf{I} \right\}^{-1}, \quad \mathbf{m}_{\mathbf{w}_j} = \frac{k}{\tau^2} \mathbf{V}_{\mathbf{w}_j} (\mathbf{y}_j - \mathbf{X}_j \beta); \quad (110)$$

therefore, (108) and (110) imply that the complete conditional distribution of  $\mathbf{w}_j^*$  has density  $N(\mathbf{m}_{\mathbf{w}_j^*}, \mathbf{V}_{\mathbf{w}_j^*})$ , where

$$\mathbf{m}_{\mathbf{w}_j^*} = \mathbb{E}(\mathbf{w}_j^* \mid \text{rest}) = \mathbf{C}_{*,j}(\alpha) \mathbf{C}_{j,j}^{-1}(\alpha) \mathbb{E}(\mathbf{w}_j \mid \text{rest})$$

$$= \mathbf{C}_{*,j}(\boldsymbol{\alpha}) \left\{ \mathbf{C}_{j,j}(\boldsymbol{\alpha}) + \frac{\tau_j^2}{k} \mathbf{I} \right\}^{-1} (\mathbf{y}_j - \mathbf{X}_j \boldsymbol{\beta}) \quad (111)$$

and

$$\begin{aligned} \mathbf{V}_{\mathbf{w}_j^*} &= \text{var}(\mathbf{w}_j^* \mid \text{rest}) = \mathbb{E} \{ \text{var}(\mathbf{w}_j^* \mid \mathbf{w}_j) \mid \text{rest} \} + \text{var} \{ \mathbb{E}(\mathbf{w}_j^* \mid \mathbf{w}_j) \mid \text{rest} \} \\ &= \mathbf{C}_{*,*}(\boldsymbol{\alpha}) - \mathbf{C}_{*,j}(\boldsymbol{\alpha}) \mathbf{C}_{j,j}^{-1}(\boldsymbol{\alpha}) \mathbf{C}_{j,*}(\boldsymbol{\alpha}) + \mathbf{C}_{*,j}(\boldsymbol{\alpha}) \mathbf{C}_{j,j}^{-1}(\boldsymbol{\alpha}) \mathbf{V}_{\mathbf{w}_j} \mathbf{C}_{j,j}^{-1}(\boldsymbol{\alpha}) \mathbf{C}_{j,*}(\boldsymbol{\alpha}). \end{aligned} \quad (112)$$

Finally, we derive the posterior predictive distribution of  $\mathbf{y}_j^*$  given the rest. If  $\boldsymbol{\beta}_j$ ,  $\tau_j^2$ ,  $\mathbf{w}_j^*$  are the samples from the  $j$ th subset posterior distribution of  $\boldsymbol{\beta}$ ,  $\tau^2$ , and  $\mathbf{w}^*$ , then (101) implies that  $\mathbf{y}_j^*$  given the rest is sampled as

$$\mathbf{y}_j^* = \mathbf{X}_j \boldsymbol{\beta}_j + \mathbf{w}_j^* + \boldsymbol{\epsilon}_j^*, \quad \boldsymbol{\epsilon}_j^* \sim N(\mathbf{0}, \tau_j^2 \mathbf{I});$$

therefore, the complete conditional distribution of  $\mathbf{y}_j^*$  is  $N(\boldsymbol{\mu}_{\mathbf{y}_j^*}, \mathbf{V}_{\mathbf{y}_j^*})$ , where

$$\boldsymbol{\mu}_{\mathbf{y}_j^*} = \mathbf{X}_j \boldsymbol{\beta}_j + \mathbf{w}_j^*, \quad \mathbf{V}_{\mathbf{y}_j^*} = \tau_j^2 \mathbf{I}. \quad (113)$$

All full conditionals except that of  $\boldsymbol{\alpha}$  are analytically tractable in terms of standard distributions in subset  $j$  ( $j = 1, \dots, k$ ). The Gibbs sampler with a Metropolis-Hastings step iterates between the following four steps until sufficient number of samples of  $\boldsymbol{\beta}_j$ ,  $\boldsymbol{\alpha}_j$ ,  $\mathbf{w}_j^*$ , and  $\mathbf{y}_j^*$  are drawn post convergence to the stationary distribution:

1. Sample  $\boldsymbol{\beta}_j$  from  $N(\boldsymbol{\mu}_{j\boldsymbol{\beta}}, \mathbf{V}_{j\boldsymbol{\beta}})$ , where  $\boldsymbol{\mu}_{j\boldsymbol{\beta}}$  and  $\mathbf{V}_{j\boldsymbol{\beta}}$  are defined in (106).
2. Sample  $\boldsymbol{\alpha}_j$  using the Metropolis-Hastings algorithm from the  $j$ th subset posterior density (up to constants) of  $\boldsymbol{\alpha}_j$  in (107) with a normal random walk proposal.
3. Sample  $\mathbf{w}_j^*$  from  $N(\boldsymbol{\mu}_{\mathbf{w}_j^*}, \mathbf{V}_{\mathbf{w}_j^*})$ , where  $\boldsymbol{\mu}_{\mathbf{w}_j^*}$  and  $\mathbf{V}_{\mathbf{w}_j^*}$  are defined in (111) and (112).
4. Sample  $\mathbf{y}_j^*$  from  $N(\boldsymbol{\mu}_{\mathbf{y}_j^*}, \mathbf{V}_{\mathbf{y}_j^*})$ , where  $\boldsymbol{\mu}_{\mathbf{y}_j^*}$  and  $\mathbf{V}_{\mathbf{y}_j^*}$  are defined in (113).

## 4 Sampling from the subset posterior distributions using a low-rank GP prior

For clarity, we focus on the modified predictive process (MPP) prior as a representative example of low-rank GP prior. The Gibbs sampling algorithm derived in this section is easily extended to other low-rank GP priors. Following the setup in Section 3, we assume that  $C_{\boldsymbol{\alpha}}(\mathbf{s}_{ji}, \mathbf{s}_{ji'}) = \sigma^2 \rho(\mathbf{s}_{ji}, \mathbf{s}_{ji'}; \phi)$  and  $D_{\boldsymbol{\alpha}}(\mathbf{s}_{ji}, \mathbf{s}_{ji'}) = \mathbf{1}(i = i') \tau^2$ ,  $\boldsymbol{\alpha} = (\sigma^2, \tau^2, \phi)$ , the prior distributions on  $\boldsymbol{\beta}$  and  $\boldsymbol{\alpha}$  have the same forms as in (102), and  $\mathcal{S}_j$  contains the locations in subset  $j$ . The only change in this section is that the spatial process  $w(\cdot)$  in (101) is assigned a MPP prior derived from parent GP prior in (103). MPP projects the parent GP  $w(\cdot)$  onto a subspace spanned by its realization over a set of  $r$  locations,  $\mathcal{S}^{(0)} = \{\mathbf{s}_1^{(0)}, \dots, \mathbf{s}_r^{(0)}\}$ , known as the “knots”, where no conditions are imposed on

$\mathcal{S} \cap \mathcal{S}^{(0)}$ . Let  $\mathbf{c}(\cdot, \mathcal{S}^{(0)}) = \{C_{\alpha}(\cdot, \mathbf{s}_1^{(0)}), \dots, C_{\alpha}(\cdot, \mathbf{s}_r^{(0)})\}^T$  and  $\mathbf{w}^{(0)} = \{w(\mathbf{s}_1^{(0)}), \dots, w(\mathbf{s}_r^{(0)})\}^T$  be  $r \times 1$  vectors and  $\mathbf{C}(\mathcal{S}^{(0)})$  be an  $r \times r$  matrix whose  $(i, j)$ th entry is  $C_{\alpha}(\mathbf{s}_i^{(0)}, \mathbf{s}_j^{(0)})$ . The MPP prior defines

$$\tilde{w}(\cdot) = \mathbf{c}^T(\cdot, \mathcal{S}^{(0)}) \mathbf{C}(\mathcal{S}^{(0)})^{-1} \mathbf{w}^{(0)} + \tilde{\epsilon}(\cdot), \quad (114)$$

where the processes  $\tilde{\epsilon}(\cdot)$  and  $w(\cdot)$  are mutually independent and  $\tilde{\epsilon}(\cdot)$  is a GP with mean 0,  $\text{cov}\{\tilde{\epsilon}(\mathbf{a}), \tilde{\epsilon}(\mathbf{b})\} = \delta(\mathbf{a}) \mathbf{1}(\mathbf{a} = \mathbf{b})$  for any  $\mathbf{a}, \mathbf{b} \in \mathcal{D}$ , and

$$\delta(\mathbf{s}_{ji}) = C_{\alpha}(\mathbf{s}_{ji}, \mathbf{s}_{ji}) - \mathbf{c}^T(\mathbf{s}_{ji}, \mathcal{S}^{(0)}) \mathbf{C}(\mathcal{S}^{(0)})^{-1} \mathbf{c}(\mathbf{s}_{ji}, \mathcal{S}^{(0)}).$$

The process  $\tilde{w}(\cdot)$  is a low-rank GP with mean 0 and

$$\text{cov}\{\tilde{w}(\mathbf{a}), \tilde{w}(\mathbf{b})\} = \mathbf{c}^T(\mathbf{a}, \mathcal{S}^{(0)}) \mathbf{C}(\mathcal{S}^{(0)})^{-1} \mathbf{c}(\mathbf{b}, \mathcal{S}^{(0)}) + \delta(\mathbf{a}) \mathbf{1}_{\mathbf{a}=\mathbf{b}}$$

for any  $\mathbf{a}, \mathbf{b} \in \mathcal{D}$ . If we replace  $w(\cdot)$  by  $\tilde{w}(\cdot)$  in (101), then

$$y(\mathbf{s}_{ji}) = \mathbf{x}(\mathbf{s}_{ji})^T \boldsymbol{\beta} + \tilde{w}(\mathbf{s}_{ji}) + \epsilon(\mathbf{s}_{ji}), \quad j = 1, \dots, k, \quad i = 1, \dots, m. \quad (115)$$

and our definition in (114) implies that  $\tilde{w}(\cdot)$  is assigned a MPP prior [24].

We start by defining mean and covariance functions specific to univariate spatial regression using MPP. Let  $\tilde{\mathbf{w}}_j = \{\tilde{w}(\mathbf{s}_{j1}), \dots, \tilde{w}(\mathbf{s}_{jm})\}$  and  $\tilde{\mathbf{w}}_j^* = \{\tilde{w}(\mathbf{s}_1), \dots, \tilde{w}(\mathbf{s}_l)\}$ . The MPP prior is identical to the FITC approximation in sparse approximate GP regression, so we use the FITC notations to simplify the description of posterior computations [55]. Define  $\mathbf{Q}_{j,j} = \mathbf{C}_{j,0}(\boldsymbol{\alpha}) \mathbf{C}^{-1}(\mathcal{S}^{(0)}) \mathbf{C}_{0,j}(\boldsymbol{\alpha})$ , where  $\text{cov}\{w(\mathbf{s}_{ja}), w(\mathbf{s}_b^{(0)})\} = \{\mathbf{C}_{j,0}(\boldsymbol{\alpha})\}_{a,b}$  ( $a = 1, \dots, m; b = 1, \dots, r$ ) and  $\mathbf{C}_{0,j}(\boldsymbol{\alpha}) = \mathbf{C}_{j,0}^T(\boldsymbol{\alpha})$ . The density of  $(\tilde{\mathbf{w}}_j, \tilde{\mathbf{w}}_j^*)$  under the GP prior implied by MPP is  $N\{\mathbf{0}, \tilde{\mathbf{C}}(\boldsymbol{\alpha})\}$ , where  $2 \times 2$  block form of  $\tilde{\mathbf{C}}(\boldsymbol{\alpha})$  is defined using

$$\begin{aligned} \tilde{\mathbf{C}}_{j,j}(\boldsymbol{\alpha}) &= \mathbf{Q}_{j,j} + \text{diag}\{\mathbf{C}_{j,j}(\boldsymbol{\alpha}) - \mathbf{Q}_{j,j}\} = \text{cov}(\tilde{\mathbf{w}}_j, \tilde{\mathbf{w}}_j), & \tilde{\mathbf{C}}_{j,*}(\boldsymbol{\alpha}) &= \mathbf{Q}_{j,*} = \text{cov}(\tilde{\mathbf{w}}_j, \tilde{\mathbf{w}}_j^*), \\ \tilde{\mathbf{C}}_{*,*}(\boldsymbol{\alpha}) &= \mathbf{Q}_{*,*} + \text{diag}\{\mathbf{C}_{*,*}(\boldsymbol{\alpha}) - \mathbf{Q}_{*,*}\} = \text{cov}(\tilde{\mathbf{w}}_j^*, \tilde{\mathbf{w}}_j^*), & \tilde{\mathbf{C}}_{*,j}(\boldsymbol{\alpha}) &= \mathbf{Q}_{*,j} = \text{cov}(\tilde{\mathbf{w}}_j^*, \tilde{\mathbf{w}}_j). \end{aligned} \quad (116)$$

Stochastic approximation is implemented following Section 3. First, consider stochastic approximation for the likelihood of  $\boldsymbol{\beta}$  and  $\boldsymbol{\alpha}$ . Integrating out  $\tilde{\mathbf{w}}_j$  in (115) gives

$$\mathbf{y}_j = \mathbf{X}_j \boldsymbol{\beta} + \tilde{\boldsymbol{\eta}}_j, \quad \tilde{\boldsymbol{\eta}}_j \sim N\{\mathbf{0}, \tilde{\mathbf{C}}_{j,j}(\boldsymbol{\alpha}) + \tau^2 \mathbf{I}\}. \quad (117)$$

The likelihood of  $\boldsymbol{\beta}$  and  $\boldsymbol{\alpha}$  given  $\mathbf{y}_j, \mathbf{X}_j$  after stochastic approximation is

$$\{l_j(\boldsymbol{\beta}, \boldsymbol{\alpha})\}^k = (2\pi)^{-mk/2} |\tilde{\mathbf{C}}_{j,j}(\boldsymbol{\alpha}) + \tau^2 \mathbf{I}|^{-k/2} e^{-\frac{k}{2}(\mathbf{y}_j - \mathbf{X}_j \boldsymbol{\beta})^T \{\tilde{\mathbf{C}}_{j,j}(\boldsymbol{\alpha}) + \tau^2 \mathbf{I}\}^{-1} (\mathbf{y}_j - \mathbf{X}_j \boldsymbol{\beta})}. \quad (118)$$

The prior distribution for  $\boldsymbol{\beta}$  in (102), the pseudo likelihood in (118), and Bayes rule implies that

the density of the  $j$ th subset posterior distribution for  $\beta$  given the rest is

$$\beta \mid \text{rest} \propto e^{-\frac{1}{2}(\mathbf{y}_j - \mathbf{X}_j \beta)^T [k^{-1}\{\tilde{\mathbf{C}}_{j,j}(\alpha) + \tau^2 \mathbf{I}\}]^{-1}(\mathbf{y}_j - \mathbf{X}_j \beta)} e^{-\frac{1}{2}(\beta - \mu_\beta)^T \Sigma_\beta^{-1}(\beta - \mu_\beta)}.$$

This implies that the complete conditional distribution of  $\beta_j$  has density  $N(\tilde{\mathbf{m}}_{j\beta}, \tilde{\mathbf{V}}_{j\beta})$ , where

$$\tilde{\mathbf{V}}_{j\beta} = \left[ k \mathbf{X}_j^T \{ \tilde{\mathbf{C}}_{j,j}(\alpha) + \tau^2 \mathbf{I} \}^{-1} \mathbf{X}_j + \Sigma_\beta^{-1} \right]^{-1}, \quad \tilde{\mathbf{m}}_{j\beta} = \tilde{\mathbf{V}}_{j\beta} \left[ k \mathbf{X}_j^T \{ \tilde{\mathbf{C}}_{j,j}(\alpha) + \tau^2 \mathbf{I} \}^{-1} \mathbf{y}_j + \Sigma_\beta^{-1} \mu_\beta \right]. \quad (119)$$

Following Section 3, the density of the  $j$ th subset posterior distribution for  $\alpha$  given the rest is

$$\alpha \mid \text{rest} \propto |\tilde{\mathbf{C}}_{j,j}(\alpha) + \tau^2 \mathbf{I}|^{-k/2} e^{-\frac{1}{2}(\mathbf{y}_j - \mathbf{X}_j \beta)^T [k^{-1}\{\tilde{\mathbf{C}}_{j,j}(\alpha) + \tau^2 \mathbf{I}\}]^{-1}(\mathbf{y}_j - \mathbf{X}_j \beta)} (\sigma^2)^{-a_\sigma - 1} e^{-b_\sigma/\sigma^2} (\tau^2)^{-a_\tau - 1} e^{-b_\tau/\tau^2} (b_\phi - a_\phi)^{-1}. \quad (120)$$

This density does not have a standard form, so we use a Metropolis-Hastings step with a normal random walk proposal and sample  $\alpha_j$  using the `metrop` function in the R package `mcmc`.

Second, we derive the posterior predictive distribution of  $\tilde{\mathbf{w}}_j^*$  given the rest. The MPP prior on  $(\tilde{\mathbf{w}}_j, \tilde{\mathbf{w}}_j^*)$  implies that the density of  $\tilde{\mathbf{w}}_j^*$  given  $\tilde{\mathbf{w}}_j$  is

$$\tilde{\mathbf{w}}_j^* \mid \tilde{\mathbf{w}}_j \sim N \left\{ \tilde{\mathbf{C}}_{*,j}(\alpha) \tilde{\mathbf{C}}_{j,j}^{-1}(\alpha) \tilde{\mathbf{w}}_j, \tilde{\mathbf{C}}_{*,*}(\alpha) - \tilde{\mathbf{C}}_{*,j}(\alpha) \tilde{\mathbf{C}}_{j,j}^{-1}(\alpha) \tilde{\mathbf{C}}_{j,*}(\alpha) \right\}. \quad (121)$$

Given  $\alpha, \beta, \mathbf{y}_j$ , and  $\mathbf{X}_j$ , (115) implies that the likelihood of  $\tilde{\mathbf{w}}_j$  after stochastic approximation is

$$\{l_j(\tilde{\mathbf{w}}_j)\}^k = (2\pi)^{-mk/2} |\tau^2 \mathbf{I}|^{-k/2} e^{-\frac{k}{2\tau^2}(\mathbf{y}_j - \mathbf{X}_j \beta - \tilde{\mathbf{w}}_j)^T (\mathbf{y}_j - \mathbf{X}_j \beta - \tilde{\mathbf{w}}_j)}. \quad (122)$$

The MPP prior on  $\tilde{\mathbf{w}}_j$ , the pseudo likelihood in (122), and Bayes rule implies that the density of the subset posterior distribution for  $\tilde{\mathbf{w}}_j$  given the rest is

$$\tilde{\mathbf{w}}_j \mid \text{rest} \propto e^{-\frac{1}{2\tau^2/k}(\mathbf{y}_j - \mathbf{X}_j \beta - \tilde{\mathbf{w}}_j)^T (\mathbf{y}_j - \mathbf{X}_j \beta - \tilde{\mathbf{w}}_j)} e^{-\frac{1}{2} \tilde{\mathbf{w}}_j^T \tilde{\mathbf{C}}_{j,j}^{-1}(\alpha) \tilde{\mathbf{w}}_j}.$$

This implies that the complete conditional distribution of  $\tilde{\mathbf{w}}_j$  has density  $N(\mathbf{m}_{\tilde{\mathbf{w}}_j}, \mathbf{V}_{\tilde{\mathbf{w}}_j})$ , where

$$\mathbf{V}_{\tilde{\mathbf{w}}_j} = \left\{ \tilde{\mathbf{C}}_{j,j}^{-1}(\alpha) + \frac{k}{\tau^2} \mathbf{I} \right\}^{-1}, \quad \mathbf{m}_{\tilde{\mathbf{w}}_j} = \frac{k}{\tau^2} \mathbf{V}_{\tilde{\mathbf{w}}_j} (\mathbf{y}_j - \mathbf{X}_j \beta); \quad (123)$$

therefore, (121) and (123) imply that the complete conditional distribution of  $\tilde{\mathbf{w}}_j^*$  has density  $N(\mathbf{m}_{\tilde{\mathbf{w}}_j^*}, \mathbf{V}_{\tilde{\mathbf{w}}_j^*})$ , where

$$\begin{aligned} \mathbf{m}_{\tilde{\mathbf{w}}_j^*} &= \mathbb{E}(\tilde{\mathbf{w}}_j^* \mid \text{rest}) = \tilde{\mathbf{C}}_{*,j}(\alpha) \tilde{\mathbf{C}}_{j,j}^{-1}(\alpha) \mathbb{E}(\tilde{\mathbf{w}}_j \mid \text{rest}) \\ &= \tilde{\mathbf{C}}_{*,j}(\alpha) \left\{ \tilde{\mathbf{C}}_{j,j}(\alpha) + \frac{\tau^2}{k} \mathbf{I} \right\}^{-1} (\mathbf{y}_j - \mathbf{X}_j \beta) \end{aligned} \quad (124)$$



and

$$\begin{aligned} \mathbf{V}_{\tilde{\mathbf{w}}_j^*} &= \text{var}(\tilde{\mathbf{w}}_j^* \mid \text{rest}) = \mathbb{E} \{ \text{var}(\tilde{\mathbf{w}}_j^* \mid \tilde{\mathbf{w}}_j) \mid \text{rest} \} + \text{var} \{ \mathbb{E}(\tilde{\mathbf{w}}_j^* \mid \tilde{\mathbf{w}}_j) \mid \text{rest} \} \\ &= \tilde{\mathbf{C}}_{*,*}(\boldsymbol{\alpha}) - \tilde{\mathbf{C}}_{*,j}(\boldsymbol{\alpha}) \tilde{\mathbf{C}}_{j,j}^{-1}(\boldsymbol{\alpha}) \tilde{\mathbf{C}}_{j,*}(\boldsymbol{\alpha}) + \tilde{\mathbf{C}}_{*,j}(\boldsymbol{\alpha}) \tilde{\mathbf{C}}_{j,j}^{-1}(\boldsymbol{\alpha}) \mathbf{V}_{\tilde{\mathbf{w}}_j} \tilde{\mathbf{C}}_{j,j}^{-1}(\boldsymbol{\alpha}) \tilde{\mathbf{C}}_{j,*}(\boldsymbol{\alpha}). \end{aligned} \quad (125)$$

Finally, we derive the posterior predictive distribution of  $\mathbf{y}_j^*$  given the rest. If  $\beta_j$ ,  $\tau_j^2$ ,  $\tilde{\mathbf{w}}_j^*$  are the samples from the  $j$ th subset posterior distribution of  $\beta$ ,  $\tau^2$ , and  $\tilde{\mathbf{w}}^*$ , then (115) implies that  $\mathbf{y}_j^*$  given the rest is sampled as

$$\mathbf{y}_j^* = \mathbf{X}_j \beta_j + \tilde{\mathbf{w}}_j^* + \boldsymbol{\epsilon}_j^*, \quad \boldsymbol{\epsilon}_j^* \sim N(\mathbf{0}, \tau_j^2 \mathbf{I});$$

therefore, the complete conditional distribution of  $\mathbf{y}_j^*$  has density  $N(\tilde{\boldsymbol{\mu}}_{\mathbf{y}_j^*}, \tilde{\mathbf{V}}_{\mathbf{y}_j^*})$ , where

$$\tilde{\boldsymbol{\mu}}_{\mathbf{y}_j^*} = \mathbf{X}_j \beta_j + \tilde{\mathbf{w}}_j^*, \quad \tilde{\mathbf{V}}_{\mathbf{y}_j^*} = \tau_j^2 \mathbf{I}. \quad (126)$$

All full conditionals except that of  $\boldsymbol{\alpha}$  are analytically tractable in terms of standard distributions in subset  $j$  ( $j = 1, \dots, k$ ). The Gibbs sampler with a Metropolis-Hastings step iterates between the following four steps until sufficient number of samples of  $\beta_j$ ,  $\alpha_j$ ,  $\tilde{\mathbf{w}}_j^*$ , and  $\mathbf{y}_j^*$  are drawn post convergence to the stationary distribution:

1. Sample  $\beta_j$  from  $N(\tilde{\boldsymbol{\mu}}_{j\beta}, \tilde{\mathbf{V}}_{j\beta})$ , where  $\tilde{\boldsymbol{\mu}}_{j\beta}$  and  $\tilde{\mathbf{V}}_{j\beta}$  are defined in (119).
2. Sample  $\alpha_j$  using the Metropolis-Hastings algorithm from the  $j$ th subset posterior density (up to constants) of  $\alpha_j$  in (120) with a normal random walk proposal.
3. Sample  $\tilde{\mathbf{w}}_j^*$  from  $N(\boldsymbol{\mu}_{\tilde{\mathbf{w}}_j^*}, \mathbf{V}_{\tilde{\mathbf{w}}_j^*})$ , where  $\boldsymbol{\mu}_{\tilde{\mathbf{w}}_j^*}$  and  $\mathbf{V}_{\tilde{\mathbf{w}}_j^*}$  are defined in (124) and (125).
4. Sample  $\mathbf{y}_j^*$  from  $N(\tilde{\boldsymbol{\mu}}_{\mathbf{y}_j^*}, \tilde{\mathbf{V}}_{\mathbf{y}_j^*})$ , where  $\tilde{\boldsymbol{\mu}}_{\mathbf{y}_j^*}$  and  $\tilde{\mathbf{V}}_{\mathbf{y}_j^*}$  are defined in (126).

## 5 Computation time comparisons

We report the run-times of all the methods used in the simulated and real data analysis in Section 4 of the main paper; see Tables 6, 7, and 8 for the run-times in  $\log_{10}$  seconds in Simulation 1, Simulation 2, and sea surface temperature data analysis, respectively. The run-times cannot be compared directly from the tables due to the differences in implementation. Specifically, DISK (GP) and DISK (MPP) for all values of  $r$  and  $k$  are implemented in R, whereas most competitors are implemented in R and a higher-level language, such as C/C++ and Fortran.

## References

- [1] Agueh, M. and G. Carlier (2011). Barycenters in the Wasserstein space. *SIAM Journal on Mathematical Analysis* 43(2), 904–924.

Table 6: Run-time (in  $\log_{10}$  seconds) of all the methods used in Simulation 1. The numbers in parentheses are standard deviations over 10 simulation replications. CMC and SDP have identical run-times

laGP	LatticeKrig	GP	MPP ( $r = 200$ )	MPP ( $r = 200$ )
0.4998 (0.0142)	1.2598 (0.0134)	4.5927 (0.0050)	4.3377 (0.0217)	4.6040 (0.0165)
NNGP				
NN = 5	NN = 15	NN = 25		
2.8400 (0.0346)	3.5027 (0.0278)	3.7688 (0.0202)		
CMC				
MPP ( $r = 200, k = 10$ )	MPP ( $r = 200, k = 20$ )	MPP ( $r = 200, k = 30$ )	MPP ( $r = 200, k = 40$ )	MPP ( $r = 200, k = 50$ )
3.3373 (0.1280)	3.6980 (0.0571)	3.2867 (0.0110)	3.1158 (0.0028)	3.0196 (0.0051)
MPP ( $r = 400, k = 10$ )	MPP ( $r = 400, k = 20$ )	MPP ( $r = 400, k = 30$ )	MPP ( $r = 400, k = 40$ )	MPP ( $r = 400, k = 50$ )
3.7804 (0.0423)	4.2968 (0.1206)	4.0720 (0.2151)	4.0024 (0.0135)	3.8587 (0.0805)
DISK				
GP ( $k = 10$ )	GP ( $k = 20$ )	GP ( $k = 30$ )	GP ( $k = 40$ )	GP ( $k = 50$ )
3.9945 (0.0066)	3.6647 (0.1368)	3.4965 (0.0596)	3.4423 (0.0255)	3.3940 (0.0359)
MPP ( $r = 200, k = 10$ )	MPP ( $r = 200, k = 20$ )	MPP ( $r = 200, k = 30$ )	MPP ( $r = 200, k = 40$ )	MPP ( $r = 200, k = 50$ )
3.8061 (0.0019)	3.3998 (0.0158)	3.3207 (0.0042)	3.3096 (0.0283)	3.2936 (0.0138)
MPP ( $r = 400, k = 10$ )	MPP ( $r = 400, k = 20$ )	MPP ( $r = 400, k = 30$ )	MPP ( $r = 400, k = 40$ )	MPP ( $r = 400, k = 50$ )
3.8370 (0.0100)	3.3874 (0.0172)	3.4000 (0.0107)	3.3644 (0.0035)	3.3563 (0.0031)

Table 7: Run-time (in  $\log_{10}$  seconds) of all the methods used in Simulation 2. The numbers in parentheses are standard deviations over 10 simulation replications

laGP	DISK (MPP, $r = 400, k = 500$ )	DISK (MPP, $r = 600, k = 500$ )
3.67 (0.19)	4.36 (0.00)	4.37 (0.00)

Table 8: Run-time (in  $\log_{10}$  seconds) of all the methods used in the sea surface temperature data analysis. The numbers in parentheses are standard deviations over 10 simulation replications. CMC and SDP have identical run-times

laGP	CMC (MPP, $r = 400, k = 300$ )	DISK (MPP, $r = 400, k = 300$ )
0.93 (0.28)	4.90 (0.03)	5.16 (0.08)

- [2] Álvarez-Esteban, P. C., E. del Barrio, J. Cuesta-Albertos, and C. Matrán (2016). A fixed-point approach to barycenters in Wasserstein space. *Journal of Mathematical Analysis and Applications* 441(2), 744–762.
- [3] Banerjee, A., D. B. Dunson, and S. T. Tokdar (2012). Efficient Gaussian process regression for large datasets. *Biometrika* 100(1), 75–89.
- [4] Banerjee, S., B. P. Carlin, and A. E. Gelfand (2014). *Hierarchical Modeling and Analysis for Spatial Data*. CRC Press.
- [5] Banerjee, S., A. O. Finley, P. Waldmann, and T. Ericsson (2010). Hierarchical spatial process models for multiple traits in large genetic trials. *Journal of the American Statistical Association* 105(490), 506–521.
- [6] Banerjee, S., A. E. Gelfand, A. O. Finley, and H. Sang (2008). Gaussian predictive process models for large spatial data sets. *Journal of the Royal Statistical Society: Series B (Statistical Methodology)* 70(4), 825–848.
- [7] Berliner, L. M., C. K. Wikle, and N. Cressie (2000). Long-lead prediction of pacific ssts via bayesian dynamic modeling. *Journal of Climate* 13(22), 3953–3968.

- [8] Bickel, P. J. and D. A. Freedman (1981). Some asymptotic theory for the bootstrap. *The Annals of Statistics* 9(6), 1196–1217.
- [9] Carlier, G., A. Oberman, and E. Oudet (2015). Numerical methods for matching for teams and Wasserstein barycenters. *ESAIM: Mathematical Modelling and Numerical Analysis* 49(6), 1621–1642.
- [10] Chalupka, K., C. K. Williams, and I. Murray (2012). A framework for evaluating approximation methods for Gaussian process regression. *arXiv preprint arXiv:1205.6326*.
- [11] Cheng, G. and Z. Shang (2017). Computational limits of divide-and-conquer method. *Journal of Machine Learning Research (to appear)*.
- [12] Cressie, N. and G. Johannesson (2008). Fixed rank kriging for very large spatial data sets. *Journal of the Royal Statistical Society: Series B (Statistical Methodology)* 70(1), 209–226.
- [13] Cressie, N. and C. Wikle (2011). *Statistics for Spatio-Temporal Data*. Wiley, Hoboken, NJ.
- [14] Cuturi, M. and A. Doucet (2014). Fast computation of Wasserstein barycenters. In *Proceedings of the 31st International Conference on Machine Learning, JMLR W&CP*, Volume 32.
- [15] Datta, A., S. Banerjee, A. O. Finley, and A. E. Gelfand (2016). Hierarchical nearest-neighbor Gaussian process models for large geostatistical datasets. *Journal of the American Statistical Association* 111(514), 800–812.
- [16] Datta, A., S. Banerjee, A. O. Finley, N. A. Hamm, and M. Schaap (2016). Nonseparable dynamic nearest neighbor Gaussian process models for large spatio-temporal data with an application to particulate matter analysis. *The Annals of Applied Statistics* 10(3), 1286–1316.
- [17] Deisenroth, M. P. and J. W. Ng (2015). Distributed Gaussian processes. *arXiv preprint arXiv:1502.02843*.
- [18] Di Lorenzo, E., N. Schneider, K. Cobb, P. Franks, K. Chhak, A. Miller, J. McWilliams, S. Bograd, H. Arango, E. Curchitser, et al. (2008). North Pacific gyre oscillation links ocean climate and ecosystem change. *Geophysical Research Letters* 35(8).
- [19] Du, J., H. Zhang, V. Mandrekar, et al. (2009). Fixed-domain asymptotic properties of tapered maximum likelihood estimators. *The Annals of Statistics* 37(6A), 3330–3361.
- [20] Eidsvik, J., B. A. Shaby, B. J. Reich, M. Wheeler, and J. Niemi (2014). Estimation and prediction in spatial models with block composite likelihoods. *Journal of Computational and Graphical Statistics* 23(2), 295–315.
- [21] Finley, A., A. Datta, and S. Banerjee (2017). *spNNGP: Spatial Regression Models for Large Datasets using Nearest Neighbor Gaussian Processes*. R package version 0.1.1.

- [22] Finley, A. O., S. Banerjee, and A. E. Gelfand (2015). spBayes for large univariate and multivariate point-referenced spatio-temporal data models. *Journal of Statistical Software* 63(i13).
- [23] Finley, A. O., A. Datta, B. C. Cook, D. C. Morton, H. E. Andersen, and S. Banerjee (2017). Applying nearest neighbor Gaussian processes to massive spatial data sets: Forest canopy height prediction across Tanana Valley Alaska. *arXiv preprint arXiv:1702.00434*.
- [24] Finley, A. O., H. Sang, S. Banerjee, and A. E. Gelfand (2009). Improving the performance of predictive process modeling for large datasets. *Computational Statistics & Data Analysis* 53(8), 2873–2884.
- [25] Furrer, R., M. G. Genton, and D. Nychka (2006). Covariance tapering for interpolation of large spatial datasets. *Journal of Computational and Graphical Statistics*.
- [26] Gal, Y., M. van der Wilk, and C. E. Rasmussen (2014). Distributed variational inference in sparse Gaussian process regression and latent variable models. In *Advances in Neural Information Processing Systems*, pp. 3257–3265.
- [27] Gelfand, A. E., S. Banerjee, C. Sirmans, Y. Tu, and S. E. Ong (2007). Multilevel modeling using spatial processes: Application to the singapore housing market. *Computational Statistics & Data Analysis* 51(7), 3567–3579.
- [28] Gelfand, A. E., P. Diggle, P. Guttorp, and M. Fuentes (Eds.) (2010). *Handbook of Spatial Statistics*. Boca Raton, FL: CRC Press.
- [29] Gramacy, R. B. (2016). laGP: Large-scale spatial modeling via local approximate gaussian processes in R. *Journal of Statistical Software* 72(1), 1–46.
- [30] Gramacy, R. B. and D. W. Apley (2015). Local gaussian process approximation for large computer experiments. *Journal of Computational and Graphical Statistics* 24(2), 561–578.
- [31] Gramacy, R. B. and H. K. Lee (2008). Bayesian treed Gaussian process models with an application to computer modeling. *Journal of the American Statistical Association* 103(483), 1119–1130.
- [32] Green, P. J., K. Łatuszyński, M. Pereyra, and C. P. Robert (2015). Bayesian computation: a summary of the current state, and samples backwards and forwards. *Statistics and Computing* 25(4), 835–862.
- [33] Guhaniyogi, R. and S. Banerjee (2017). Meta-kriging: Scalable Bayesian modeling and inference for massive spatial datasets. *UCSC Technical Report*.
- [34] Guhaniyogi, R., A. O. Finley, S. Banerjee, and A. E. Gelfand (2011). Adaptive Gaussian predictive process models for large spatial datasets. *Environmetrics* 22(8), 997–1007.

- [35] Guhaniyogi, R. and B. Sanso (2017). Large multiscale spatial modeling using tree shrinkage priors. *UCSC Technical Report*.
- [36] Guinness, J. (2016). Permutation methods for sharpening Gaussian process approximations. *arXiv preprint arXiv:1609.05372*.
- [37] Haran, M. (2011). Gaussian random field models for spatial data. *Handbook of Markov Chain Monte Carlo*, 449–478.
- [38] Harville, D. A. (1997). *Matrix algebra from a statistician’s perspective*, Volume 1. Springer.
- [39] Higdon, D. (1998). A process-convolution approach to modelling temperatures in the north atlantic ocean. *Environmental and Ecological Statistics* 5(2), 173–190.
- [40] Katzfuss, M. (2017). A multi-resolution approximation for massive spatial datasets. *Journal of the American Statistical Association* 112(517).
- [41] Kaufman, C. G., M. J. Schervish, and D. W. Nychka (2008). Covariance tapering for likelihood-based estimation in large spatial data sets. *Journal of the American Statistical Association* 103(484), 1545–1555.
- [42] Lemos, R. T. and B. Sansó (2006). Spatio-temporal variability of ocean temperature in the portugul current system. *Journal of Geophysical Research: Oceans* 111(C4).
- [43] Lemos, R. T. and B. Sansó (2009). A spatio-temporal model for mean, anomaly, and trend fields of north Atlantic sea surface temperature. *Journal of the American Statistical Association* 104(485), 5–18.
- [44] Li, C., S. Srivastava, and D. B. Dunson (2017). Simple, scalable and accurate posterior interval estimation. *Biometirka* 104(3), 665–680.
- [45] Liang, F., Y. Cheng, Q. Song, J. Park, and P. Yang (2013). A resampling-based stochastic approximation method for analysis of large geostatistical data. *Journal of the American Statistical Association* 108(501), 325–339.
- [46] Minsker, S., S. Srivastava, L. Lin, and D. Dunson (2014). Scalable and robust Bayesian inference via the median posterior. In *Proceedings of the 31st International Conference on Machine Learning (ICML-14)*, pp. 1656–1664.
- [47] Minsker, S., S. Srivastava, L. Lin, and D. B. Dunson (2017). Robust and scalable Bayes via a median of subset posterior measures. *Journal of Machine Learning Research (to appear)*.
- [48] Minsker, S. and N. Strawn (2017). Distributed statistical estimation and rates of convergence in normal approximation. *arXiv preprint arXiv:1704.02658*.

- [49] Miroshnikov, A. and E. Conlon (2014). *parallelMCMCcombine: Methods for combining independent subset Markov chain Monte Carlo (MCMC) posterior samples to estimate a posterior density given the full data set*. R package version 1.0.
- [50] Neiswanger, W., C. Wang, and E. Xing (2014). Asymptotically exact, embarrassingly parallel MCMC. In *Proceedings of the 30th International Conference on Uncertainty in Artificial Intelligence*, pp. 623–632.
- [51] Ng, J. W. and M. P. Deisenroth (2014). Hierarchical mixture-of-experts model for large-scale Gaussian process regression. *arXiv preprint arXiv:1412.3078*.
- [52] Nychka, D., S. Bandyopadhyay, D. Hammerling, F. Lindgren, and S. Sain (2015). A multiresolution Gaussian process model for the analysis of large spatial datasets. *Journal of Computational and Graphical Statistics* 24(2), 579–599.
- [53] Nychka, D., D. Hammerling, S. Sain, and N. Lenssen (2016). Latticekrig: Multiresolution kriging based on markov random fields. R package version 6.4.
- [54] Park, C. and D. Apley (2017). Patchwork kriging for large-scale gaussian process regression. *arXiv preprint arXiv:1701.06655*.
- [55] Quiñonero-Candela, J. and C. E. Rasmussen (2005). A unifying view of sparse approximate gaussian process regression. *Journal of Machine Learning Research* 6(Dec), 1939–1959.
- [56] R Development Core Team (2017). *R: A Language and Environment for Statistical Computing*. Vienna, Austria: R Foundation for Statistical Computing.
- [57] Raskutti, G., M. J. Wainwright, and B. Yu (2012). Minimax-optimal rates for sparse additive models over kernel classes via convex programming. *Journal of Machine Learning Research* 13(Feb), 389–427.
- [58] Rasmussen, C. E. and C. K. Williams (2006). Gaussian processes for machine learning. *MIT Press*.
- [59] Rue, H., S. Martino, and N. Chopin (2009). Approximate Bayesian inference for latent Gaussian models by using integrated nested Laplace approximations. *Journal of the Royal Statistical Society: Series B (Statistical Methodology)* 71(2), 319–392.
- [60] Sang, H. and J. Z. Huang (2012). A full scale approximation of covariance functions for large spatial data sets. *Journal of the Royal Statistical Society: Series B (Statistical Methodology)* 74(1), 111–132.
- [61] Savitsky, T. D. and S. Srivastava (2017). Scalable Bayes under informative sampling. *Scandinavian Journal of Statistics (to appear)*.

- [62] Scott, S. L., A. W. Blocker, F. V. Bonassi, H. A. Chipman, E. I. George, and R. E. McCulloch (2016). Bayes and big data: the consensus Monte Carlo algorithm. *International Journal of Management Science and Engineering Management* 11(2), 78–88.
- [63] Shaby, B. and D. Ruppert (2012). Tapered covariance: Bayesian estimation and asymptotics. *Journal of Computational and Graphical Statistics* 21(2), 433–452.
- [64] Shang, Z. and G. Cheng (2015). Nonparametric Bayesian aggregation for massive data. *arXiv preprint arXiv:1508.04175*.
- [65] Shang, Z. and G. Cheng (2017). Gaussian approximation of general nonparametric posterior distributions. *Information and Inference (to appear)*.
- [66] Snelson, E. and Z. Ghahramani (2006). Sparse gaussian processes using pseudo-inputs. In *Advances in Neural Information Processing Systems*, pp. 1257–1264.
- [67] Srivastava, S., V. Cevher, Q. Dinh, and D. Dunson (2015). WASP: Scalable Bayes via barycenters of subset posteriors. In *Proceedings of the 18th International Conference on Artificial Intelligence and Statistics*, pp. 912–920.
- [68] Srivastava, S., C. Li, and D. B. Dunson (2015). Scalable Bayes via Barycenter in Wasserstein Space. *arXiv preprint arXiv:1508.05880*.
- [69] Staib, M., S. Clatici, J. Solomon, and S. Jegelka (2017). Parallel streaming Wasserstein barycenters. *arXiv preprint arXiv:1705.07443*.
- [70] Stein, M. L., Z. Chi, and L. J. Welty (2004). Approximating likelihoods for large spatial data sets. *Journal of the Royal Statistical Society: Series B (Statistical Methodology)* 66(2), 275–296.
- [71] Stroud, J. R., M. L. Stein, and S. Lysen (2017). Bayesian and maximum likelihood estimation for gaussian processes on an incomplete lattice. *Journal of Computational and Graphical Statistics* 26(1), 108–120.
- [72] Szabo, B. and H. van Zanten (2017). An asymptotic analysis of distributed nonparametric methods. *arXiv preprint arXiv:1711.03149*.
- [73] van der Vaart, A. and H. van Zanten (2011). Information rates of nonparametric Gaussian process methods. *Journal of Machine Learning Research* 12(Jun), 2095–2119.
- [74] van der Vaart, A. W. and J. H. van Zanten (2008). Reproducing kernel Hilbert spaces of Gaussian priors. In *Pushing the limits of contemporary statistics: contributions in honor of Jayanta K. Ghosh*, pp. 200–222. Institute of Mathematical Statistics.
- [75] Vecchia, A. V. (1988). Estimation and model identification for continuous spatial processes. *Journal of the Royal Statistical Society: Series B (Statistical Methodology)*, 297–312.

- [76] Wang, X. and D. B. Dunson (2013). Parallel MCMC via Weierstrass sampler. *arXiv preprint arXiv:1312.4605*.
- [77] Wang, X., F. Guo, K. A. Heller, and D. B. Dunson (2015). Parallelizing MCMC with random partition trees. In *Advances in Neural Information Processing Systems*, pp. 451–459.
- [78] Wikle, C. K. (2010). Low-rank representations for spatial processes. *Handbook of Spatial Statistics*, 107–118.
- [79] Wikle, C. K. and S. H. Holan (2011). Polynomial nonlinear spatio-temporal integro-difference equation models. *Journal of Time Series Analysis* 32(4), 339–350.
- [80] Xue, J. and F. Liang (2017). A double-parallel MCMC algorithm for Bayesian analysis of big data. *Statistics and Computing (to appear)*.
- [81] Yang, Y., M. Pilanci, M. J. Wainwright, et al. (2017). Randomized sketches for kernels: Fast and optimal nonparametric regression. *The Annals of Statistics* 45(3), 991–1023.
- [82] Zhang, R., C. D. Lin, and P. Ranjan (2016). Local Gaussian process model for large-scale dynamic computer experiments. *arXiv preprint arXiv:1611.09488*.
- [83] Zhang, T. (2005). Learning bounds for kernel regression using effective data dimensionality. *Neural Computation* 17(9), 2077–2098.
- [84] Zhang, Y., J. C. Duchi, and M. J. Wainwright (2015). Divide and conquer kernel ridge regression: a distributed algorithm with minimax optimal rates. *Journal of Machine Learning Research* 16, 3299–3340.